INVESTIGATING THE EFFECT OF DIFFERENT NUMBER OF HORIZONTAL AS WELL AS VERTICAL GROUND MOTIONS ON BASE ISOLATED STRUCTURES WITH DIFFERENT HEIGHTS

A THESIS SUBMITTED TO
THE GRADUATE SCHOOL OF NATURAL AND APPLIED SCIENCES
OF
MIDDLE EAST TECHNICAL UNIVERSITY

BY

BENGÜ ELCIK EROL

IN PARTIAL FULFILLMENT OF THE REQUIREMENTS
FOR
THE DEGREE OF MASTER OF SCIENCE
IN
CIVIL ENGINEERING

SEPTEMBER 2019

Approval of the thesis:

INVESTIGATING THE EFFECT OF DIFFERENT NUMBER OF HORIZONTAL AS WELL AS VERTICAL GROUND MOTIONS ON BASE ISOLATED STRUCTURES WITH DIFFERENT HEIGHTS

submitted by **BENGÜ ELCIK EROL** in partial fulfillment of the requirements for the degree of **Master of Science in Civil Engineering Department, Middle East Technical University** by,

Prof. Dr. Halil Kalıpçılar
Dean, Graduate School of **Natural and Applied Sciences**

Prof. Dr. Ahmet Türer
Head of Department, **Civil Engineering**

Prof. Dr. Uğurhan Akyüz
Supervisor, **Civil Engineering, METU**

Examining Committee Members:

Prof. Dr. Alp Caner
Civil Engineering, METU

Prof. Dr. Uğurhan Akyüz
Civil Engineering, METU

Prof. Dr. Ahmet Yakut
Civil Engineering, METU

Prof. Dr. Murat Altuğ Erberik
Civil Engineering, METU

Assoc. Prof. Dr. Alper Aldemir
Civil Engineering, Hacettepe University

Date: 10.09.2019

I hereby declare that all information in this document has been obtained and presented in accordance with academic rules and ethical conduct. I also declare that, as required by these rules and conduct, I have fully cited and referenced all material and results that are not original to this work.

Name, Surname: Bengü Elcik Erol

Signature:

ABSTRACT

INVESTIGATING THE EFFECT OF DIFFERENT NUMBER OF HORIZONTAL AS WELL AS VERTICAL GROUND MOTIONS ON BASE ISOLATED STRUCTURES WITH DIFFERENT HEIGHTS

Elcik Erol, Bengü
Master of Science, Civil Engineering
Supervisor: Prof. Dr. Uğurhan Akyüz

September 2019, 130 pages

The main goal of this study is to investigate the effects of the changes in selecting procedure of real ground motion records to be used in non-linear time history analysis on base isolated structures with friction-pendulum system. The revision involves selecting 11 ground motion records instead of 7 records and taking into account the vertical components of earthquakes instead of considering just horizontal components. Specific to this study, the main parameters employed for investigation will be base reactions, inter-storey drift ratios, peak floor accelerations, isolator displacements and axial loads on isolators. The main reason for selecting these parameters is that the inter-storey drift ratio and peak floor acceleration are the main parameters affecting structural system design, and base reactions, isolator displacements and axial loads on isolators are the main parameters affecting isolation system design. These parameters were evaluated using non-linear time history analysis method with ground motion records, which are selected and scaled using the seismicity of Isparta, on structures having 3 different numbers of floors. The analyses performed in this work indicates that increasing the number of selected ground motion records causes a decrease in all parameters evaluated. While consideration of vertical components of ground motions do not have any identifiable effect on peak floor accelerations, inter-storey drift ratios or isolator displacements, increases the variation of axial loads on isolators and base reactions. Another conclusion is that the revision on Turkish seismic code increases the execution time for analyses.

Keywords: vertical ground motion, base shear, bending moment, inter-storey drift ratio, floor acceleration, base isolation, friction pendulum

ÖZ

FARKLI ADETLERDE YATAY VE DÜŞEY DEPREM KAYDI KULLANIMINININ DEĞİŞİK YÜKSEKLİKLERDEKİ TABAN İZOLATÖRLÜ YAPILAR ÜZERİNDE ETKİSİNİN ARAŞTIRILMASI

Elcik Erol, Bengü
Yüksek Lisans, İnşaat Mühendisliği
Tez Danışmanı: Prof. Dr. Uğurhan Akyüz

Eylül 2019, 130 sayfa

Bu çalışmada, zaman-tanım alanında analizlerde kullanılacak gerçek deprem kayıtlarının adet ve özelliklerinin değişiminin, sürtünmeli sarkaç tipi sismik izolatörler kullanılarak deprem yalıtımı yapılmış yapıların davranışına olan etkisi incelenmiştir. İlgili revizyon 7 adet yerine 11 adet gerçek deprem kaydının kullanılmasını ve sadece yatay bileşenler yerine, depremlerin düşey bileşenlerinin de göz önünde bulundurulmasını içermektedir. Bu çalışma özelinde değerlendirmede esas alınan başlıca parametreler taban kesme ve moment kuvvetleri, göreli kat ötelenmeleri, kat ivmeleri, izolatör yer değiştirmeleri ve izolatörler üzerinde oluşan düşey kuvvetler olacaktır. Bu parametrelerin seçilme sebebi, kat ötelenmeleri ve kat ivmelerinin yapı tasarımını etkileyen başlıca parametreler olması, taban kuvvetleri, izolatör yer değiştirmeleri ve izolatörler üzerinde oluşan kuvvetlerin ise izolatör tasarımını etkileyen başlıca parametreler olmasıdır. Bu parametreler 3 farklı kat adedine sahip olan yapılar üzerinde, Isparta depremselliği kullanılarak seçilen ve ölçeklendirilen gerçek deprem kayıtları kullanılarak yapılan zaman tanım alanında doğrusal olmayan analiz yöntemi kullanılarak değerlendirilmiştir. Bu çalışmada elde edilen sonuçlara göre deprem kayıt adedinin artırılması ilgili parametrelerin tümünde bir azalmaya sebep olmaktadır. Depremlerin düşey bileşenlerinin analizlere dahil edilmesi ise kat

ötelenmesi, kat ivmesi ve izolatör deplasmanları üzerinde tanımlanabilir bir etki göstermezken, izolatörler üzerine etkiyen düşey kuvvetlerin dağılımının değişmesine ve taban kuvvetlerinde artışlara sebebiyet vermektedir. Bu çalışmada elde edilen başka bir sonuç ise ilgili yönetmelik revizyonunun analiz sürelerinde ciddi uzamalara sebep olacağıdır.

Anahtar Kelimeler: düşey yer hareketi, taban kesmesi, eğilme momenti, göreli kat ötelenmesi, kat ivmesi, sismik izolasyon, sürtünmeli sarkaç

To my beloved parents

ACKNOWLEDGEMENTS

I would like to express the deepest appreciation to my thesis supervisor Prof. Dr. Uğurhan Akyüz for his guidance and support during my study.

I would also like to thank my thesis committee, Prof. Dr. Ahmet Yakut, Prof. Dr. Alp Caner, Prof. Dr. Murat Altuğ Erberik and Assoc. Prof. Dr. Alper Aldemir, for their vulnerable comments and suggestions on my thesis work.

I would like to thank my grandmothers and my grandfathers, Ayfer Çukurca, Dudu Elcik, Fazıl Çukurca and Mustan Elcik, for their prayers that have always been with me since I was a child.

I owe thanks to my beloved husband, Mustafa Erol, for patiently enduring the difficulties of my entire work process and for standing by me in any circumstances. I always feel his love and support.

Finally, I give my deepest thanks to my precious parents Fatma Feza Çukurca Elcik and Atila Elcik. They have always believed and trusted in me since my childhood. There are not enough words to tell about my love and respect against them. I am proud to be a part of this family.

TABLE OF CONTENTS

LIST OF TABLES

TABLES

LIST OF FIGURES

FIGURES

LIST OF ABBREVIATIONS

ABBREVIATIONS	
NRB	Natural Rubber Bearing
LRB	Lead Rubber Bearing
HRB	High Damping Rubber Bearing
FPS	Friction Pendulum System
TBEC2019	Turkish Building Earthquake Code 2019
TEC2007	Turkish Earthquake Code 2007
ISO2	Base Isolated 2-Storey Structure
ISO4	Base Isolated 4-Storey Structure
ISO7	Base Isolated 7-Storey Structure
GM	Ground Motion
ELF	Equivalent Lateral Force
ASCE	American Society of Civil Engineers
g	Gravitational Acceleration
RSA	Response Spectrum Analysis
NTHA	Nonlinear Time History Analysis
DBE	Design Basis Earthquake
MCE	Maximum Considered Earthquake
PSHA	Probabilistic Seismic Hazard Assessment
SRSS	Square Root of Sum of the Squares

PSD	Peak Spectral Displacement
PFA	Peak Floor Acceleration
IDR	Inter-Storey Drift Ratio
ISD	Isolator Displacement

CHAPTER 1

INTRODUCTION

Earthquakes are natural disasters that cause loss of life and give economic damages to a great extent. The classical design approach in order to design safe buildings against earthquakes is increasing the ductility of structures. Installation of seismic isolation systems in structures is one of the effective design approaches for reduction of earthquake damage.

Base isolation applications have been increased in Turkey with the help of the Technical Statement of Ministry of Health, which obligates the designers to use base isolation in the design of hospitals having the capacity of 100 and more inpatients and located in the first or second seismic zone. Real ground motion records are selected and scaled for non-linear time history analyses of these structures. Ground motions are characterized by two horizontal components and a vertical component. It is a contemporary acceptance that primarily the horizontal components of an earthquake causing major damage to the structure. Despite vertical seismic loads are neglected in designs of earthquake resistant structures, the response of base-isolated structures could be affected by them [3].

1.1. Base Isolation Philosophy

Seismic isolation approach is depended on providing additional energy dissipation capability and flexibility by establishing technological devices between the foundation and superstructure. The isolation system absorbs some of the earthquake energy and transfers the rest to the superstructure by increasing the dominant periods of structure. The limits of displacements at isolation level are determined by the damping or energy dissipation capacity in the isolators [2].

Inter-storey drift and storey accelerations have to be minimized to provide excellent seismic resistance to a structure. Large inter-storey drifts cause destruction of non-structural elements within the buildings. Increasing the stiffness of structure minimize the inter-storey drifts however, this leads to an increase in storey accelerations. Although the storey accelerations could be minimized by increasing the flexibility of structure, this causes an increase in inter-storey drifts. The practical solution to this dilemma is using base isolation systems in buildings [14].

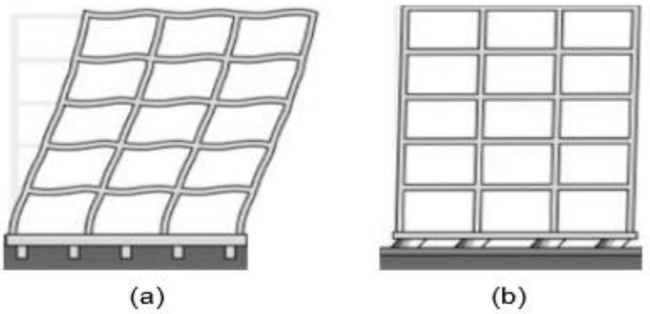

Figure 1.1. Change of Deflection Pattern While Using Isolator; (a) Conventional Structure, and (b) Base-isolated Structure [10]

The philosophy of base isolation is decoupling the structure from ground motion with the help of low stiffness elements (isolation devices) interposed between the foundation and superstructure. This implementation gives the structure a fundamental period that is much higher than its fixed-based period [14]. The period shift due to the isolation system causes a reduction in accelerations, which means that the inertia forces affected the structure, will be lower. On the other hand, overabundant displacements due to period increase should be limited by increasing the damping in the isolation system [15].

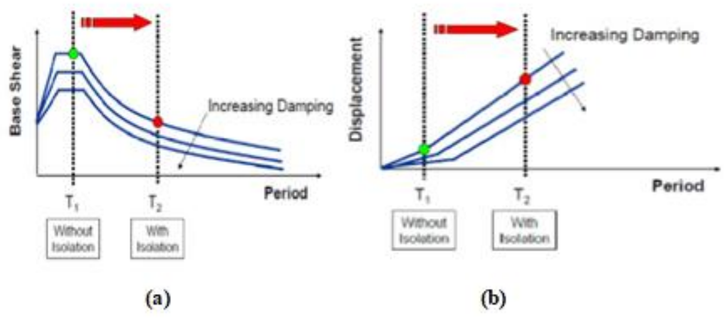

Figure 1.2. Effect of Period Shift in Isolated Structures; (a) on Accelerations, and (b) on Displacements [21]

1.1.1. Types of Base Isolation Devices

1.1.1.1. Elastomeric Bearings

Elastomeric bearings are discussed in three major groups as follows:

- Low Damping Natural and Synthetic Rubber Bearing (NRB)
- Lead Rubber Bearing (LRB)
- High Damping Rubber Bearing (HRB).

A low damping natural rubber bearing consists of two thick steel endplates and many thin steel shims. A typical scheme of an NRB is demonstrated in Figure1.3. The vulcanized rubber is bonded to the steel with the help of heat and pressure in a single operation. The horizontal stiffness of the bearing is controlled by the elastomer. Steel shims provide vertical stiffness as they prevent bulging of the rubber [14].

A lead rubber bearing (LRB) is a version of NRB that one or more lead plugs are inserted into holes, as shown in Figure 1.3. The steel shims cause a shear force on the lead plug. The lateral forces deformed the lead core and increase the period of the structure. Along with this situation, the dissipation of energy takes place [14].

The components of a high damping rubber bearing are rubber layers and steel shims. At small strains (strains <20%), the material shows non-linear behaviour. The bearing has high stiffness and damping and minimizes the response under high-frequency vibrations like wind, small earthquakes or vertical vibrations caused by environmental situations [14].

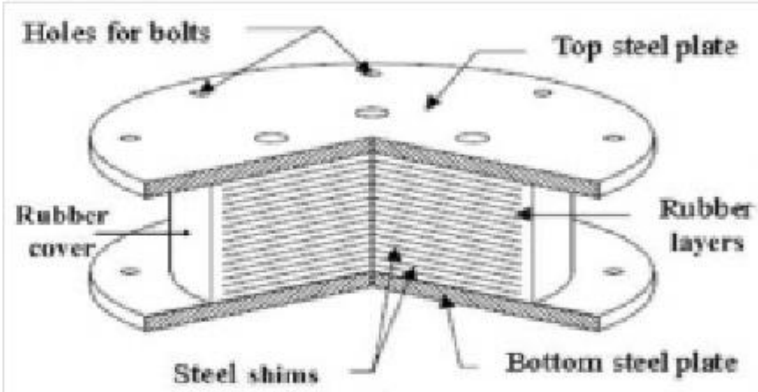

Figure 1.3. Natural Rubber Bearing (NRB) [11]

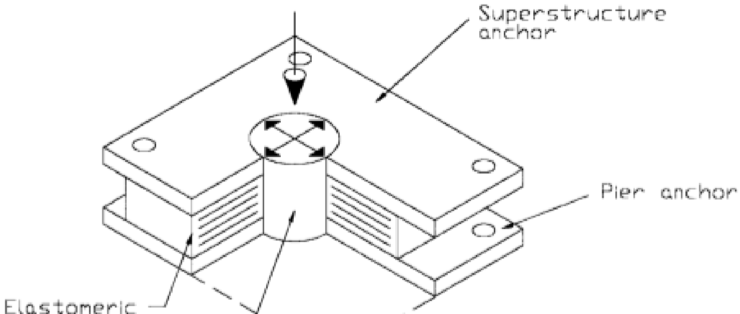

Figure 1.4. Lead Plug Bearing (LRB) [14]

1.1.1.2. Friction Sliding Devices

There are pieces of evidence of the use of sliding bearings in antique Persia by pouring gravelled material between the bearing walls and the ground. This application would work as a sliding mechanism under an earthquake. This mechanism is provided by using the friction between stainless steel and Teflon® at the present time [11].

The most popular frictional isolation system is friction pendulum system (FPS) in Turkey. This type of bearing combines a restoring force and sliding by geometry. The bearing has a stainless steel spherical surface and an articulated slider moving on this surface. There is low-friction material that is coated between the side of the slider and the spherical surface [14].

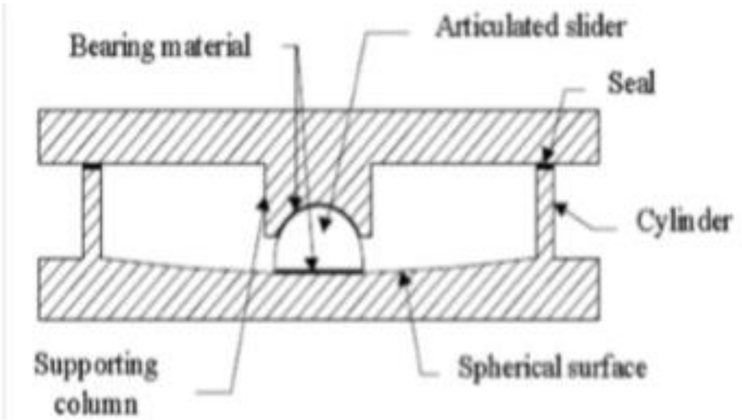

Figure 1.5. Friction Pendulum System (FPS) [11]

Damping of the isolator is generated by the friction between the slider and spherical surface. The radius of curvature of the concave surface determines the stiffness of isolator, that is to say, the period of the base isolated structure [14]. FPS is selected as the base isolation system for this study.

1.2. Literature Survey

Scottish engineer David Stevenson generated an idea called "asymmetric joint" in order to improve the resistance of lighthouses against earthquake hazard in Japan. The rolling-bearing device, which is designed by Stevenson, consists of balls and cups. Even though the correct formulation of the base isolation philosophy has been improved by Stevenson, acceptance of the base isolation system as a sophisticated technology has taken a long time [7].

In literature, effects of vertical components of ground motions are generally investigated for the same purposes as isolator displacements, base shears and axial loads on isolators. In the study of Amaral, and Guerreiro [3], a based isolated three-floor real structure and a test structure are evaluated in two cases. Two types of ground motion records, one of them is short-distance and lower magnitude GM and the other one is long-distance and higher magnitude GM, are used for the evaluation. The study has focuses on the real structure. The authors state that for both types of seismic action, the value of maximum displacement is not influenced by the vertical component of GM. In addition, the vertical component of ground motion does not change the influence of friction on the response of the isolation system. On the other hand, according to the obtained results from this research, the maximum axial loads acting on isolators non-uniformly increase. Moreover, the probability of occurrence of tensile loads on bearings, which is a situation to be avoided by designers, also increases when the vertical component of ground motions is included [3].

Another work [13], focused on the effects of the vertical acceleration on the response of base-isolated structures with high damping rubber bearings subjected to near-fault ground motions. Mazza and Vulcano evaluate six cases for HRDB. The cases are three different values of fundamental vibration period (T_1= 2s, 3s and 4s) and for each vibration period, two subsoil classes. The results of the research show that the isolators can undergo tensile loads under vertical acceleration. Moreover, it is concluded that the variation of axial loads acting on bearings is evident when the ratio of $PGA_{vertical}$

to PGA $_{horizontal}$ increases [13]. On the other hand, the ductility demand is not influenced by the vertical component of ground motion even if the ratio of peak ground accelerations increases [13].

Another research that evaluates the base-isolated structures subjected to near-fault motions is the study of Petti, Polichetti, Lodato and Palazzo [17]. In this study, a 2D model in MATLAB and a 3D model in SAP2000 are used in order to evaluate the response of FPS under vertical acceleration. The authors state that the results obtained from both models validate each other. Based on the results of the study, when the peak ground acceleration of vertical component of ground motion reaches 1g, the base reactions increase up to almost the double of the case without vertical seismic component. On the other hand, the vertical component of motion has no influence on the relative displacement of FPS [17].

In the study of Rabiei [19], the effects of vertical accelerations on FPS systems are investigated. An idealized three-dimensional single storey structure resting on FPS is used for the evaluation. The record of Tabas earthquake is used for NTHA. According to the results of the study, the error caused by neglecting the vertical component of the motion is approximately 30% for the base shear value however; this error decreases as the fundamental vibration period of structure increases [19].

1.3. Aim and Scope of Work

In Turkey, until Turkish Building Earthquake Code 2019 (TBEC2019) [25] is published, there was not a regulation for seismically isolated structures in seismic codes. In 2019, not only design basis for base isolated structures are included in the earthquake code, but also the selection and scaling procedure of real ground motions for time history analysis are changed. The first major revision about time history analysis is that the designer has to select 11 GMs rather than 7 GMs and use the mean of these GMs in design. The other important revision is that the vertical components of the ground motions have to be taken into consideration when designing an earthquake resistant structure.

In this study, the effects of selecting 11 GMs instead of 7 GMs by considering vertical components of them on seismic response of base isolated structures are investigated. Selected structure for analysis is one of the blocks of a building complex serving as a hospital in Turkey. Isparta is decided to be the seismic region and GMs are selected by using the site-specific response spectrum curve of Isprata. Friction pendulum system (FPS) is chosen as base isolation system. In order to make evaluations, different sets of GMs are created and three different buildings are modelled as two-storey, four-storey and seven-storey structures resting on base isolators. Non-linear time history analysis methods of base isolated systems regulated in TEC2007 [26] and TBEC2019 [25] are compared in terms of

- Base shear
- Peak floor accelerations
- Inter-Storey drift ratios
- Isolation system displacements
- Bending moments of columns and shear walls
- Axial loads acting on isolators

CHAPTER 2

CASE STUDIES

The aim of case studies is to investigate the performance of friction pendulum isolation system (FPS) by using different 3 sets of GMs for buildings having different number of floors. Detailed information about selected ground motions is further explained in section 2.4. One fix based and one base isolated finite element models of each structures having different numbers of storeys namely 2-storey, 4-storey and 7-storey, are prepared for comparison. Structural system descriptions are listed in Table 2.1.

Table 2.1. Structural System Descriptions

ISO2	Base Isolated System with 2 Storeys
ISO4	Base Isolated System with 4 Storeys
ISO7	Base Isolated System with 7 Storeys

Description of selected building and analysis models, method of analysis, seismicity and major characteristics of base isolation systems are discussed on the following sections.

2.1. Description of Building

Selected structure for analysis is one of the blocks of a hospital complex. Identified architectural dimensions are listed in Table 2.2.

2.2. Structural Modelling and Design

Fixed based 7-storey building is modelled as the basic model, and structural models of other ones are generated from the fixed based model of 7-storey building. ProtaStructure2018 software [18] is used to analyze and design the structure.

Element self-weights, additional dead loads and live loads are applied to the slabs by considering the specifications in Design Loads for Buildings (TS498) [23] in accordance with the architectural plan.

Table 2.2. Architectural Dimensions

Plan Dimensions	61.20 m (x direction) 51.20 m (y direction)
Span Lengths	7.90 m (x,y direction) 4.20 m (x,y direction)
Storey Height	4.5 m

Columns and beams are defined as frame elements. In order to avoid prolonged executing times, for definition of shear walls, middle column approach is accepted instead of shell elements. For the same reason, slab loads are transferred to frame beams and slabs are not included physically in analysis models. Foundation is not modelled; column and shear wall bottom joints are assigned as fix restraints.

For dynamic analysis, site-specific response spectrum is used. The structure used in this work is a building in which seismic loads are resisted by frames and coupled structural walls as defined in Turkish Earthquake Code 2007(TEC2007) [26] and Structural Behaviour Factor (R) is decided to be 7 for fixed base systems as required in TEC2007 [26].

Building Code Requirements for Reinforced Concrete (TS500) [24] is followed in order to design the structural elements. Determined element dimensions are presented in Table 2.3.

Table 2.3. Structural Element Dimensions

Typ. Column Size	80x80 cm
Typ. Beam Size	40x75 cm
Typ. Slab Thickness	20 cm
Typ. Shear wall Thickness	40 cm

Dimensions of structural elements of 2-storey and 4-storey systems are directly adopted from 7-storey system, and their structural models are prepared by generating the model of the 7-storey system. Formwork plan of a typical floor is presented in Figure 2.1.

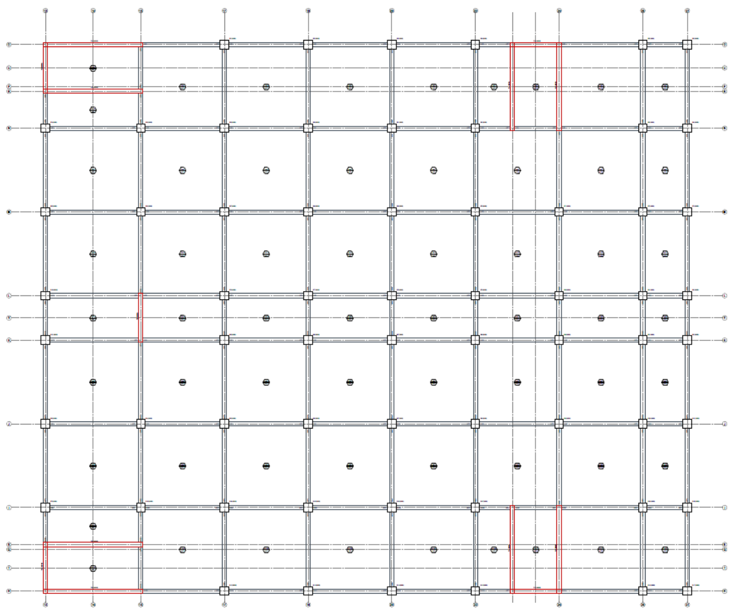

Figure 2.1. Formwork Plan of a Typical Floor of Building

ISO2, ISO4 and ISO7 systems are modelled by defining link elements at the bottoms of structural models of fixed based 2-storey, 4-storey and 7-storey systems, respectively. Link elements represent the base isolators and they are modelled as nonlinear friction isolator type links. Effective Stiffness (K_{eff}) and Effective Damping (β_{eff}) are assigned as linear parameters and Elastic Stiffness (K1), coefficient of friction (μ) and Radius of Curvature (R) values are assigned as nonlinear paroperties of isolators. Nominal values of these parameters are used in analysis. Major characteristics of chosen isolators are explained in detail in section 2.5.

11 ground motions (GM) are determined and defined as time history functions in base isolated models. With these GMs, nonlinear time history load cases are defined for analysis. Information about selected GMs and analysis methods are further explained in parts 2.4 and 2.3, respectively.

Sap2000 V20.0.0 [9] is used for analysis of the systems stated in this chapter. 3D model of ISO7 system is demonstrated in Figure 2.2.

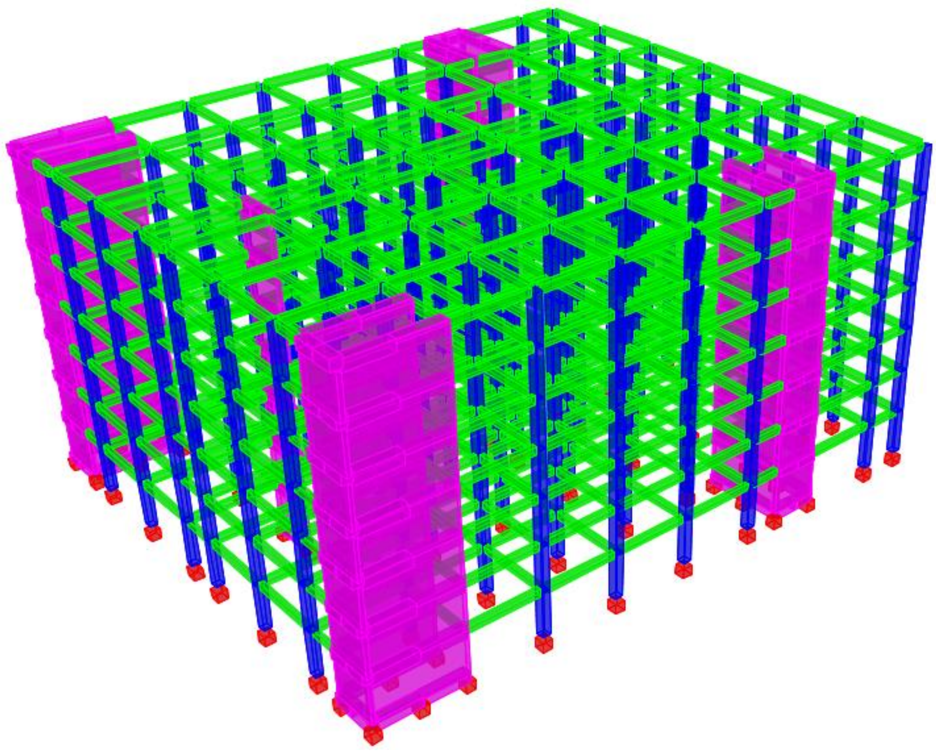

Figure 2.2. 3D Finite Element Model of ISO7 Model

2.3. Analysis Methods

2.3.1. Equivalent Lateral Force (ELF) Procedure

The equivalent lateral force (ELF) procedure of ASCE [4] utilizes the higher effective damping values of base isolated structures in computing the response of the structures by modifying code-specified or site-specific 5%-damped spectra. The effective stress and the effective damping at the calculated displacement are used in order to represent the structure [15].

The design displacement, D_D, is the displacement at the centre of rigidity of the isolation system at DBE motion and it is computed by using Eq. 2.1:

$$D_D = \frac{g S_{D1} T_D}{4\pi^2 B_D} \tag{2.1}$$

where

g = acceleration due to gravity (m/s^2)

S_{D1}= design %5 damped spectral acceleration parameter at 1–second period in units of g

T_D= Effective design period of the isolated structure (seconds)

B_D= Numerical coefficient related to the effective damping of the isolations system at the design displacement, β_D, as set forth in Table 2.4.

$$T_D = 2\pi \sqrt{\frac{W}{K_{Dmin}\, g}} \tag{2.2}$$

where

W = effective seismic weight of the structure above the isolation interface (kN)

K_{Dmin}= effective stiffness of the isolation system at the design displacement in horizontal direction (kN/m)

Table 2.4. Damping Coefficient, BD or BM

Effective Damping, β_D or β_M (percentage of critical)	B_D or B_M Factor
≤2	0.8
5	1.0
10	1.2
20	1.5
30	1.7
40	1.9
≥50	2.0

The total design displacement, D_{TD}, is computed with Eq.2.3:

$$D_{TD} = D_D \left(1 + y \frac{12e}{b^2 + e^2}\right) \tag{2.3}$$

where

D_D = design displacement at centre of rigidity of the isolation system

y= the distance between the centres of rigidity of the isolated system and the element of interest measured perpendicular to the seismic loading under consideration

e= the actual eccentricity measured in plan between the centre of mass of the structure above the isolation interface and the centre of rigidity of the isolation system, plus accidental eccentricity, taken as %5 of the longest plan dimension of the structure perpendicular to the direction of force under consideration

b= the shortest plan dimension of the structure measured perpendicular to d

d= the longest plan dimension of the structure

Plan dimensions that are used for calculation of total design displacement are demonstrated in Figure 2.3.

The minimum lateral seismic shear force that the structure above the isolation is given by the Eq.2.4:

$$V_s = K_{D,max} D_D \tag{2.4}$$

where $K_{D,max}$ is the maximum effective stiffness of the isolation system.

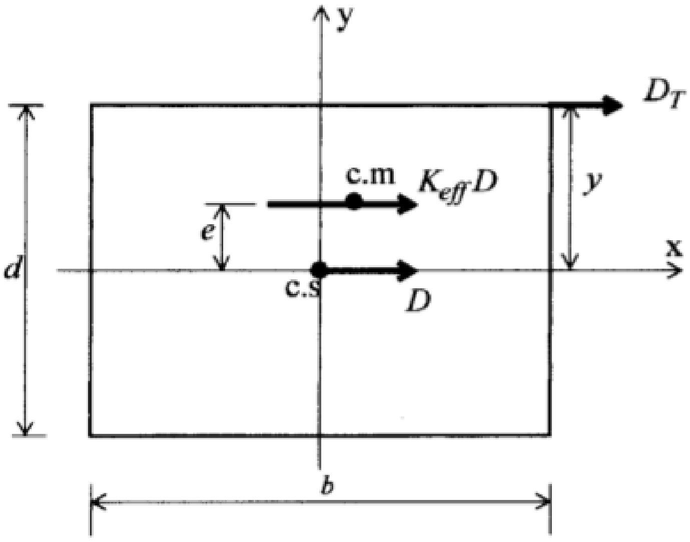

Figure 2.3. Plan Dimensions for Calculation of DTD [14]

The shear force should be distributed over the height of the structure. Lateral force at level x, F_x, is computed by using Eq.2.5:

$$F_x = \frac{V_S h_x w_x}{\sum_{i=1}^{n} w_i h_i} \tag{2.5}$$

where

w_x= portion of that is located at level x

h_x= height above the base of level x

2.3.2. Response Spectrum Analysis (RSA)

%5 damped site-specific spectrum is used for the response spectrum analysis. Although only the use of the spectrum in the horizontal direction is required in TEC2007 [26], Turkish Building Earthquake Code 2019 (TBEC2019) [25] involves the use of the vertical spectrum in RSA. In this study, RSA analyses are performed for FB7 system in order to design the structure.

2.3.3. Nonlinear Time History Analysis (NTHA)

Nonlinear time history analysis is used to investigate the performance of seismic isolation under horizontal and vertical seismic forces. TEC2007 [26] states:

"In linear and nonlinear analysis, in case of using three ground motions the maximum of results, and in case of using at least seven ground motions average of results shall be taken for the design."

However, TBEC2019 [25] requires selecting eleven GMs instead of seven GMs for time history analysis. Moreover, while only horizontal components of GMs are included in analysis according to TEC2007, TBEC2019 requires the consideration of vertical components of GMs for analysis.

In this study, isolated system models are analysed by using three different sets of GMs for comparison. Set 1 consists of 7 ground motions having two horizontal ground motion acceleration components. Set 2 contains 11 ground motions having two horizontal ground motion acceleration components. Set 3 consists of 11 ground motions having two horizontal and one vertical ground motion acceleration components. The results of three different sets are presented in detail in Chapter 3.

2.4. Seismicity

For the analysis in this work, Design Basis Earthquake (DBE) is used for evaluations of the structures. Isparta, which is in the first-degree seismic zone of Turkey, is selected as the seismic region for this study. Probabilistic Seismic Hazard Assessment (PSHA) for Isparta has been used to obtain the SRSS horizontal target response spectrum curve of DBE level earthquake. For non-linear time history analysis, time histories are selected and scaled based on the site-specific spectrum. Vertical response spectrum curve has been obtained from TEC2007 [23]. Response spectrum curve of DBE level earthquake for Isparta that has been obtained from PSHA is presented in Figure 2.4. Related spectral acceleration values for specific periods are demonstrated in Table 2.5 and Table 2.6.

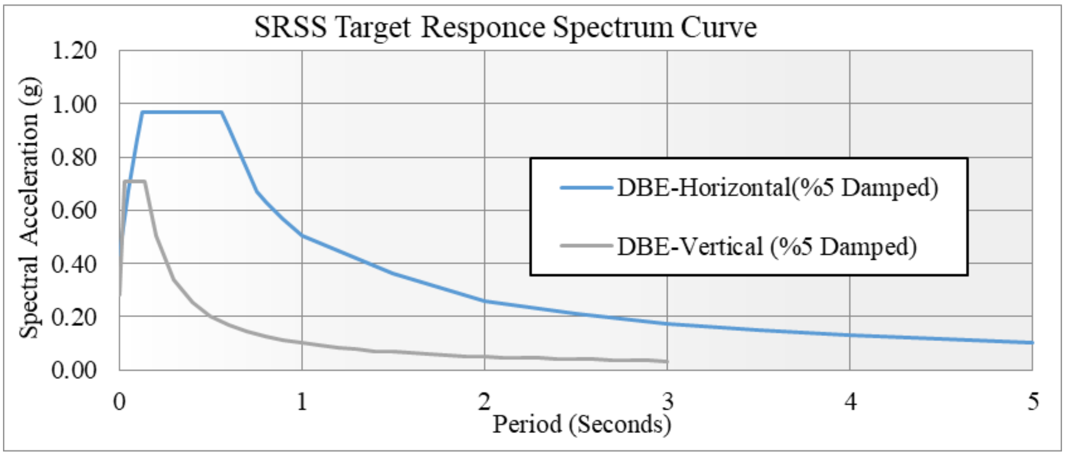

Figure 2.4. Site Specific SRSS Response Spectra for Isparta (%5 Damped)

Table 2.5. Site Specific Horizontal SRSS Spectral Accelerations for Isparta

(%5 Damped)

Period (s)	**Sa (g)**
0	0.4329
0.05	0.6753
0.1	0.8703
0.105	0.8922
0.128	0.9677
0.2	0.968
0.3	0.968
0.4	0.968
0.5	0.968
0.562	0.968
0.6	0.9073
0.9	0.5647
1	0.505
2	0.2603
3	0.1733
4	0.1293

Table 2.6. Site Specific Vertical SRSS Spectral Accelerations for Isparta

(%5 Damped)

Period (s)	**Sa (g)**
0	0.284
0.028606	0.709
0.14303	0.709
0.2	0.507
0.3	0.338
0.4	0.254
0.5	0.203
0.6	0.169
0.7	0.145
0.8	0.127
0.9	0.113
1	0.101
1.5	0.068
2	0.051
2.5	0.041
3	0.034

2.4.1. Selecting and Scaling Procedure of Ground Motion Records

In this study, the total of 11 ground motions is selected and scaled based on site-specific target spectrum. These 11 ground motions are separated into three different sets for comparison as stated previously in part 2.3. Shear wave velocity (Vs_{30}), type of mechanism, fault distance parameters and soil conditions are considered for selecting procedure [5]. Site Specific Probabilistic Seismic Hazard Analysis for Isparta [16] is used for getting information about these seismic parameters. Selected ground motions are listed in Table 2.7.

Time history plots in three directions are provided in Figures 2.5 to 2.37.

Table 2.7. Selected Ground Motion Records

Record #	Event	Mag	Mechanism	Rjb(km)	Vs30 (m/s)	PGA (g)	PGV (cm/s)
15	Kern County	7.36	Reverse	38.42	385.43	0.217	21.909
68	San Fernando	6.61	Reverse	22.77	316.46	0.227	22.104
187	Imperial Valley-06	6.53	strike slip	12.69	348.69	0.218	21.341
731	Loma Prieta	6.93	Reverse Oblique	41.71	391.91	0.110	25.517
826	Cape Mendocino	7.01	Reverse	40.23	337.46	0.192	28.503
880	Landers	7.28	strike slip	26.96	355.42	0.139	15.367
900	Landers	7.28	strike slip	23.62	353.63	0.246	55.942
987	Northridge-01	6.69	Reverse	20.36	321.91	0.449	26.484
1762	Hector Mine	7.13	strike slip	41.81	382.93	0.210	28.370
3749	Cape Mendocino	7.01	Reverse	16.54	355.18	0.409	38.946
6893	Darfield, New Zealand	7	strike slip	11.86	344.02	0.490	46.749

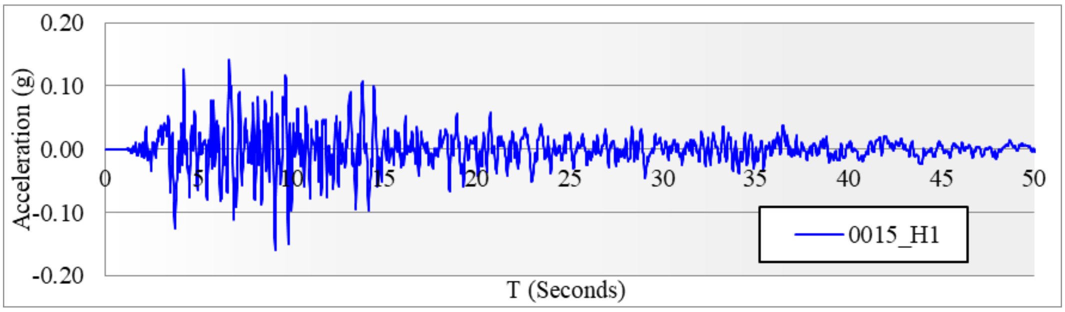

Figure 2.5. Horizontal-1 Component of GM0015

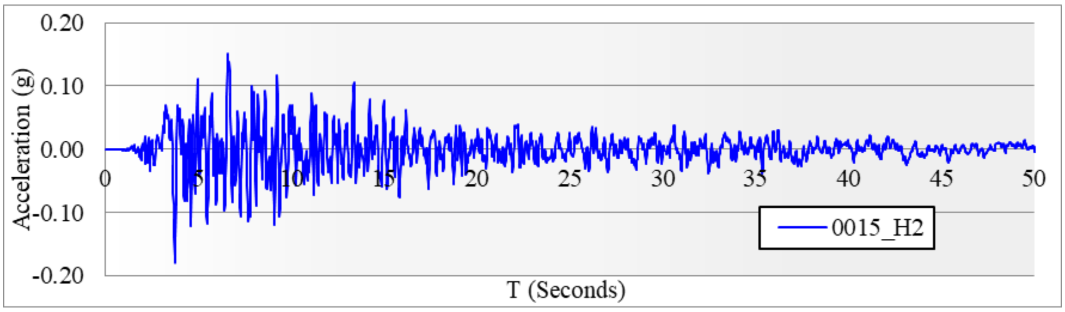

Figure 2.6. Horizontal-2 Component of GM0015

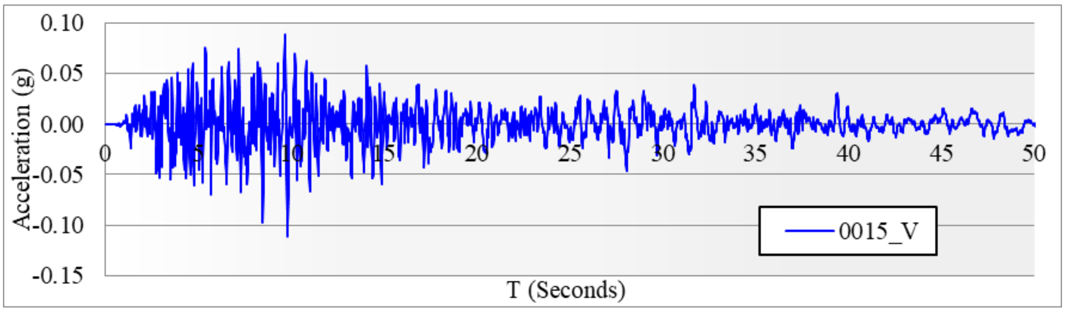

Figure 2.7. Vertical Component of GM0015

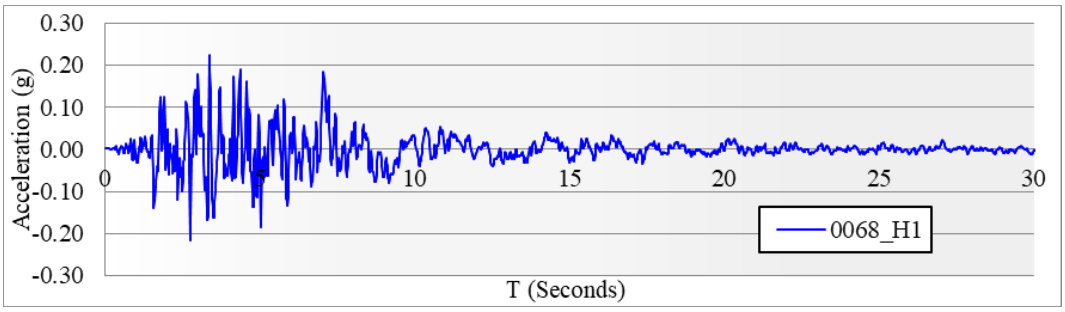

Figure 2.8. Horizontal-1 Component of GM0068

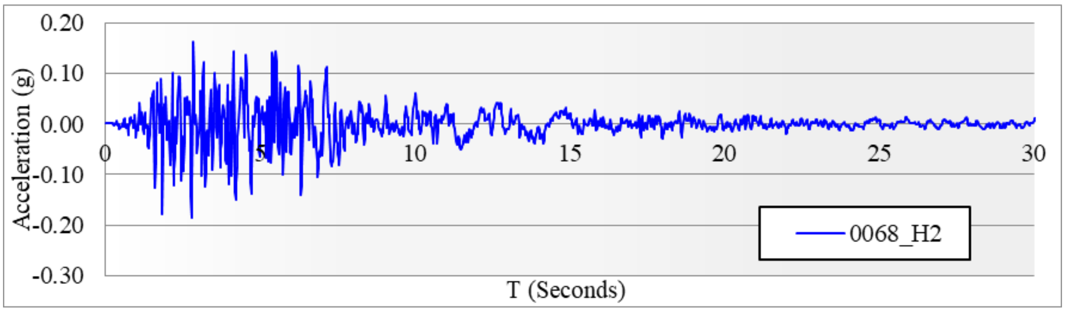

Figure 2.9. Horizontal-2 Component of GM0068

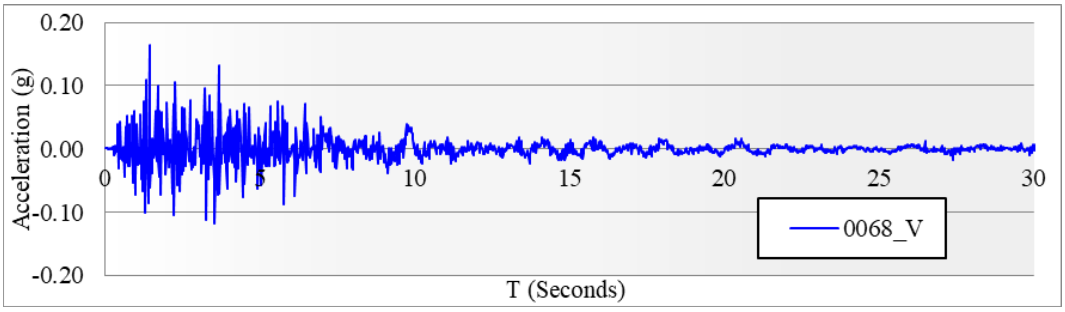

Figure 2.10. Vertical Component of GM0068

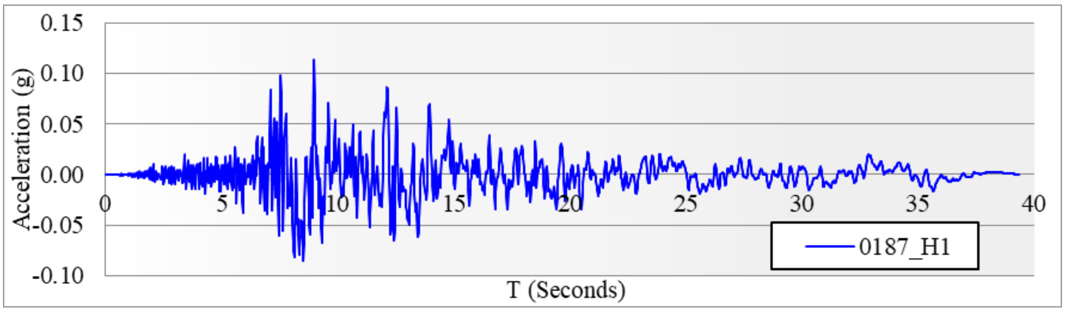

Figure 2.11. Horizontal-1 Component of GM0187

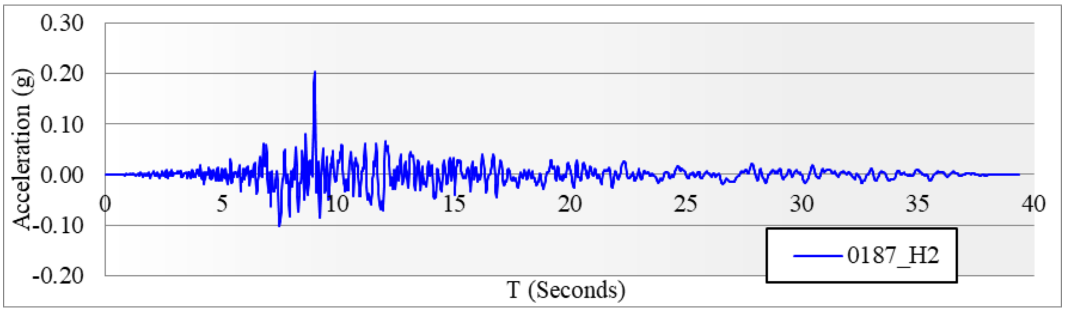

Figure 2.12. Horizontal-2 Component of GM0187

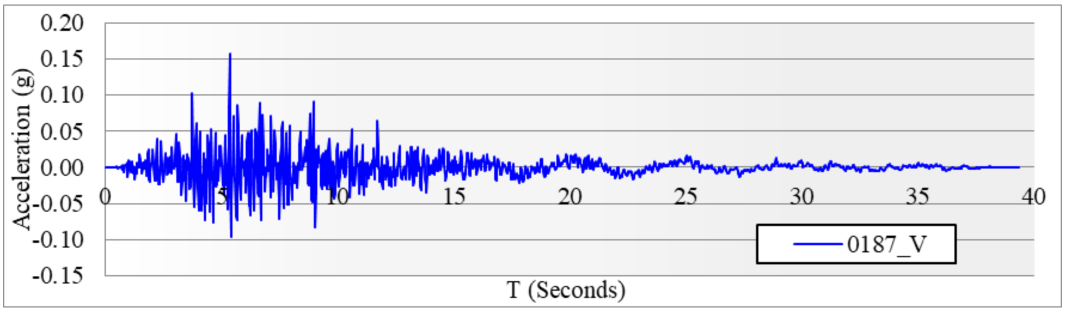

Figure 2.13. Vertical Component of GM0187

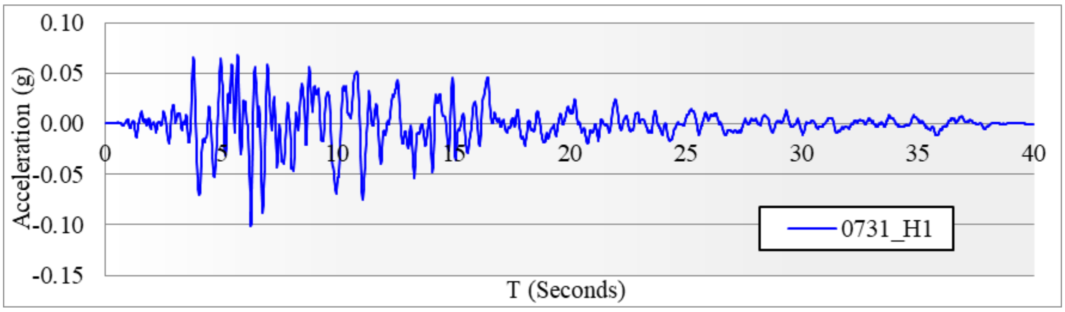

Figure 2.14 Horizontal-1 Component of GM0731

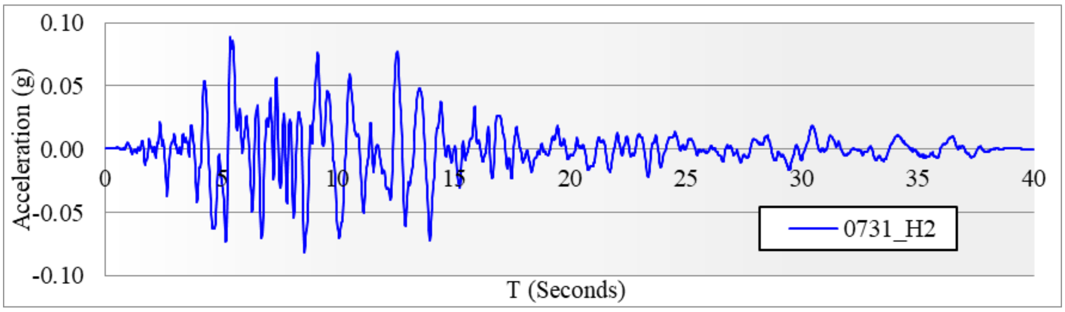

Figure 2.15. Horizontal-2 Component of GM0731

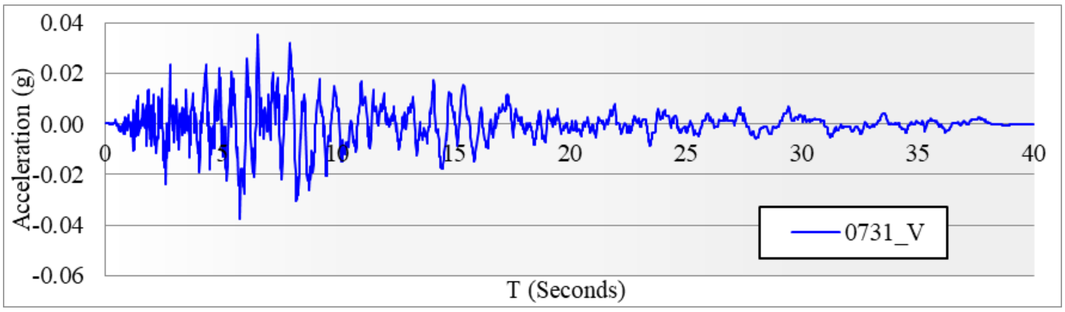

Figure 2.16. Vertical Component of GM0731

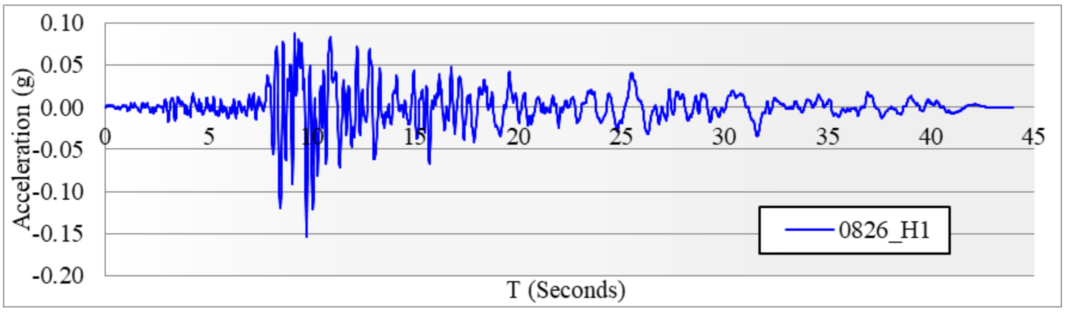

Figure 2.17. Horizontal-1 Component of GM0826

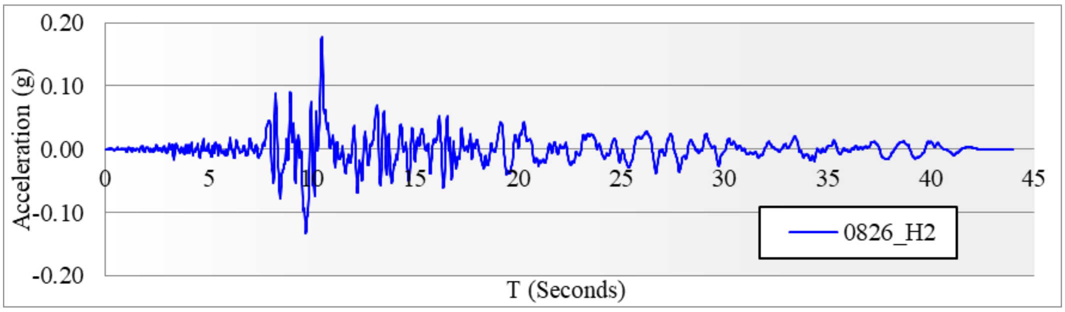

Figure 2.18. Horizontal-2 Component of GM0826

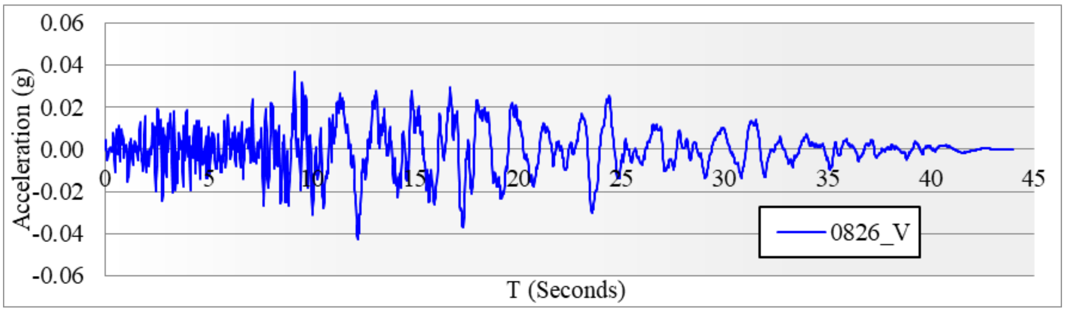

Figure 2.19. Vertical Component of GM0826

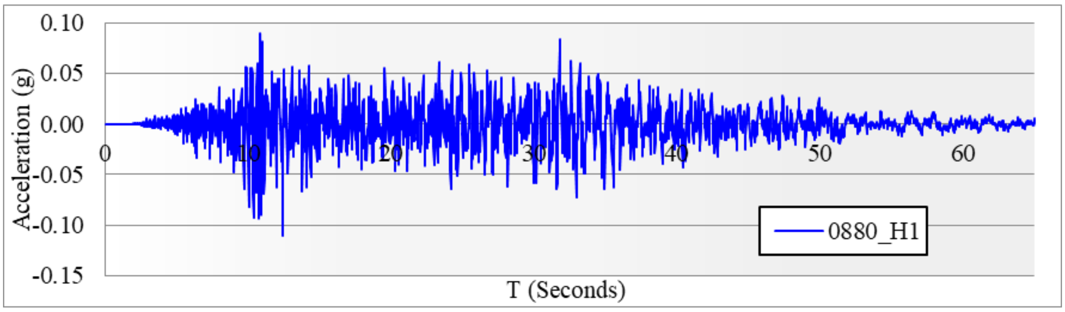

Figure 2.20. Horizontal-1 Component of GM0880

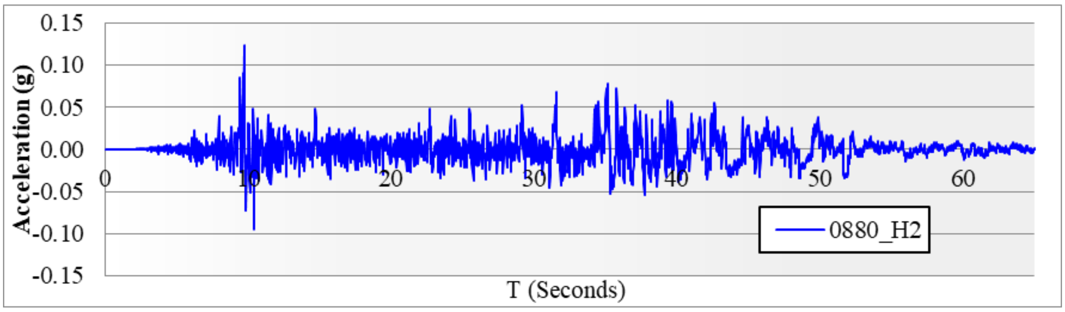

Figure 2.21. Horizontal-2 Component of GM0880

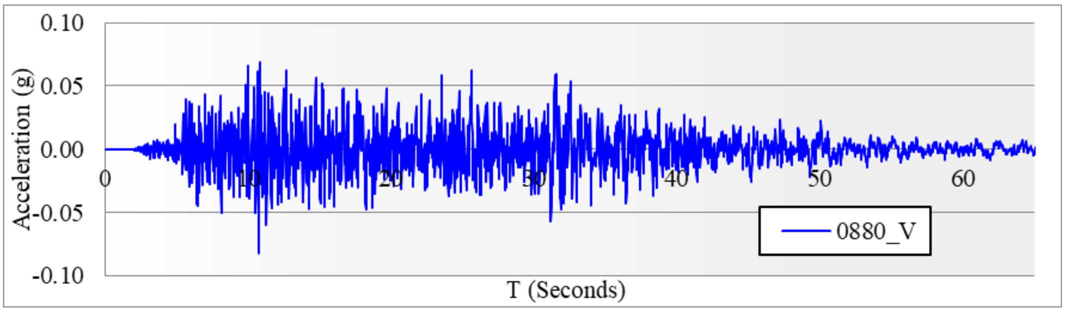

Figure 2.22. Vertical Component of GM0880

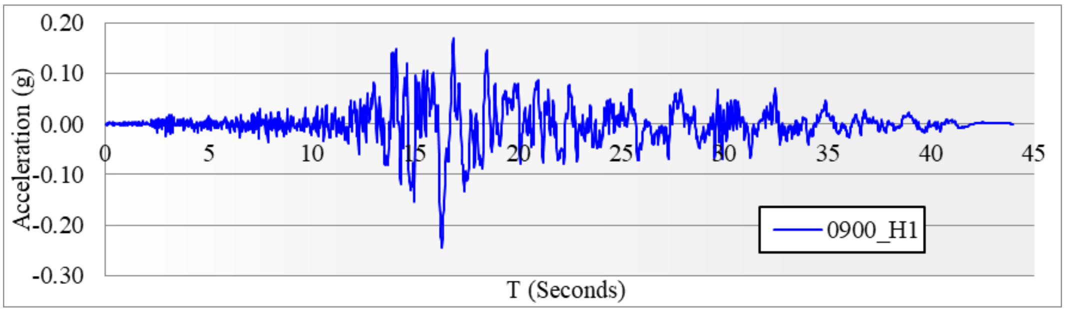

Figure 2.23. Horizontal-1 Component of GM0900

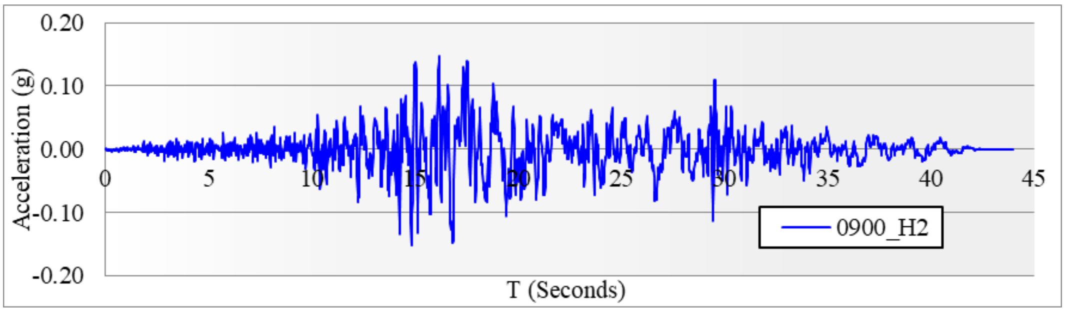

Figure 2.24. Horizontal-2 Component of GM0900

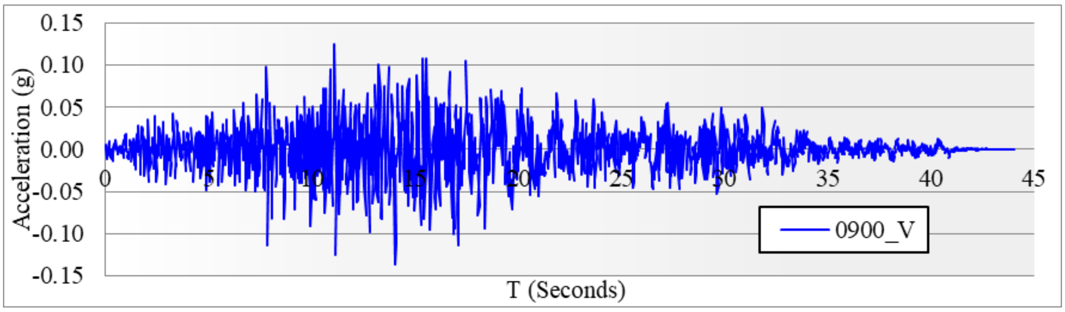

Figure 2.25. Vertical Component of GM0900

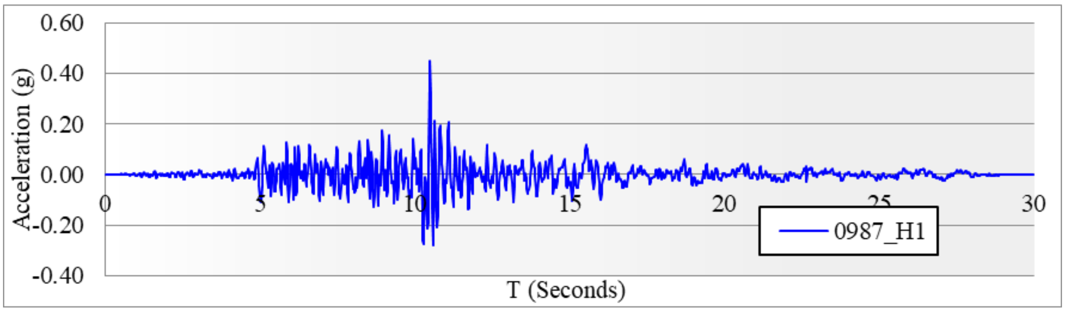

Figure 2.26. Horizontal-1 Component of GM0987

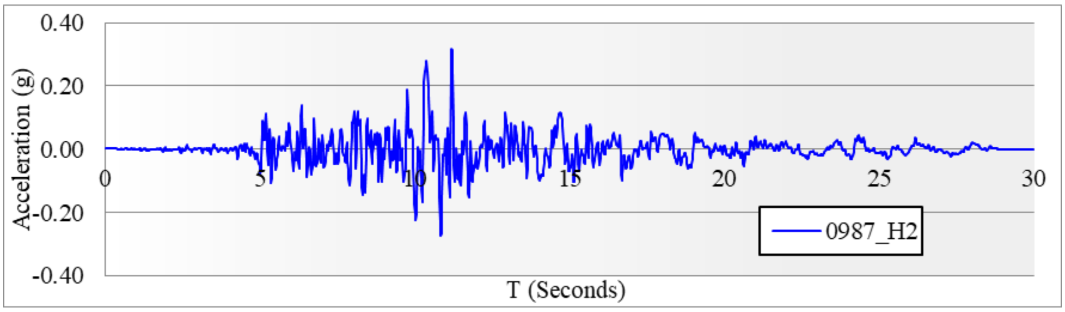

Figure 2.27. Horizontal-2 Component of GM0987

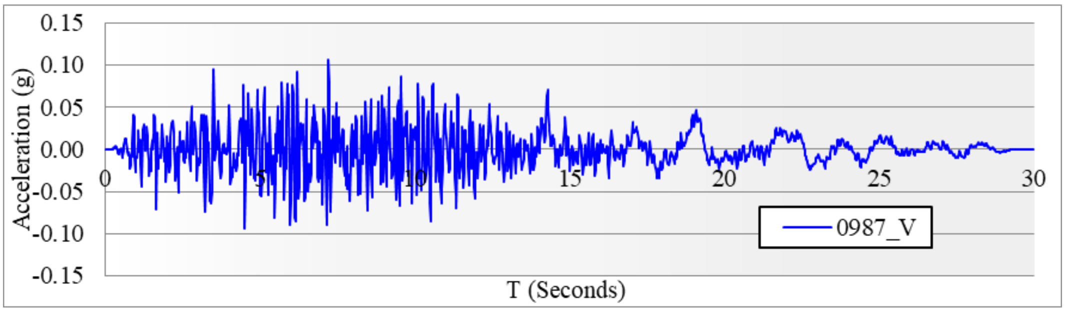

Figure 2.28. Vertical Component of GM0987

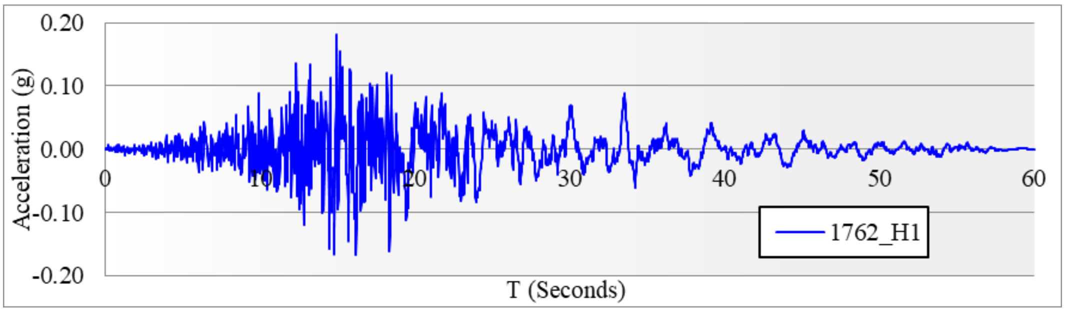

Figure 2.29. Horizontal-1 Component of GM1762

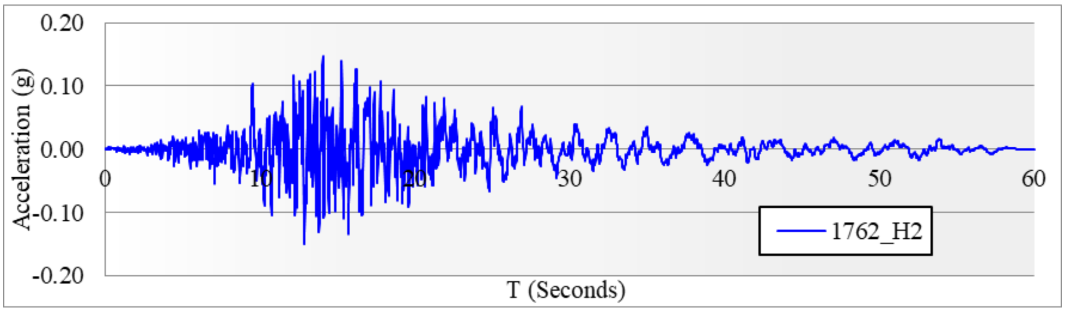

Figure 2.30. Horizontal-2 Component of GM1762

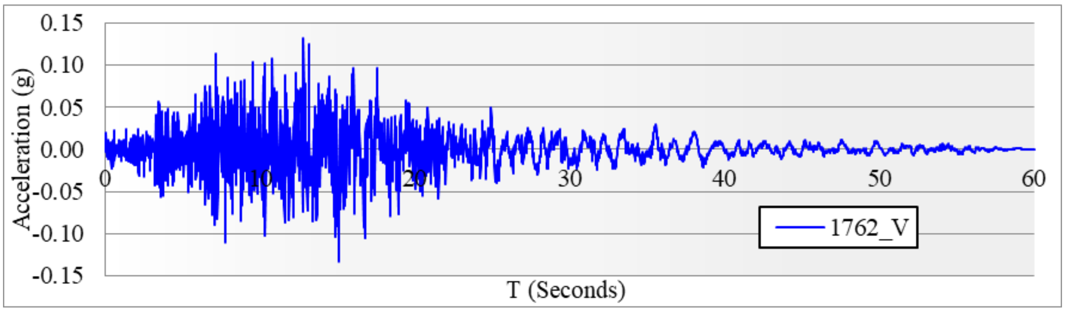

Figure 2.31. Vertical Component of GM1762

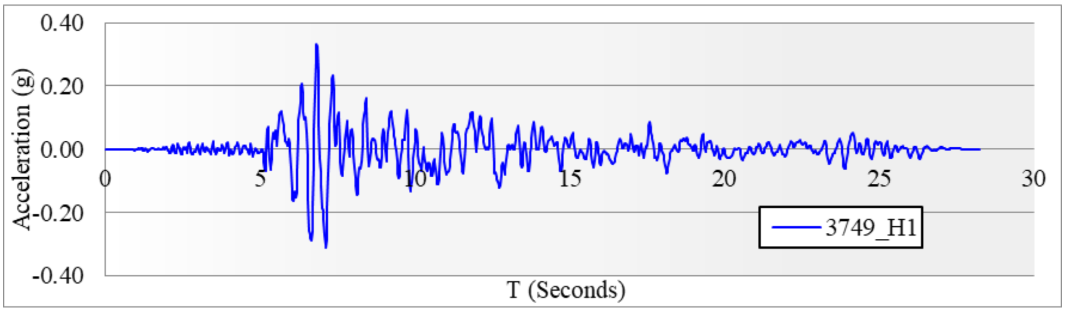

Figure 2.32. Horizontal-1 Component of GM3749

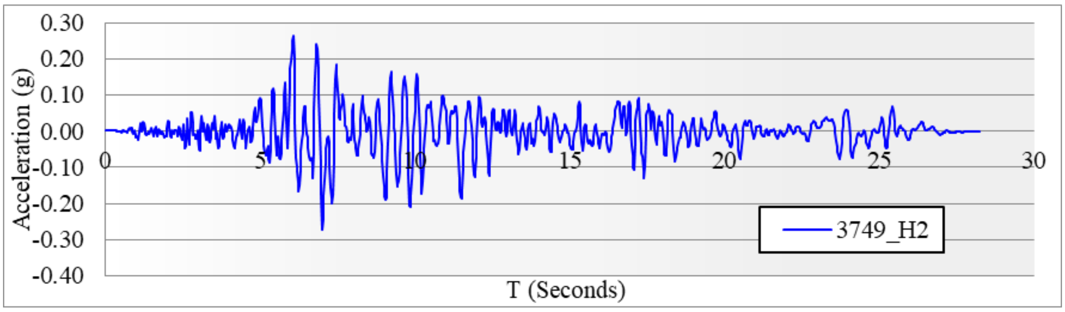

Figure 2.33. Horizontal-2 Component of GM3749

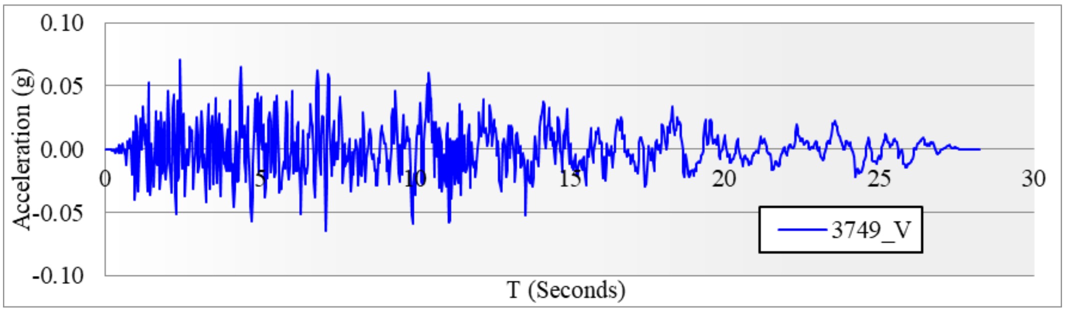

Figure 2.34. Vertical Component of GM3749

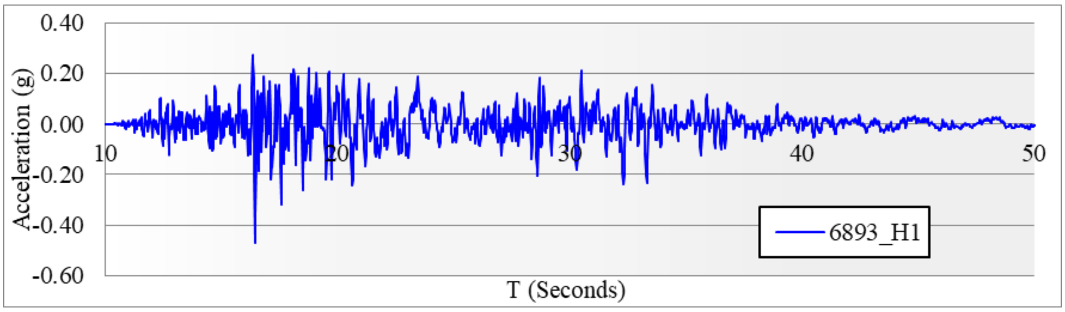

Figure 2.35. Horizontal-1 Component of GM6893

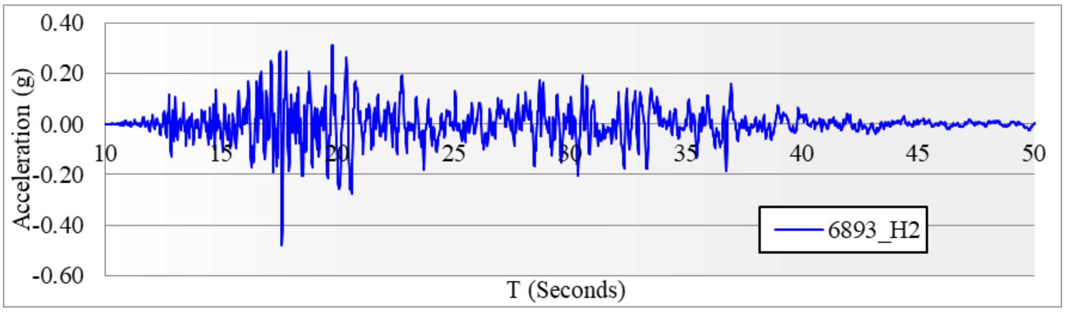

Figure 2.36. Horizontal-2 Component of GM6893

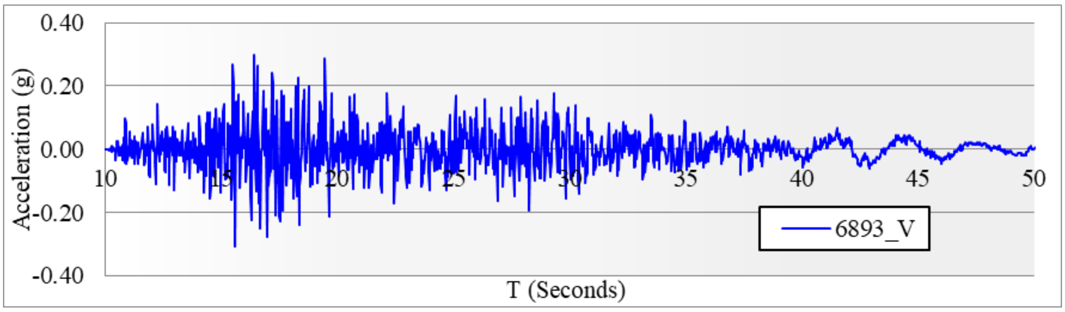

Figure 2.37. Vertical Component of GM6893

Scaling is performed in accordance with the procedure described in [5]. Scale factors are determined such that the average SRSS spectra from all horizontal component pairs do not fall below the corresponding value of the target response spectrum between $0.5T_d$ and $1.25T_m$ periods for all sets. Vertical components are scaled with respect to the determined scale factors for horizontal components. T_d is the natural period of vibration of the isolated structure at design displacement and T_m is the natural period of vibration of the isolated building at maximum displacement. Design displacement is determined at DBE level motion, which has %10 probability of exceedance in 50 years. Maximum displacement is determined at MCE level motion, which has %2 probability of exceedance in 50 years. T_d and T_m are *2.80 sec* and *3.50 sec*, respectively for this study. Therefore, scaling is between the periods of *1.40 sec* and 4*.375 sec*. Scale factors for 11-ground motion records are listed in Table 2.8, and scaled spectrums are presented in Figure 2.38. GMs 0015, 0068, 0187,0731,0880,900,3749 are included in Set1 and all 11 GMs are included in Set 2 & Set3. Arithmetic means of scaled SRSS response spectrums of all GMs sets & site-specific target spectrum in scaling period range are provided in Figure 2.39.

Table 2.8. Scale Factors of Selected Ground Motion Records

Record #	Scale Factor
15	2.7932
68	1.8525
187	1.9019
731	1.9892
826	1.3298
880	2.7831
900	1.2755
987	1.8974
1762	1.1434
3749	0.9631
6893	1.2881

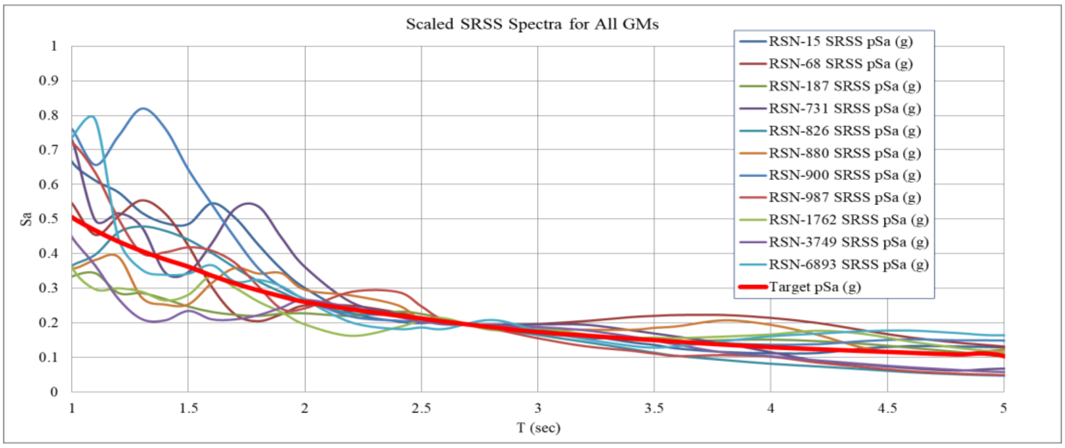

Figure 2.38. Selected SRSS Response Spectra of All GM Records & Site-Specific Target Spectrum (%5 Damped) in Scaling Period Range

2.5. Seismic Isolation System Design

In this thesis, all case studies are carried out at the DBE level earthquake.

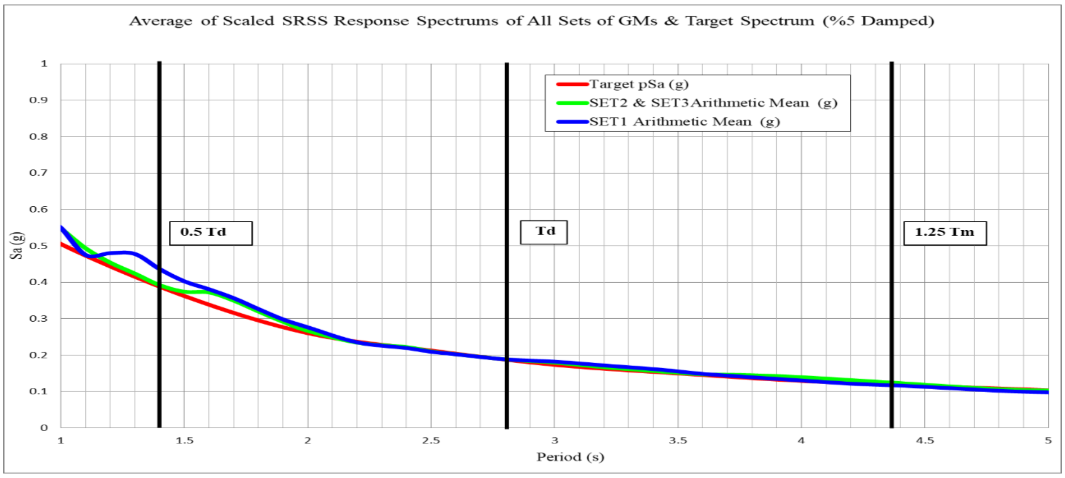

Figure 2.39. Average of Scaled SRSS Response Spectrums of All GM Sets & Site-Specific Target Spectrum (%5 Damped) in Scaling Period Range

2.5.1. Estimation of Lateral Displacements

The isolation system is designed and constructed to withstand target lateral displacement determined at the DBE motion (D_D). D_D is calculated using Eq.2.1. Numerical coefficient related to effective damping is accepted as 1.7 for this part. It is further calculated in part 2.6.

Site-specific displacement spectrum is computed from Eq.2.6:

$$PSD = S_A\left(\frac{T}{2\pi}\right)^2 \tag{2.6}$$

%5 damped SRSS displacement spectrum is demonstrated in Figure 2.40 and related spectral displacement values for specific periods are listed in Table 2.10.

Design displacement is calculated as *0.207 m*. The spectral period corresponding *0.207 m* displacement is around *2.80 sec*. when the reduction for damping of the device is applied.

The spectral acceleration is around *0.19g* at *2.80 sec.* period in Isparta. The spectral acceleration value corresponding the period of *2.80 sec.* will decrease to around

0.12 g with the help of the damping of the device. *2.80 sec* effective period is found appropriate not to exceed maximum allowable base shear of *0.2g* [22].

The minimum effective stiffness (k_{dmin}) of ISO2, ISO4 and ISO7 systems are determined using the effective design period and Eq.2.2. Target design values calculated in this part for isolated systems are listed in Table 2.9.

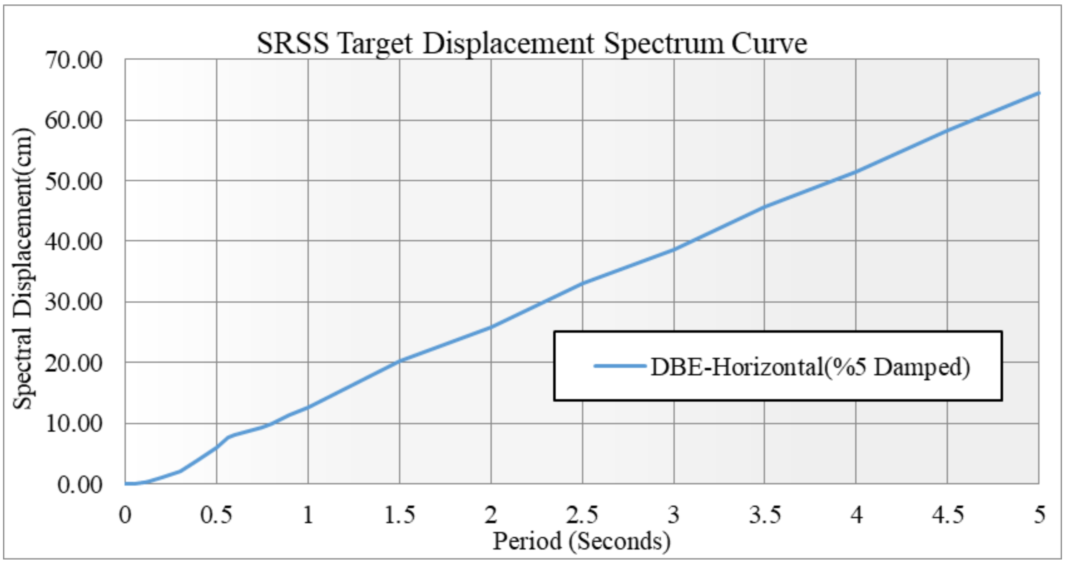

Figure 2.40. Site Specific SRSS Displacement Spectrum for Isparta (%5 Damped)

Table 2.9. Target Design Values for Isolated Structural Systems

Structural System	T_D (sec)	D_D (m)	kdmin(kN/mm)
ISO2	2.80	0.207	56275
ISO4	2.80	0.207	112550
ISO7	2.80	0.207	187900

2.5.2. Mechanical Characteristics of Isolators

The main mechanical characteristics of friction pendulum isolators are the radius of curvature (R) and coefficient of friction (μ). The effective stiffness, R and μ of isolators are determined by using Eq.2.7 in accordance with previously calculated $k_{d,min}$ values. The friction coefficient and radius of curvature are determined by remaining within limits required in [22]. The lower boundary conditions are 3 meters and 0.03; the upper boundary conditions are 6 meters and 0.06, for R and μ, respectively.

Table 2.10. SRSS Spectral Displacement Values (%5 Damped)

Period (s)	PSD
0	0
0.05	0.04195
0.1	0.21626
0.105	0.24443
0.128	0.39398
0.2	0.96215
0.4	3.84862
0.562	7.59726
0.6	8.11639
0.75	9.35239
0.8	10.0366
1	12.5488
1.5	20.2563
2	25.8728
2.5	33.0337
3	38.757
3.5	45.5992
4	51.4077
4.5	58.32
5	64.4832

$$K_{eff} = \frac{W}{R} + \frac{\mu W}{D_D} \tag{2.7}$$

where

W = Seismic Weight of Structure (kN)

R= Radius of Curvature (m)

μ= Friction coefficient

D_D= Target Lateral Displacement (m)

The effective damping (β_{eff}) is calculated with Eq. 2.8:

$$\beta_{eff} = \frac{2}{\pi} \frac{\mu}{{D_D}/{R} + \mu} \tag{2.8}$$

where

R= Radius of Curvature (m)

μ= Friction coefficient

D_{D}= Target Lateral Displacement (m)

Effective damping value is limited with %30. Damping coefficient factor (β) is determined by using Table 2.4.

There are 62 isolators located in each individual system (ISO7, ISO4 and ISO2). According to the seismic weight that they carry, these 62 isolators are divided into 2 groups for ISO2 and 3 groups for ISO4 and ISO7. Nonlinear nominal characteristics of all types of isolators located in each three systems are presented in Figures 2.41 to 2.48 individually.

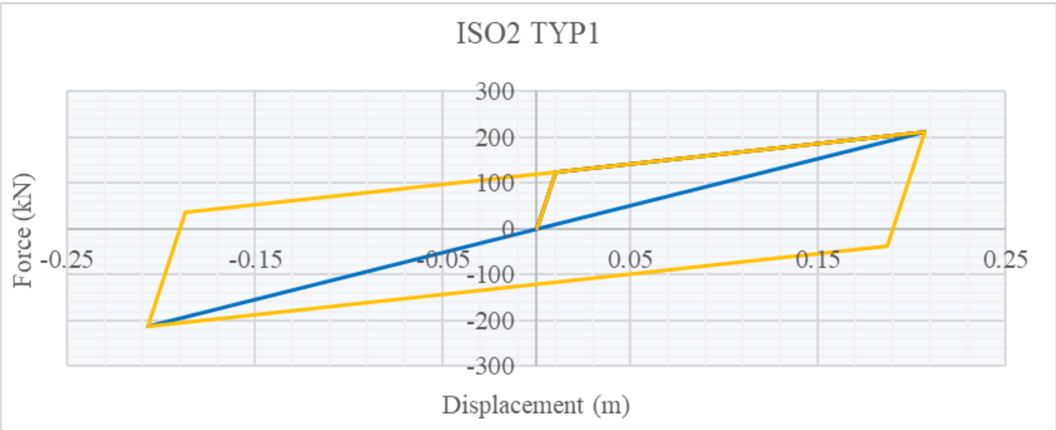

Figure 2.41. Nonlinear Nominal Properties of TYP1 Isolator for ISO2

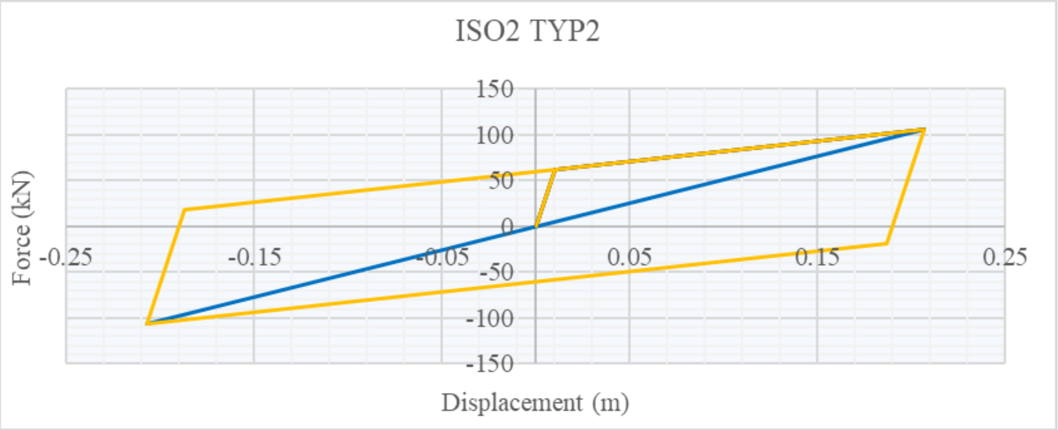

Figure 2.42. Nonlinear Nominal Properties of TYP2 Isolator for ISO2

Table 2.11. Mechanical Characteristics of the Isolators Located in ISO2 System (a)

Isolator Typ.	Average Vertical Load(kN)	Radius of Curvature (R) (m)	Friction Coefficient (μ)
1	2000	4.5	0.06
2	1000	4.5	0.06

Table 2.12. Mechanical Characteristics of the Isolators Located in ISO2 System (b)

Isolator Typ.	Effective Stiffness (kN/m)	Effective Damping (%)	Damping Coefficient (β)	Elastic Stiffness K1 (kN/m)	Post Yield Stiffness K2 (kN/m)
1	1030	34 (30) [13]	1.7	12444	444
2	515	34 (30) [13]	1.7	6222	222

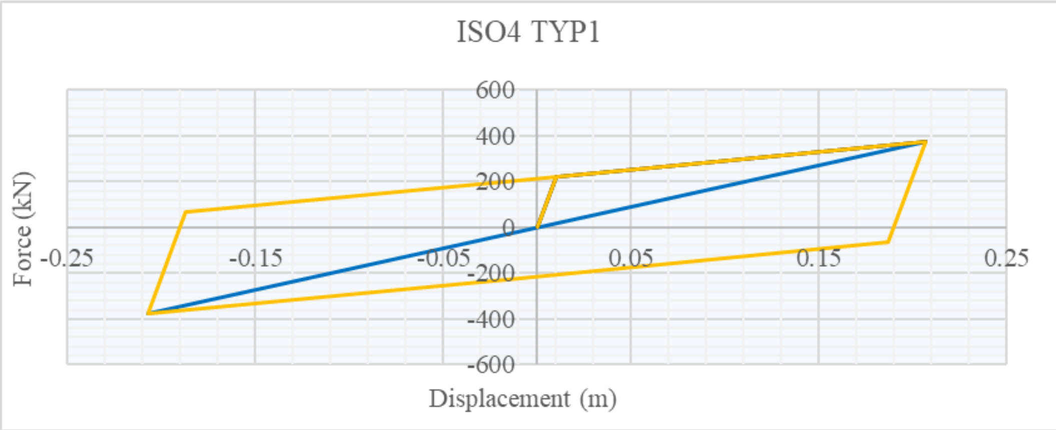

Figure 2.43. Nonlinear Nominal Properties of TYP1 Isolator for ISO4

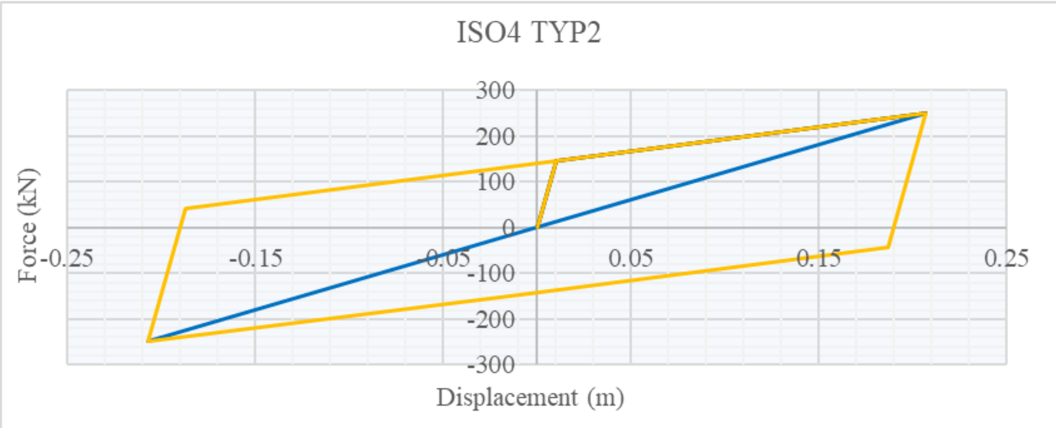

Figure 2.44. Nonlinear Nominal Properties of TYP2 Isolator for ISO4

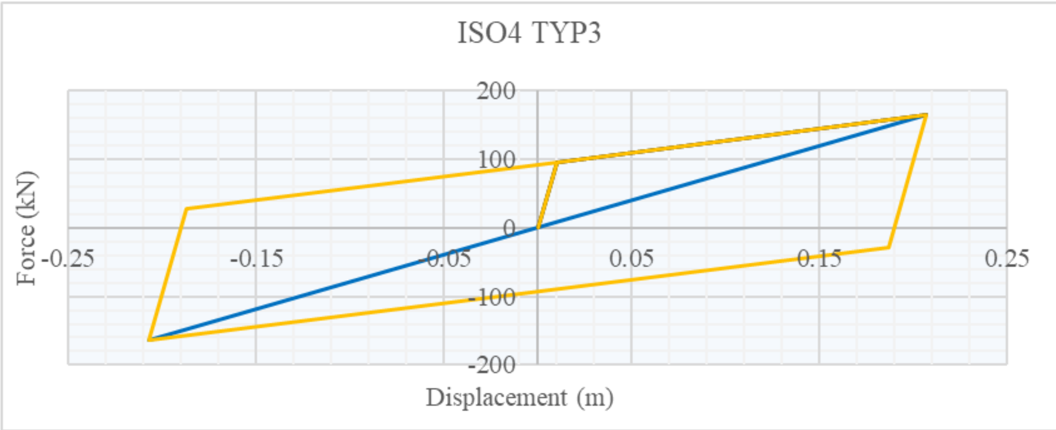

Figure 2.45. Nonlinear Nominal Properties of TYP3 Isolator for ISO4

Table 2.13. Mechanical Characteristics of the Isolators Located in ISO4 System (a)

Isolator Typ.	Average Vertical Load(kN)	Radius of Curvature (R)(m)	Friction Coefficient (μ)
1	3550	4.5	0.06
2	2350	4.5	0.06
3	1550	4.5	0.06

Table 2.14. Mechanical Characteristics of the Isolators Located in ISO4 System (b)

Isolator Typ.	Effective Stiffness (kN/m)	Effective Damping (%)	Damping Coefficient (β)	Elastic Stiffness K1 (kN/m)	Post Yield Stiffness K2 (kN/m)
1	1830	34 (30) [13]	1.7	22089	789
2	1210	34 (30) [13]	1.7	14622	522
3	800	34 (30) [13]	1.7	9644	344

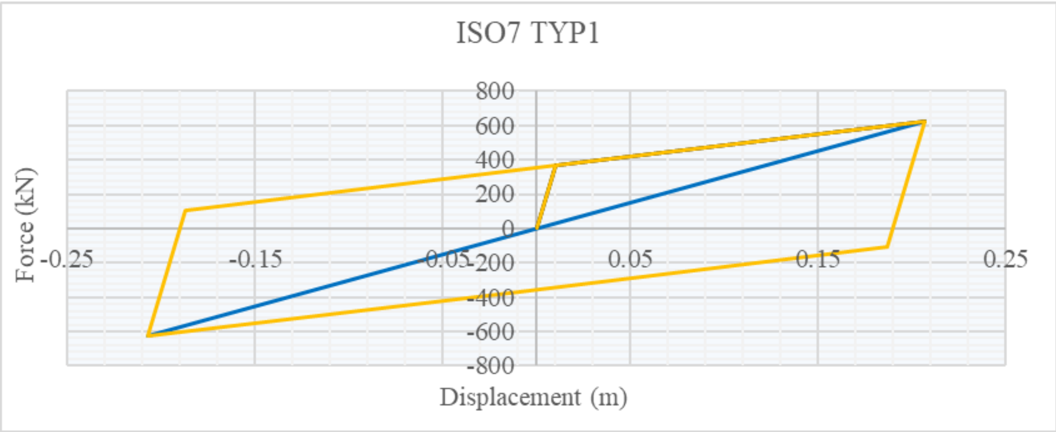

Figure 2.46. Nonlinear Nominal Properties of TYP1 Isolator for ISO7

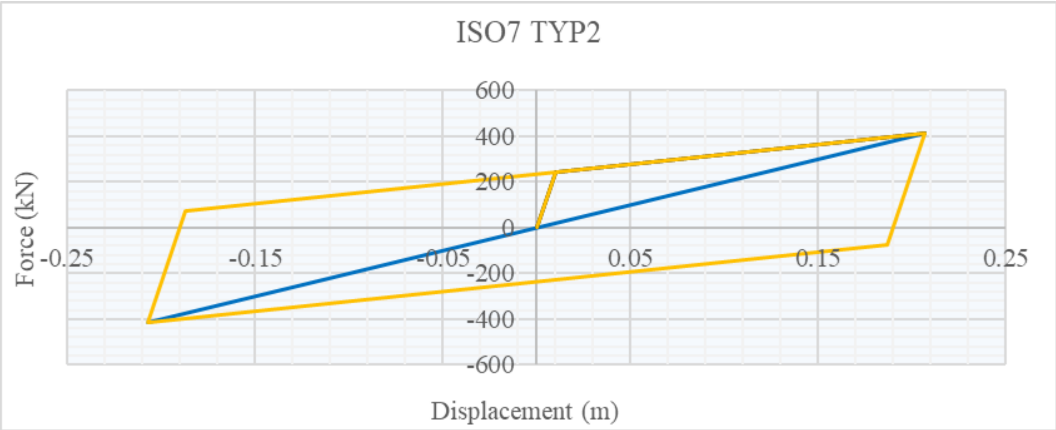

Figure 2.47. Nonlinear Nominal Properties of TYP2 Isolator for ISO7

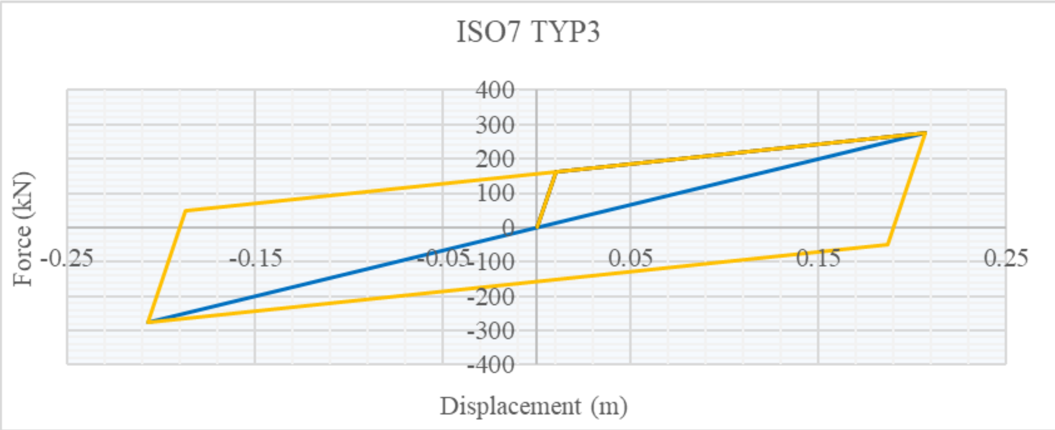

Figure 2.48. Nonlinear Nominal Properties of TYP3 Isolator for ISO7

Table 2.15. Mechanical Characteristics of the Isolators Located in ISO7 System (a)

Isolator Typ.	Average Vertical Load(kN)	Radius of Curvature (R) (m)	Friction Coefficient (μ)
1	5900	4.5	0.06
2	3900	4.5	0.06
3	2600	4.5	0.06

Table 2.16. Mechanical Characteristics of the Isolators Located in ISO7 System (b)

Isolator Typ.	Effective Stiffness (kN/m)	Effective Damping (%)	Damping Coefficient (β)	Elastic Stiffness K1 (kN/m)	Post Yield Stiffness K2 (kN/m)
1	3030	34 (30) [13]	1.7	36711	1311
2	2000	34 (30) [13]	1.7	24267	867
3	1350	34 (30) [13]	1.7	16178	578

CHAPTER 3

STRUCTURAL ANALYSIS

In this chapter, five parameters listed in Table 3.1 are evaluated to specify the behaviours of structures under selected ground motions.

Table 3.1. Parameters to be Evaluated in Analysis

Base Shear Values
Peak Floor Accelerations (PFA)
Inter-storey Drift Ratio (IDR)
Isolator Displacements (ISD)
Bending Moment Values of Columns and Shear Walls
Axial Loads on Isolators

For non-linear time history analysis, 22 different direct integration time history load cases, eleven of them contain horizontal components of ground motions only and the remaining eleven contain both horizontal and vertical components of ground motions, are used for evaluation. As discussed in detail in part 2.4., related ground motions are divided into three sets and mean results of these sets are evaluated. GMs included in the groups are listed in Table 3.2.

Base shear is the maximum lateral force at the base of the structure due to the seismic forces.

Peak Floor Acceleration (PFA) is the maximum absolute acceleration occurred at each floor of the structure. Acceleration values are determined from the geometric centres of the floors. The limitation of floor acceleration is 0.2g as specified in [22] for base isolated structures.

Inter-Storey Drift Ratio (IDR %) is a parameter calculated by dividing the displacement of two consecutive floors with the storey height. Storey displacements are determined from the geometric centres of the floors. This value is multiplied with the modification factor if reduction factor is used on seismic forces, for fixed based structures, the limitation of IDR is 0.2% [25] and for base isolated buildings, the limitation is specified as 0.5% and 1.5% in [22] and [4] respectively.

Table 3.2. Sets of GMs Used in NTHA

Set 1	GM0015, GM0068, GM0187, GM0731, GM0880, GM900, GM3749 (Horizontal components in x and y direction only)
Set 2	GM0015, GM0068, GM0187, GM0731, GM0826, GM0880, GM900, GM987, GM1762, GM3749, GM6983 (Horizontal components in x and y direction only)
Set 3	GM0015, GM0068, GM0187, GM0731, GM0826, GM0880, GM900, GM987, GM1762, GM3749, GM6983 (Horizontal components in x and y direction and vertical component)

Moreover, for base isolated buildings, isolator displacements and axial loads acting on isolators are evaluated. Because the isolation floor moves like a rigid body, system displacements are determined from the isolators located at the centre of the floors. Additionally bending moments of columns and shear walls are evaluated. One column and one shear wall closest to the geometrical centre of the structure have been selected for evaluation.

Modal mass participating ratios of all three systems are listed in Tables 3.3, 3.4 and 3.5.

Table 3.3. Modal Participating Mass Ratios (2-Storey System)

Mode #	Period (sec)	UX	UY	SumUX	SumUY	RZ	SumRZ
1	2.773	1E-05	0.84744	1E-05	0.84744	0.14796	0.14796
2	2.755	0.99539	1.2E-05	0.9954	0.84746	9.4E-09	0.14796
3	2.639	1.8E-06	0.14794	0.9954	0.9954	0.84543	0.99339
4	0.812	1.7E-06	5.2E-06	0.99541	0.9954	6.4E-05	0.99345
5	0.494	3.4E-09	2.5E-05	0.99541	0.99543	0.00022	0.99367
6	0.295	6.1E-07	3.6E-07	0.99541	0.99543	7.8E-06	0.99368
7	0.161	1.8E-08	1.4E-06	0.99541	0.99543	7.4E-06	0.99369
8	0.099	8.3E-08	1.2E-07	0.99541	0.99543	2E-06	0.99369
9	0.048	8.5E-06	4.6E-08	0.99542	0.99543	0.00018	0.99387
10	0.041	9.8E-07	4.4E-09	0.99542	0.99543	5.1E-06	0.99388
11	0.037	7.2E-09	3.4E-07	0.99542	0.99543	2.2E-05	0.9939
12	0.019	1E-05	6E-09	0.99543	0.99543	8.2E-05	0.99398

Table 3.4. Modal Participating Mass Ratios (4-Storey System)

Mode #	Period (sec)	UX	UY	SumUX	SumUY	RZ	SumRZ
1	2.834	0.99658	6.38E-06	0.99658	6.4E-06	3.5E-05	3.5E-05
2	2.825	7.21E-06	0.99621	0.99658	0.99621	0.00061	0.00064
3	2.667	4.42E-05	0.00057	0.99663	0.99678	0.99306	0.9937
4	0.985	3.32E-05	5.78E-07	0.99666	0.99678	2.2E-05	0.99373
5	0.510	1.62E-07	1.91E-05	0.99666	0.9968	0.00072	0.99444
6	0.324	1.08E-05	6.18E-05	0.99667	0.99686	1.2E-06	0.99445
7	0.165	7.73E-07	7.03E-05	0.99667	0.99693	4.1E-06	0.99445
8	0.097	1.8E-06	1.83E-05	0.99667	0.99695	7.9E-07	0.99445
9	0.075	4.18E-05	2.17E-07	0.99672	0.99695	0.00011	0.99456
10	0.057	0.00014	2.22E-06	0.99685	0.99695	0.00068	0.99524
11	0.039	1.1E-05	1.52E-05	0.99686	0.99697	4.5E-05	0.99528
12	0.038	3.39E-05	2.66E-07	0.9969	0.99697	2.4E-05	0.99531

Table 3.5. Modal Participating Mass Ratios (7-Storey System)

Mode #	Period	UX	UY	SumUX	SumUY	RZ	SumRZ
1	2.954	0.99284	0.0002	0.99284	0.0002	0.00016	0.00016
2	2.938	0.00023	0.98988	0.99308	0.99008	0.00425	0.00441
3	2.616	0.00022	0.0039	0.9933	0.99399	0.98575	0.99016
4	1.086	0.00031	1.3E-05	0.99361	0.994	3.2E-05	0.99019
5	0.502	1.8E-06	0.00028	0.99361	0.99428	0.00094	0.99113
6	0.336	7.7E-05	0.00085	0.99368	0.99513	0.00019	0.99132
7	0.177	2.2E-05	0.00092	0.99371	0.99605	0.00045	0.99177
8	0.125	0.00018	2.5E-07	0.99388	0.99605	0.00019	0.99195
9	0.096	1.2E-05	0.00012	0.99389	0.99617	4E-05	0.99199
10	0.076	0.00058	7.8E-06	0.99447	0.99618	0.00077	0.99276
11	0.053	0.00033	2.1E-05	0.9948	0.9962	0.00074	0.99351
12	0.043	0.00035	0.00012	0.99516	0.99632	6.7E-05	0.99357

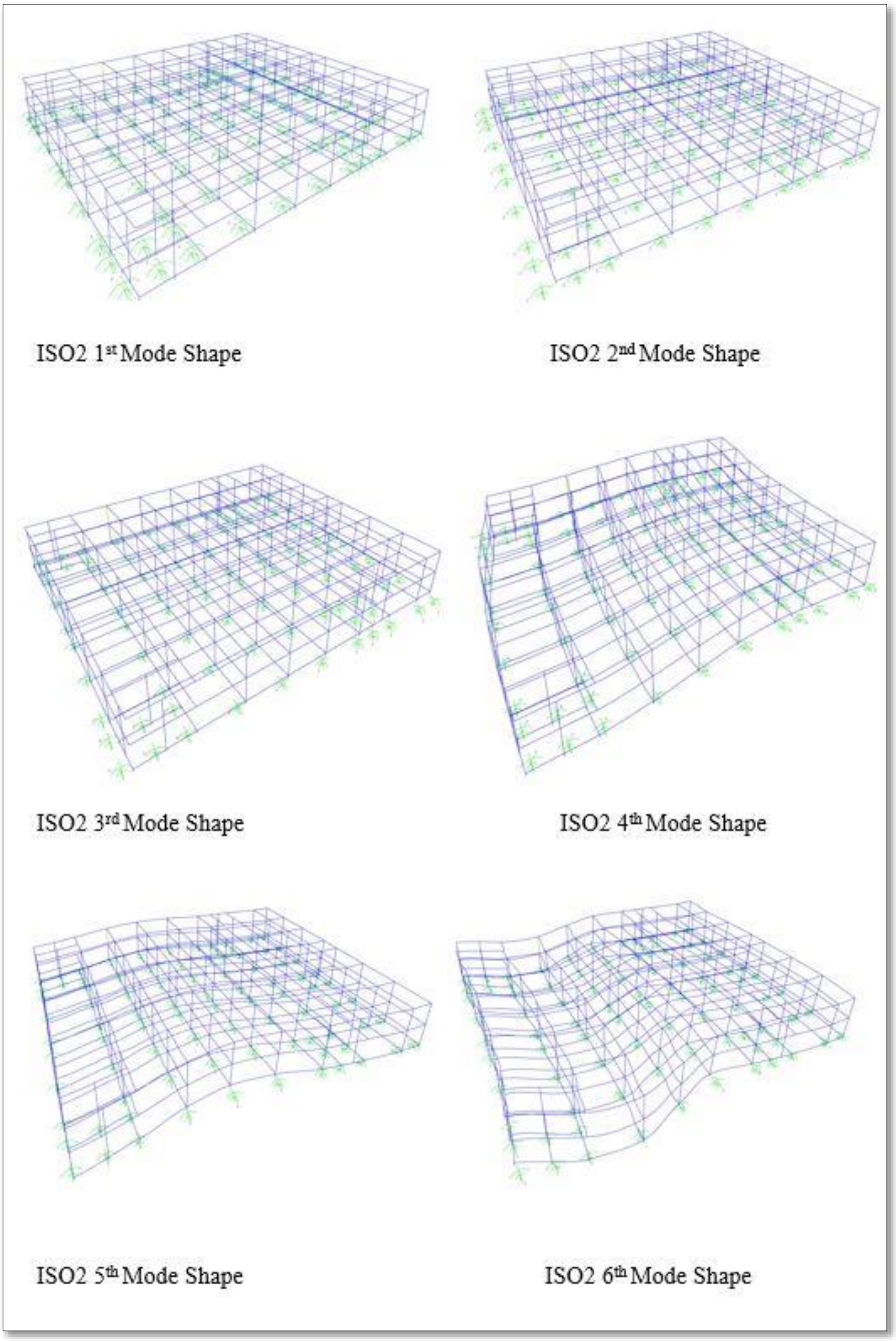

Figure 3.1. First 6 Mode Shape of 2-Storey System

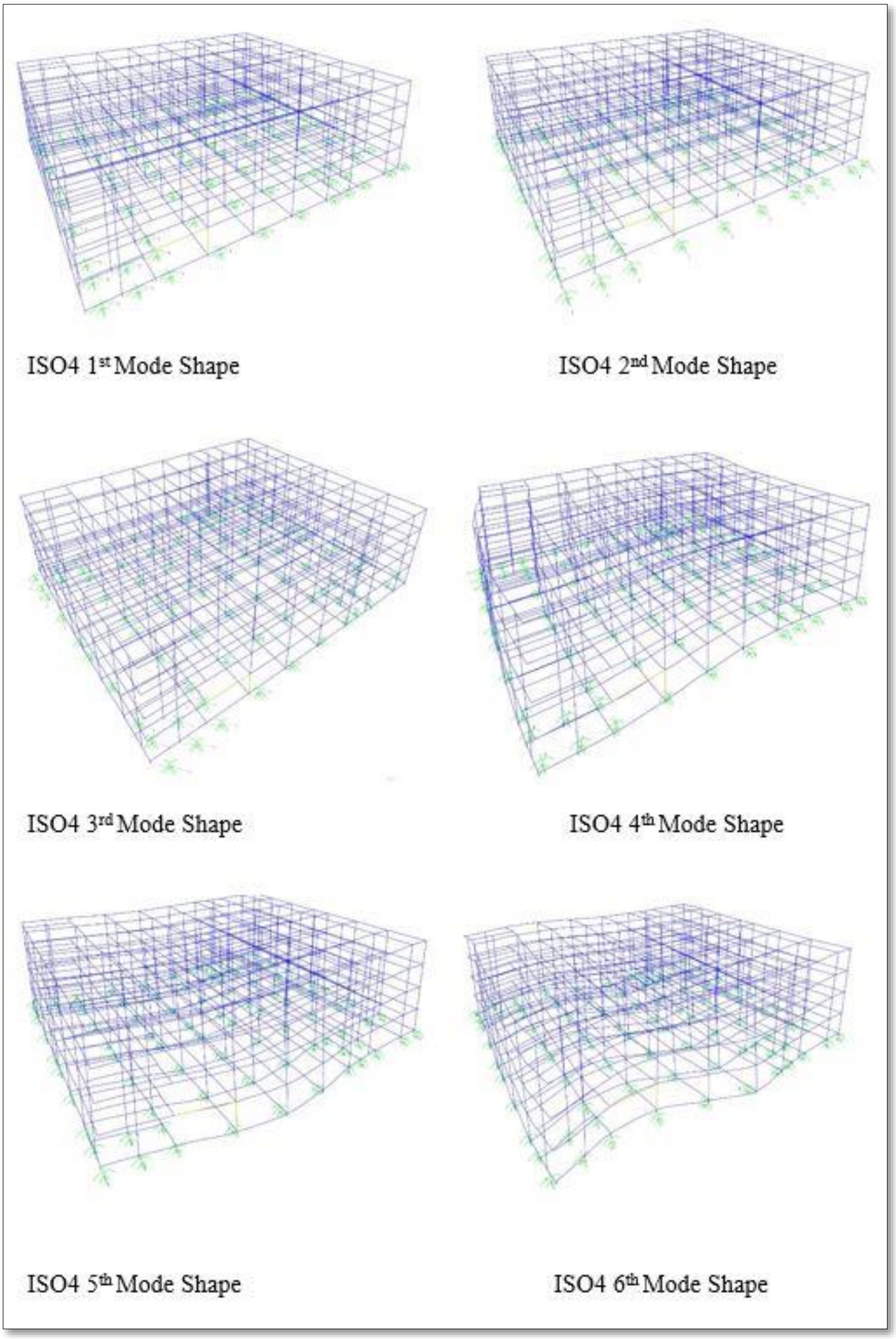

Figure 3.2. First 6 Mode Shape of 4-Storey System

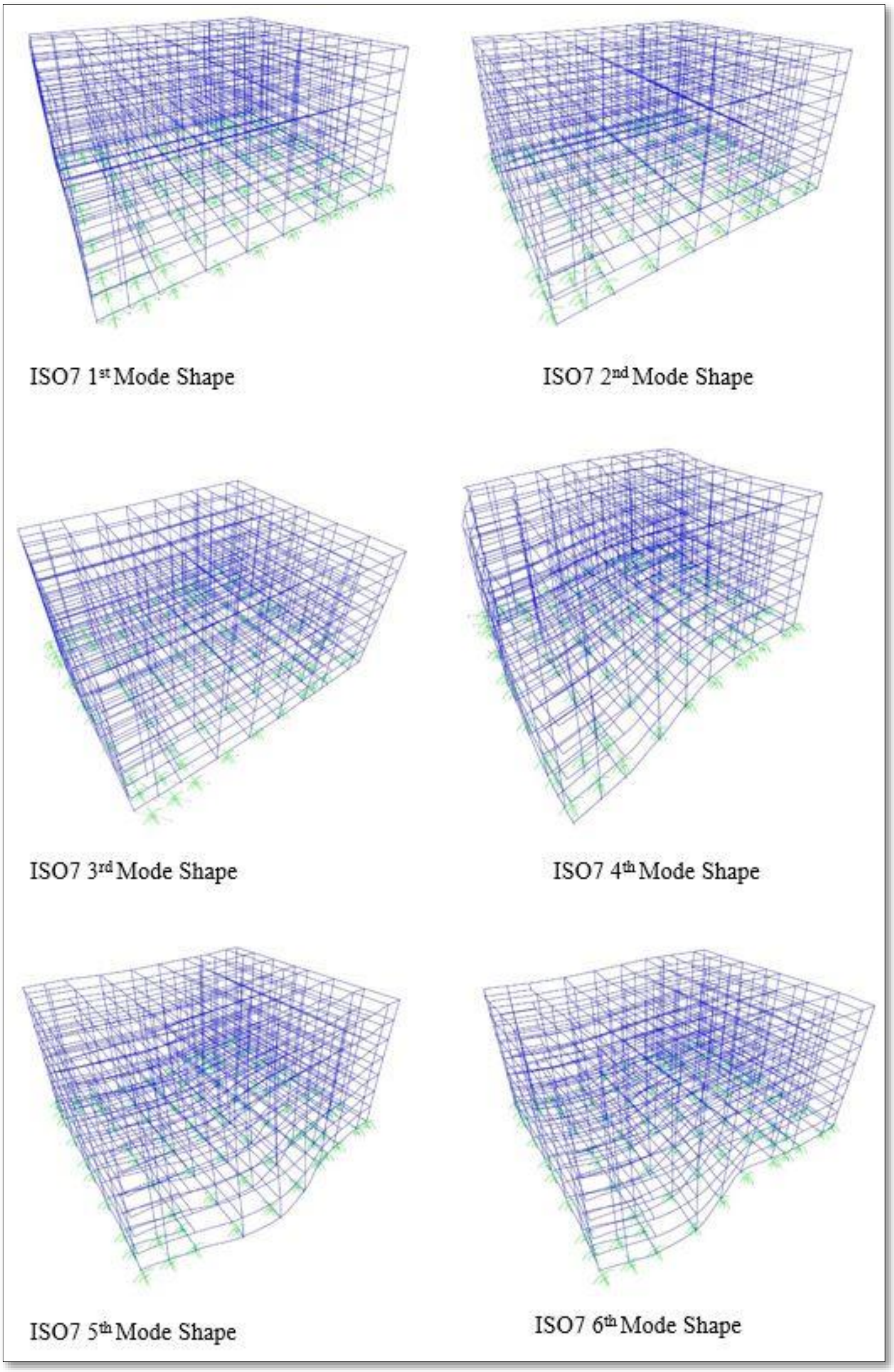

Figure 3.3. First 6 Mode Shape of 7-Storey System

3.1. NTHA Results

Non-linear time history analysis are carried out to evaluate the behaviour of FPS systems in base isolated structures. In this section, results of NTHA that are performed for the systems with different numbers of floors namely ISO2, ISO4 and ISO7 are presented to evaluate the difference in results obtained from the use of different groups of containing different numbers of ground motions.

3.1.1. Analysis Results of ISO2

3.1.1.1. Base Shear Results of ISO2

Maximum absolute base shear values are obtained from the SRSS (Square Root of the Sum of the Squares) of the reactions in x and y directions for each time instants of the ground motions. Obtained maximum SRSS base shear values for 11 GMs with and without vertical components are presented in Figure 3.4.

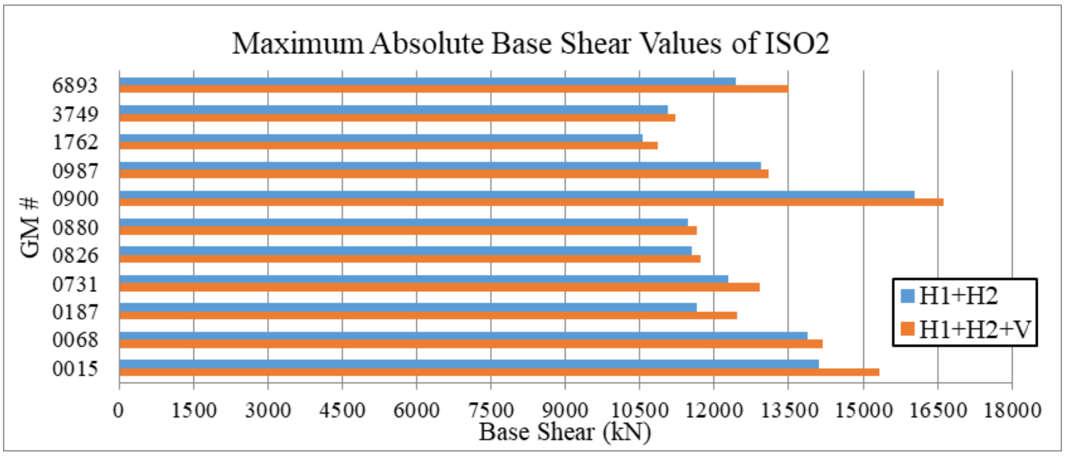

Figure 3.4. Maximum Absolute Base Shear Values of ISO2 from 11 GMs

Values of base shear of ISO2 obtained from NTHA for 11 GMs with and without vertical components are listed in Table 3.7. Mean SRSS base shear of different 3 GM sets are presented in Table 3.8.

Table 3.6. Base Shear Coefficients of ISO2 Obtained from NTHA for 11 GMs

GM #	Base Shear Coefficients	
	H1+H1	H1+H2+V
0015	11.53%	12.52%
0068	11.33%	11.59%
0187	9.52%	10.17%
0731	10.03%	10.56%
0826	9.44%	9.57%
0880	9.36%	9.52%
0900	13.09%	13.58%
0987	10.57%	10.69%
1762	8.63%	8.87%
3749	9.04%	9.16%
6893	10.16%	11.03%

Table 3.7. Base Shear Values of ISO2 Obtained from NTHA for 11GMs

GM #	Vb(kN)		
	H1+H1	H1+H2+V	Difference (%)
0015	14119.17	15329.11	8.57%
0068	13877.44	14188.81	2.24%
0187	11650.71	12457.19	6.92%
0731	12280.93	12927.39	5.26%
0826	11552.83	11720.31	1.45%
0880	11462.28	11654.88	1.68%
0900	16030.02	16624.34	3.71%
0987	12939.82	13086.47	1.13%
1762	10560.55	10860.46	2.84%
3749	11062.28	11220.28	1.43%
6893	12433.47	13501.76	8.59%

As it can be seen from figures, base shear values are higher in between 1-9 % when vertical component is included in analysis for selected 11 GMs. The change in base shear coefficients is approximately 1% for selected ground motion records.

Table 3.8. Mean Base Shear Values of each GM Set Obtained from NTHA for ISO2

GM Sets	Vb (kN)
7 GMs Horizontal Components	12926.11779
11 GMs Horizontal Components	12557.90657
11 GMs Horizontal+ Vertical Components	13036.68279

According to obtained results, selecting eleven GMs rather than seven GMs in horizontal direction does not have a significant effect on base shear values. Base shear values increase when vertical components of ground motions are taken into consideration; however, the increment ratios are relatively low.

3.1.1.2. PFA Results for ISO2

SRSS peak floor accelerations for ISO2 are demonstrated in Figure 3.5 for selected 11 GMs without vertical component.

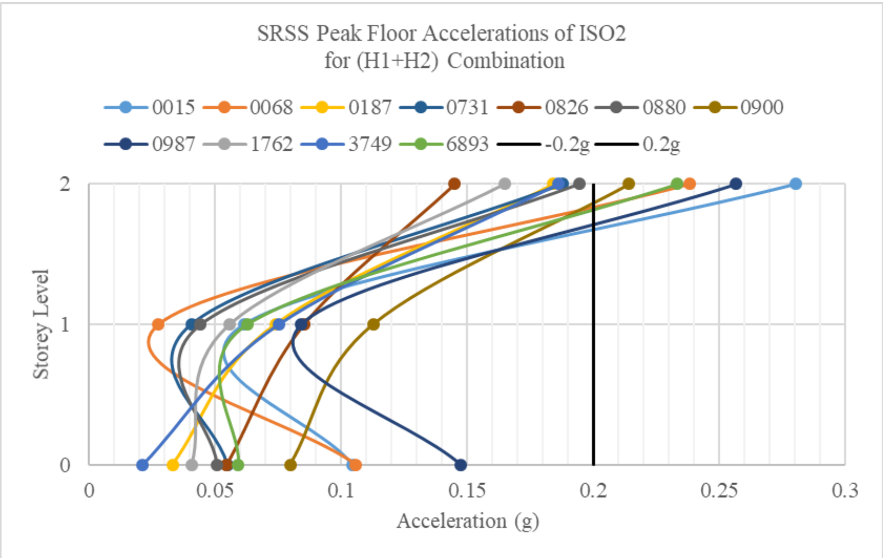

Figure 3.5. SRSS PFA of ISO2 from 11 GMs without Vertical Components

SRSS peak floor accelerations for ISO2 are demonstrated in Figure 3.6 for selected 11 GMs with vertical component.

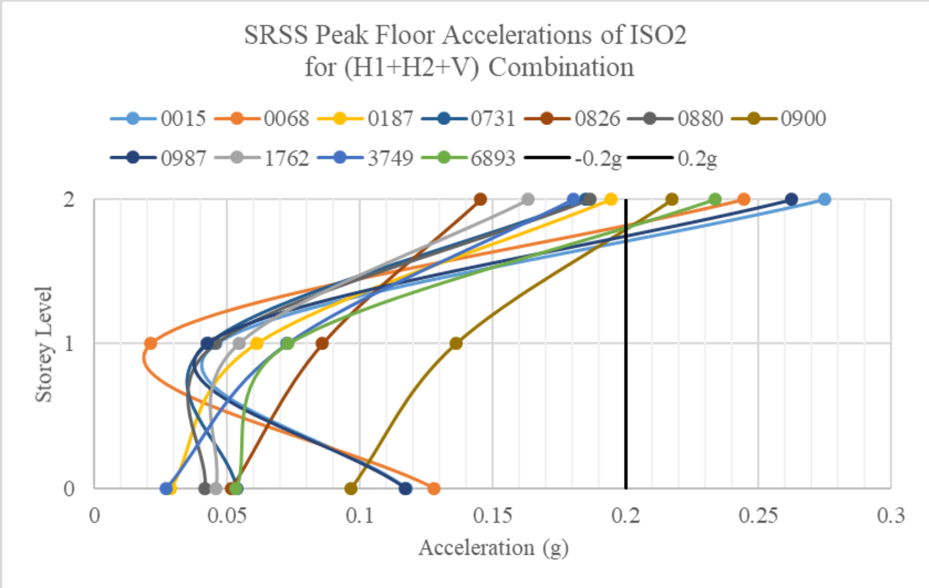

Figure 3.6. SRSS PFA of ISO2 from 11 GMs with Vertical Components

PFA results at the top floor of ISO2 system obtained from NTHA for 11 GMs with and without vertical component are listed in Table 3.9. Mean PFA values obtained from different 3 GM sets are presented in Table 3.10.

It is obvious that, selecting four more ground motions or using vertical components of GMs do not have any considerable effect on PFA values of ISO2 system.

Table 3.9. SRSS PFA (g) of ISO2 Obtained from NTHA for 11 GM Records

GM #	SRSS PFA (g)		
	H1+H1	H1+H2+V	Difference (%)
0015	0.2802	0.2747	-1.9524%
0068	0.2382	0.2445	2.6828%
0187	0.1841	0.1944	5.6051%
0731	0.1877	0.1847	-1.6224%
0826	0.1449	0.1453	0.2191%
0880	0.1944	0.1865	-4.0783%
0900	0.2140	0.2175	1.6301%
0987	0.2565	0.2625	2.3319%
1762	0.1648	0.1633	-0.9308%
3749	0.1860	0.1801	-3.1907%
6893	0.2333	0.2336	0.1361%

Table 3.10. Mean PFS (g) of each GM Set Obtained from NTHA for ISO2

GM Sets	SRSS PFA (g)
7 GMs Horizontal Components	0.2161
11 GMs Horizontal Components	0.1991
11 GMs Horizontal+ Vertical Components	0.2079

3.1.1.3. IDR (%) Results of ISO2

Inter-storey drift ratios distributed through the floors in x and y directions for ISO2 system are presented in Figures 3.7 and 3.8 for selected 11 GMs without vertical component.

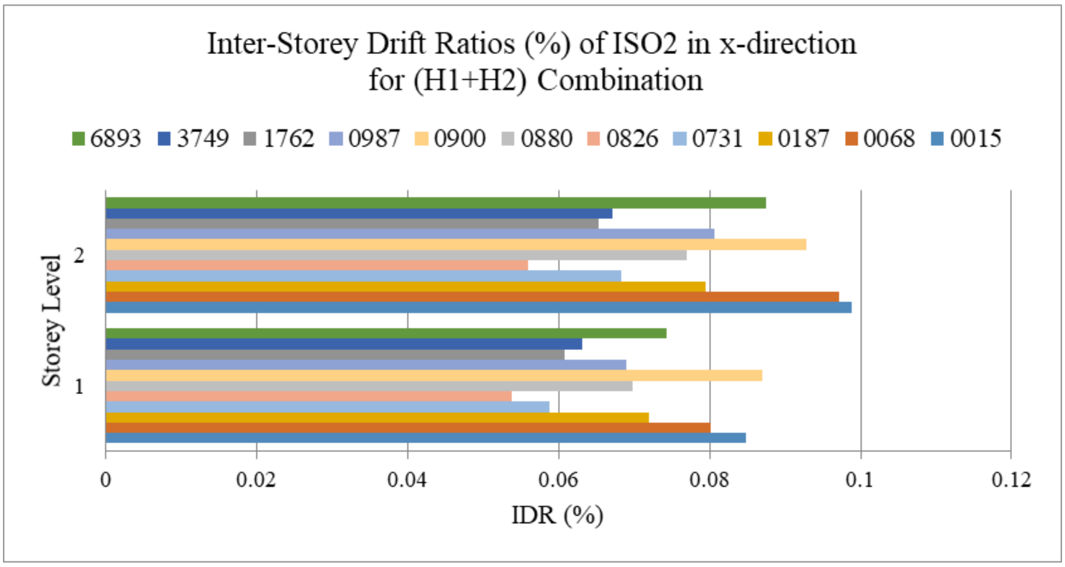

Figure 3.7. IDR (%) through Floors of ISO2 (in x-direction) from 11 GMs without Vertical Components

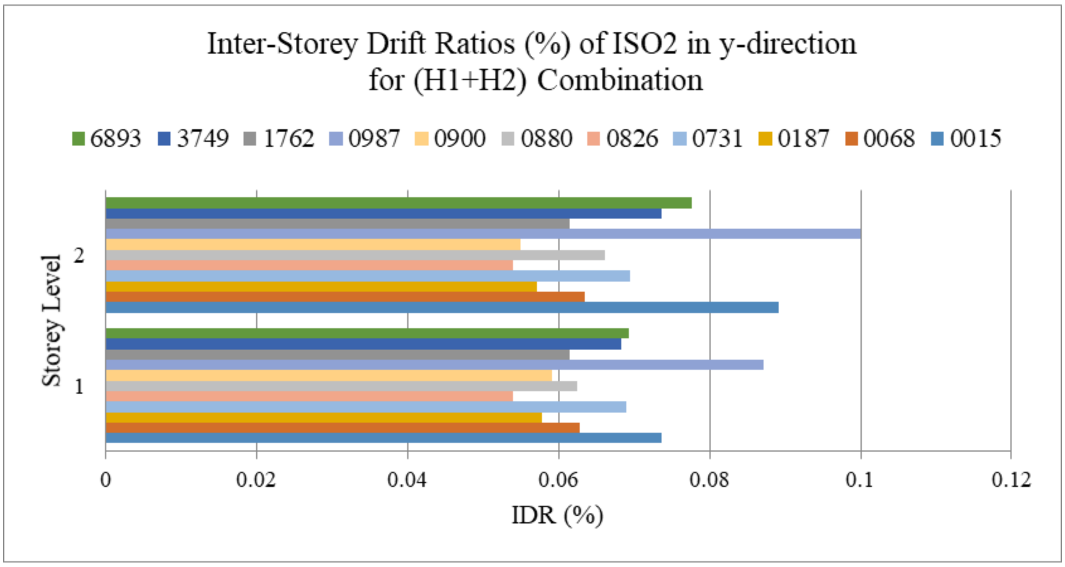

Figure 3.8. IDR (%) trough Floors of ISO2 (in y-direction) from 11 GMs without Vertical Components

Inter-storey drift ratios distributed through the floors in x and y directions for ISO2 are presented in Figures 3.9 and 3.10 for selected 11 GMs with vertical component.

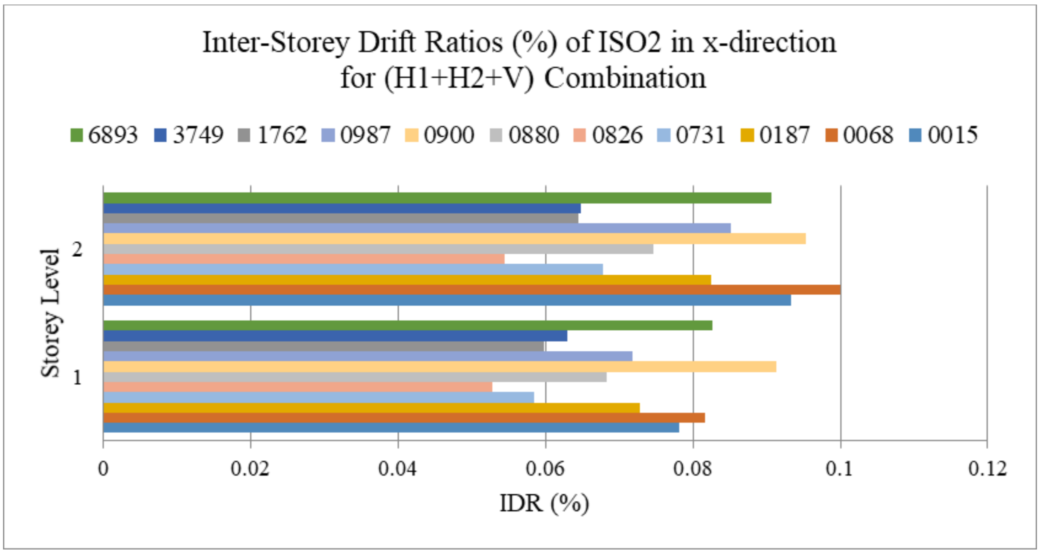

Figure 3.9. IDR (%) through Floors of ISO2 (in x-direction) from 11 GMs with Vertical Components

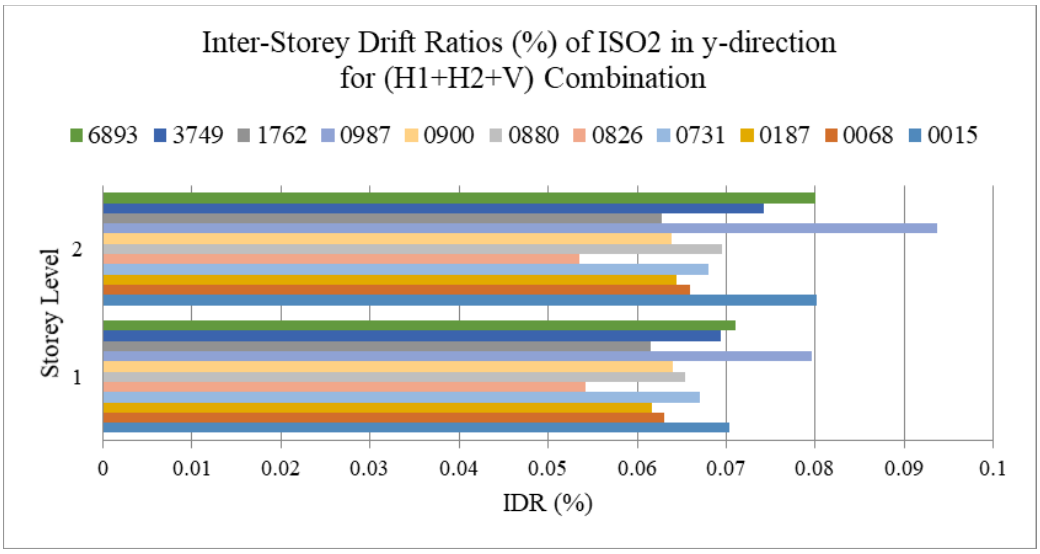

Figure 3.10. IDR (%) through Floors of ISO2 (in y-direction) from 11 GMs with Vertical Components

Maximum IDR (%) results of ISO2 system obtained from NTHA for 11 GMs with and without vertical component are listed in Table 3.11. Mean IDR (%) obtained from different 3 GM sets are presented in Table 3.12.

Any of the GMs does not exceed the maximum limits defined in specifications, which are explained in the beginning of this chapter.

According to presented results, using vertical component of GMs has not a considerable effect on IDR (%) parameters.

Table 3.11. Maximum IDR (%) Results of ISO2 Obtained from NTHA for 11 GMs

GM #	Max. IDR in x-direction (%)			Max. IDR in y-direction (%)		
	H1+H1	H1+H2+V	Difference(%)	H1+H1	H1+H2+V	Difference(%)
0015	0.0988	0.0933	-5.60%	0.0892	0.0802	-10.09%
0068	0.0971	0.1001	3.07%	0.0635	0.0660	3.92%
0187	0.0794	0.0825	3.89%	0.0571	0.0645	12.84%
0731	0.0683	0.0677	-0.85%	0.0694	0.0680	-2.08%
0826	0.0560	0.0545	-2.62%	0.0539	0.0536	-0.66%
0880	0.0770	0.0746	-3.15%	0.0662	0.0695	5.11%
0900	0.0929	0.0954	2.68%	0.0549	0.0639	16.30%
0987	0.0807	0.0852	5.65%	0.1000	0.0938	-6.24%
1762	0.0654	0.0644	-1.50%	0.0614	0.0627	2.06%
3749	0.0672	0.0648	-3.57%	0.0737	0.0742	0.63%
6893	0.0875	0.0906	3.48%	0.0776	0.0800	3.09%

Table 3.12. Mean IDR (%) of each GM Set Obtained from NTHA for ISO2

GM Sets	Max. IDR in x-direction (%)	Max. IDR in y-direction (%)
7 GMs Horizontal Components	0.0829	0.0677
11 GMs Horizontal Components	0.0791	0.0697
11 GMs Horizontal+ Vertical Components	0.0794	0.0706

Any of the GMs does not exceed the maximum limits defined in specifications, which are explained in the beginning of this chapter.

According to presented results, using vertical component of GMs has not a considerable effect on IDR parameters.

3.1.1.4. ISD Results of ISO2

Isolation system displacement (ISD) is a very important parameter in isolation system design. Sizes of isolators and isolator pedestals, dilatation distances, mechanical properties of isolators etc. are determined by using ISD. System displacement is obtained from the SRSS (Square Root of the Sum of the Squares) of the displacements in x and y directions for each time instants of the ground motions. ISD in meters for 11 GMs with and without vertical components are presented in Figures 3.11 and 3.12 respectively.

Maximum SRSS ISD values of ISO2 system for 11 GMs are represented in Table 3.13. Mean ISD obtained from different 3 GM sets are presented in Table 3.14.

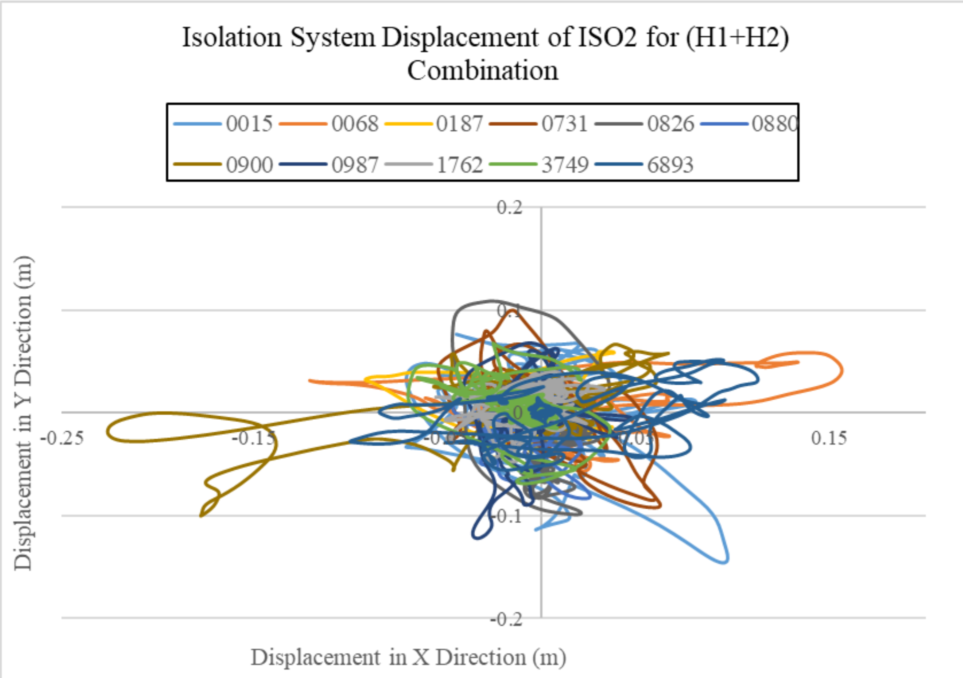

Figure 3.11. ISD of ISO2 from 11 GMs without Vertical Components

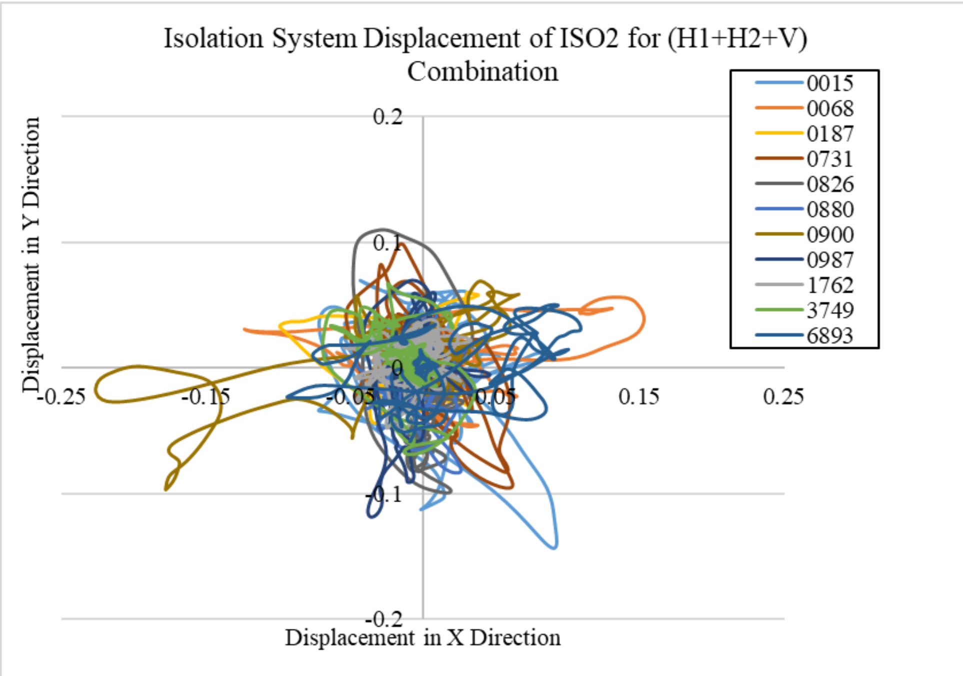

Figure 3.12. ISD of ISO2 from 11 GMs with Vertical Components

Table 3.13. Maximum SRSS ISD of ISO2 System Obtained from NTHA for 11 GMs

GM #	Isolator Displacement (cm)		
	H1+H1	H1+H2+V	Difference (%)
0015	17.41	16.97	-2.54%
0068	16.23	15.84	-2.43%
0187	9.74	10.45	7.32%
0731	11.00	11.30	2.72%
0826	11.22	11.41	1.66%
0880	8.64	8.69	0.65%
0900	22.68	22.71	0.15%
0987	12.63	12.36	-2.17%
1762	5.72	5.69	-0.61%
3749	7.85	7.80	-0.74%
6893	11.77	11.40	-3.16%

Table 3.14. Mean SRSS ISD of each GM Set Obtained from NTHA for ISO2

GM Sets	Isolator Displacement (cm)
7 GMs Horizontal Components	13.3652
11 GMs Horizontal Components	12.2641
11 GMs Horizontal+ Vertical Components	12.2380

According to the results, selecting 11 ground motions rather than 7 ground motions decreases the obtained mean ISD; including the vertical components of GMs has no effect on ISD for ISO2 system structure.

3.1.1.5. Bending Moment of Columns and Shear Walls

One shear wall and one column closest to the geometrical centre of structure have been selected for evaluation. Maximum bending moment values of the selected column in x and y directions are demonstrated in figures 3.13 and 3.14.

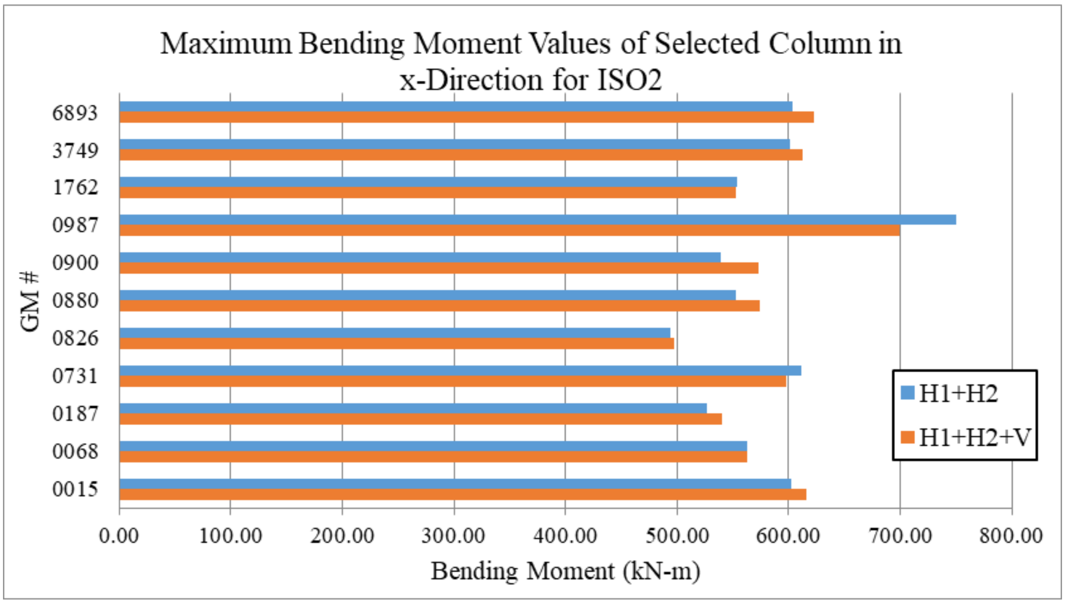

Figure 3.13. Maximum Bending Moment Values of Selected Column (in x-direction) for ISO2 from 11 GMs

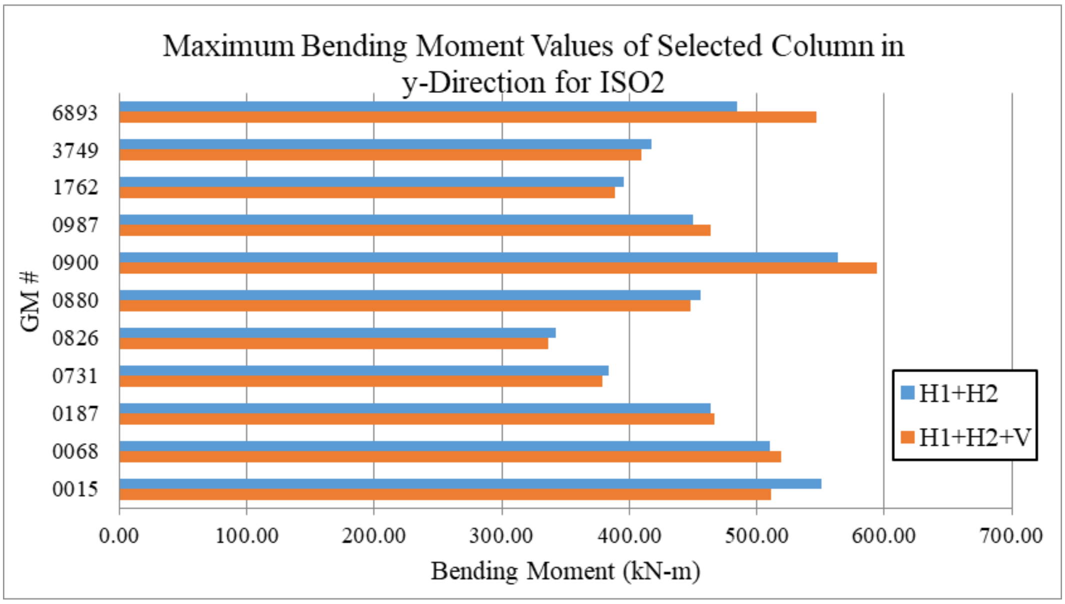

Figure 3.14. Maximum Bending Moment Values of Selected Column (in y-direction) for ISO2 from 11 GMs

Maximum bending moment values of selected column for ISO2 system for 11 GMs are represented in Tables 3.15 and mean bending moment values obtained from different 3 GM sets are presented in Table 3.16.

Table 3.15. Values of Bending Moment of Selected Column of ISO2 Obtained from NTHA for 11GMs

GM #	Mx(kNm)			My(kNm)		
	H1+H1	H1+H2+V	Difference(%)	H1+H1	H1+H2+V	Difference(%)
0015	601.80	615.97	2.35%	550.56	510.88	-7.21%
0068	562.37	562.40	0.01%	510.09	519.59	1.86%
0187	527.25	540.60	2.53%	463.62	466.45	0.61%
0731	611.75	597.74	-2.29%	383.51	378.68	-1.26%
0826	493.45	497.65	0.85%	342.71	336.93	-1.69%
0880	552.28	573.91	3.92%	456.27	447.76	-1.86%
0900	539.69	573.48	6.26%	563.51	594.52	5.50%
0987	750.22	699.66	-6.74%	450.47	464.16	3.04%
1762	553.98	552.90	-0.19%	395.45	389.15	-1.59%
3749	601.52	611.98	1.74%	417.02	409.96	-1.69%
6893	603.52	622.72	3.18%	484.39	547.07	12.94%

Table 3.16. Mean Values of Bending Moment of Selected Column of each GM Set Obtained from NTHA for ISO2

GM Sets	Mx (kNm)	My(kNm)
7 GMs Horizontal Components	570.95	477.80
11 GMs Horizontal Components	581.62	456.14
11 GMs Horizontal+ Vertical Components	586.27	460.47

According to obtained results, while selecting 4 more records increase the bending moment value in x-direction, it decreases the bending moment in y-direction.

Additionally, the effect of vertical component on bending moment values of selected column is too small to consider.

Maximum bending moment values of the selected shear wall in x and y directions are demonstrated in Figures 3.15 and 3.16.

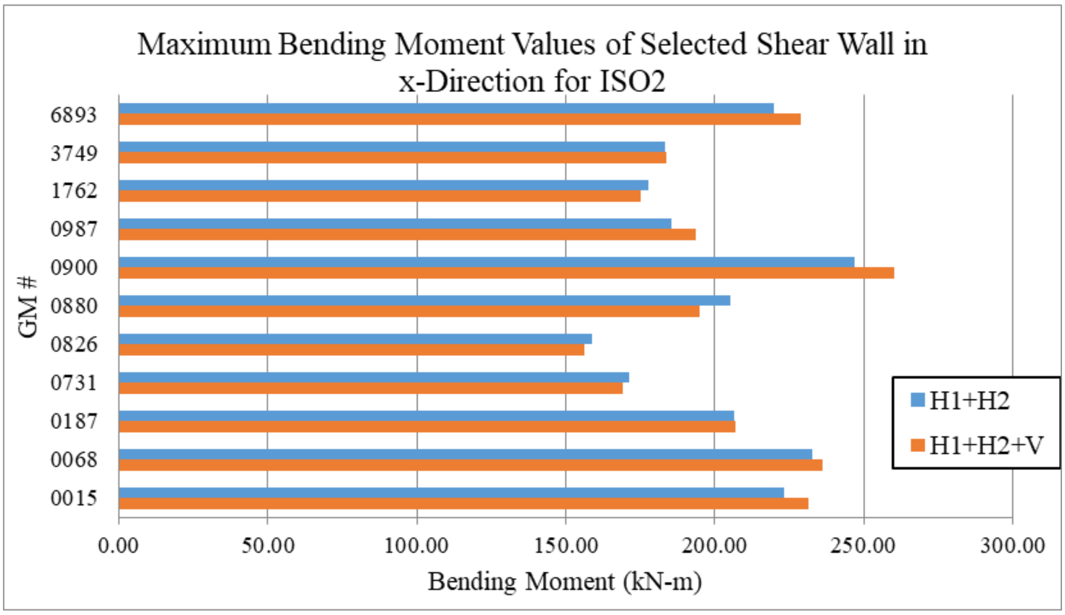

Figure 3.15. Maximum Bending Moment Values of Selected Shear Wall (in x-direction) for ISO2 from 11 GMs

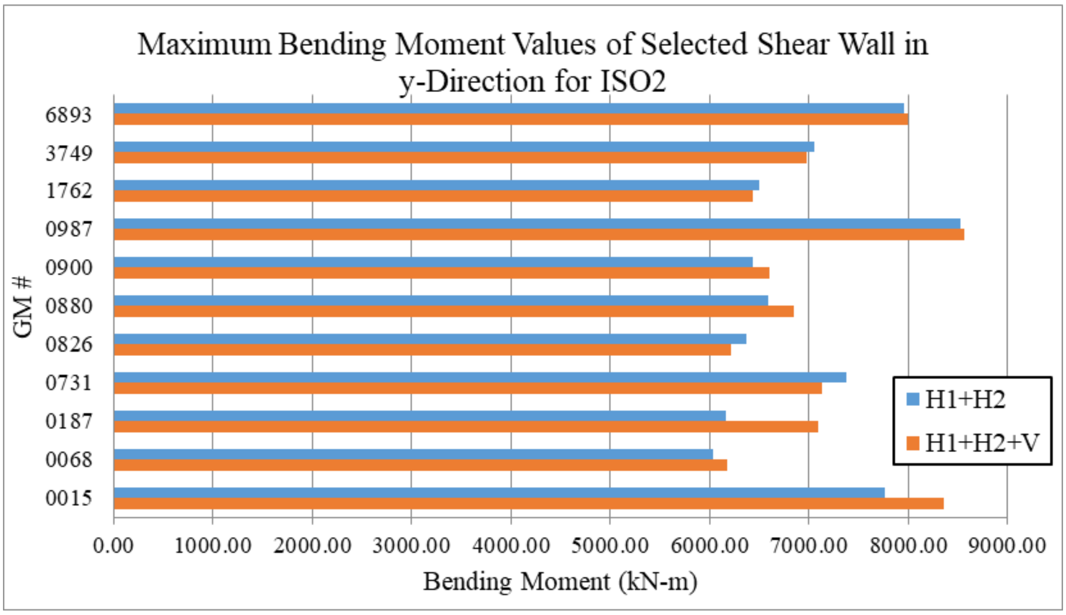

Figure 3.16. Maximum Bending Moment Values of Selected Shear Wall (in y-direction) for ISO2 from 11 GMs

Maximum bending moment values of selected shear wall for ISO2 system for 11 GMs are represented in Table 3.17 and mean bending moment values obtained from different 3 GM sets are presented in Table 3.18.

3.1.1.6. Axial Loads Acting on Isolators

One of the most important factors in design of isolation systems is the axial loads acting on the isolators located in the system. At the different time instants of a ground motion, isolators are affected by different axial load values. In this part, in order to examine the changes in axial loads acting on isolators, maximum and minimum axial loads carried by each isolator are evaluated for 11 different ground motions. While negative values represent the compression on isolators, because friction pendulum isolators do not carry any tensile load, zero values expose that the related isolators are under the influence of tension.

Table 3.17. Values of Bending Moment of Selected Shear Wall of ISO2 Obtained from NTHA for 11GMs

GM #	Mx(kNm)			My(kNm)		
	H1+H1	H1+H2+V	Difference(%)	H1+H1	H1+H2+V	Difference(%)
0015	223.40	231.69	3.71%	7767.95	8352.81	7.53%
0068	232.73	236.43	1.59%	6031.20	6172.98	2.35%
0187	206.58	206.86	0.14%	6159.46	7097.23	15.22%
0731	171.31	169.04	-1.33%	7376.12	7134.92	-3.27%
0826	158.67	156.38	-1.44%	6368.68	6218.70	-2.36%
0880	205.37	194.90	-5.10%	6587.76	6842.31	3.86%
0900	246.78	260.20	5.44%	6429.99	6604.56	2.71%
0987	185.33	193.85	4.60%	8528.15	8561.99	0.40%
1762	177.82	175.22	-1.46%	6500.60	6429.65	-1.09%
3749	183.36	183.93	0.31%	7053.46	6980.23	-1.04%
6893	219.95	229.02	4.13%	7963.85	7997.45	0.42%

Table 3.18. Mean Values of Bending Moment of Selected Shear Wall of each GM Set Obtained from NTHA for ISO2

GM Sets	GM Sets	Mx (kNm)	My(kNm)
7 GMs Horizontal Components	Set 1	209.93	6772.28
11 GMs Horizontal Components	Set2	201.03	6978.84
11 GMs Horizontal+ Vertical Components	Set 3	203.41	7126.62

Similar with the column results, selecting 4 more motions decrease the bending moment value in x-direction, and increase the value in y-direction for shear wall. While the effect of vertical ground motion is too small in weak axis of shear wall, the effect is more significant in strong axis. Even so, the effects are not so significant.

Maximum and minimum loads acting on each isolator for 11 GMs without vertical components in ISO2 system are demonstrated in Figures 3.17 and 3.18.

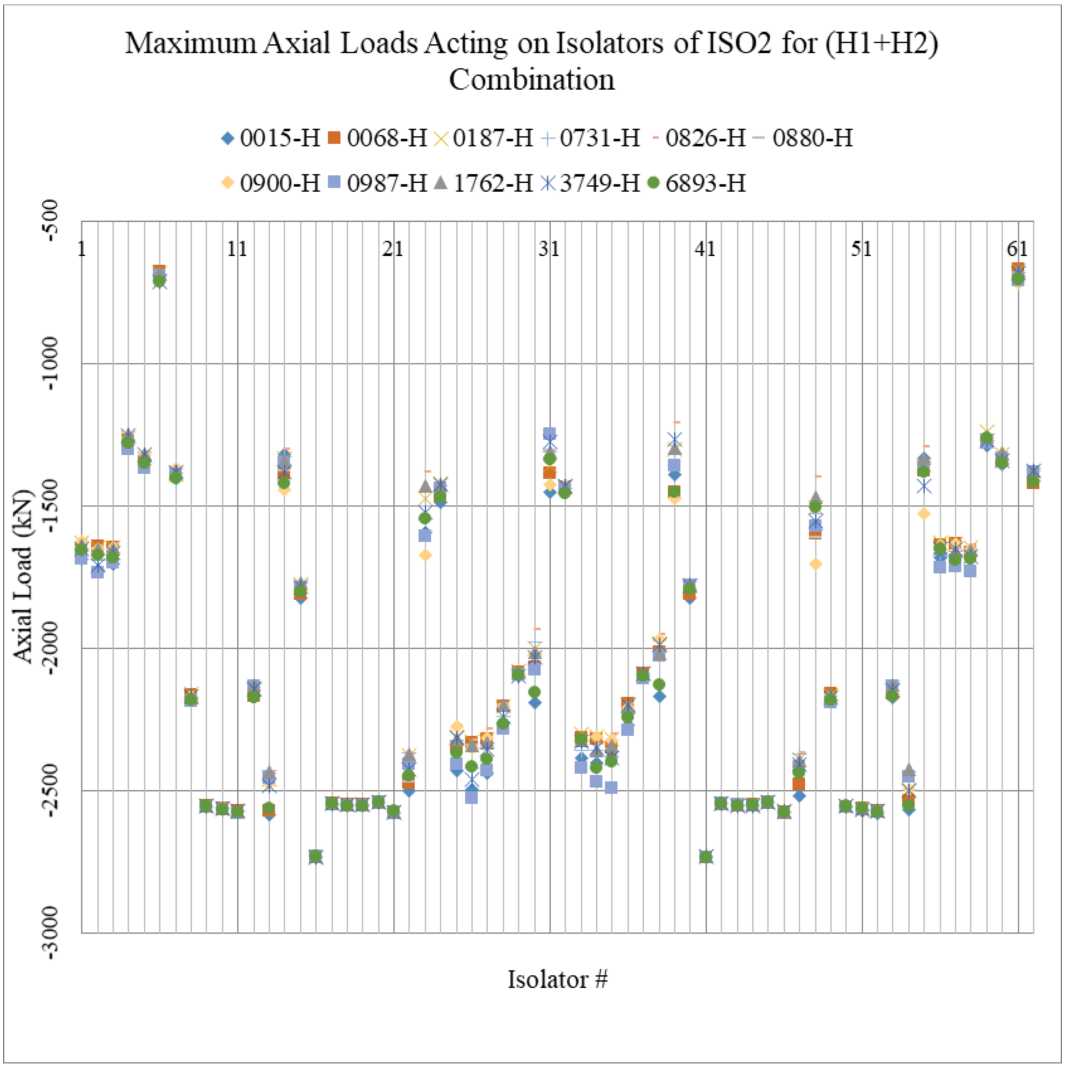

Figure 3.17. Maximum Axial Loads Acting on Each Isolator ISO2 from 11GMs without Vertical Components

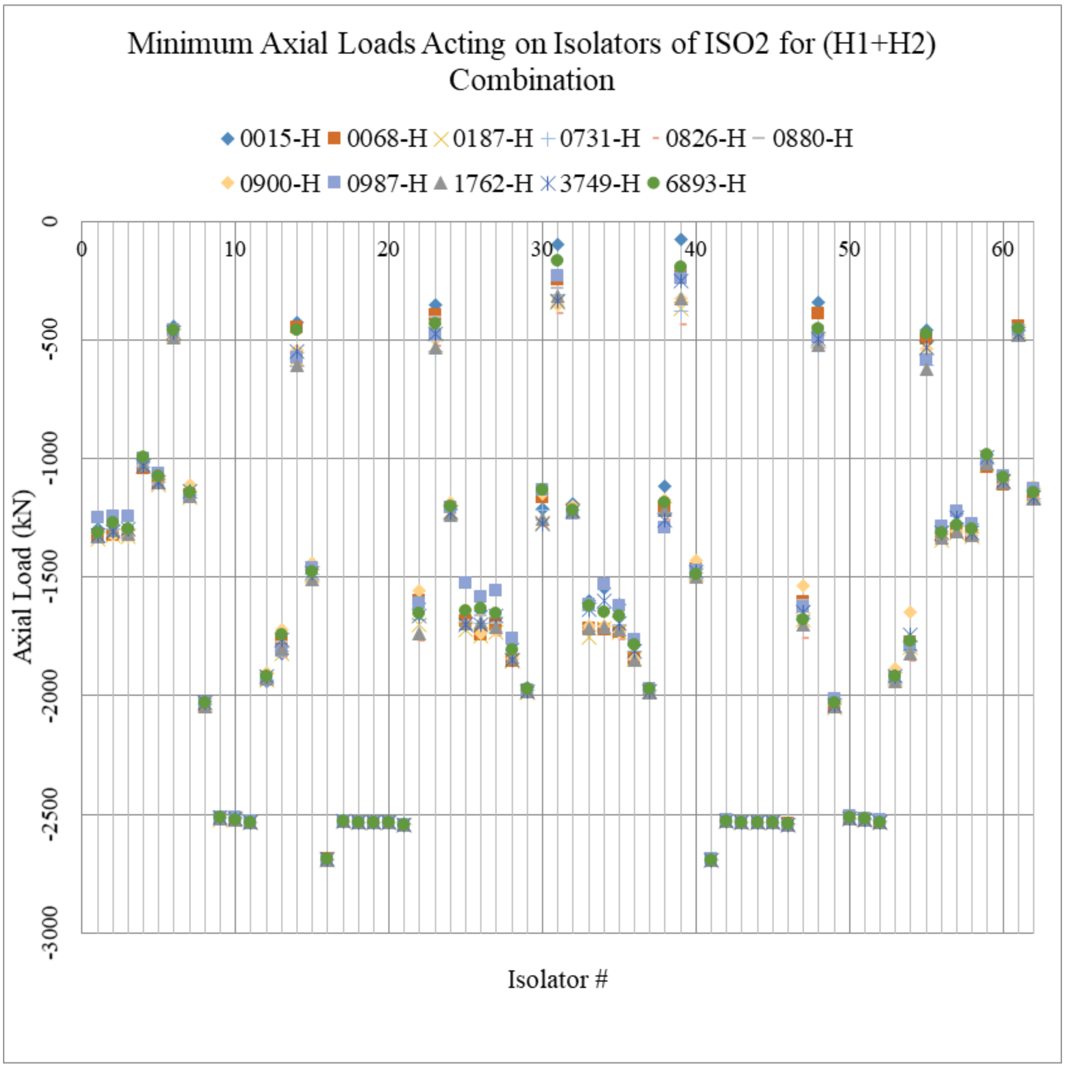

Figure 3.18. Minimum Axial Loads Acting on Each Isolator ISO2 from 11GMs without Vertical Components

While maximum axial loads are varying between 500kN and 3000 kN (compression), minimum loads scatter between 0 and 2700 kN (compression). No tensile load is generated in any isolator for 11 GMs without vertical component.

For 11 GMs with vertical components, maximum and minimum axial loads are presented in Figures 3.19 and 3.20.

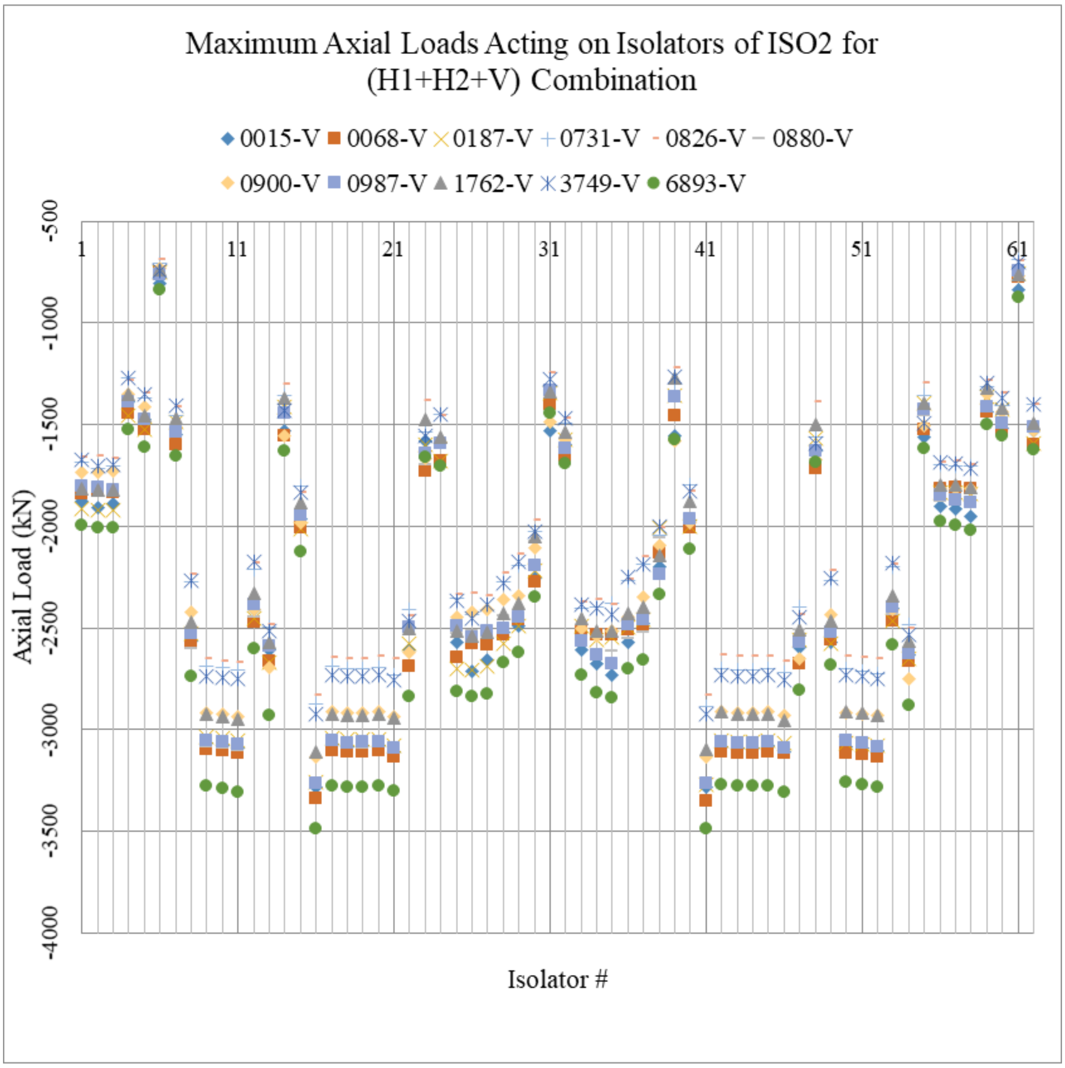

Figure 3.19. Maximum Axial Loads Acting on Each Isolator ISO2 from 11GMs with Vertical Components

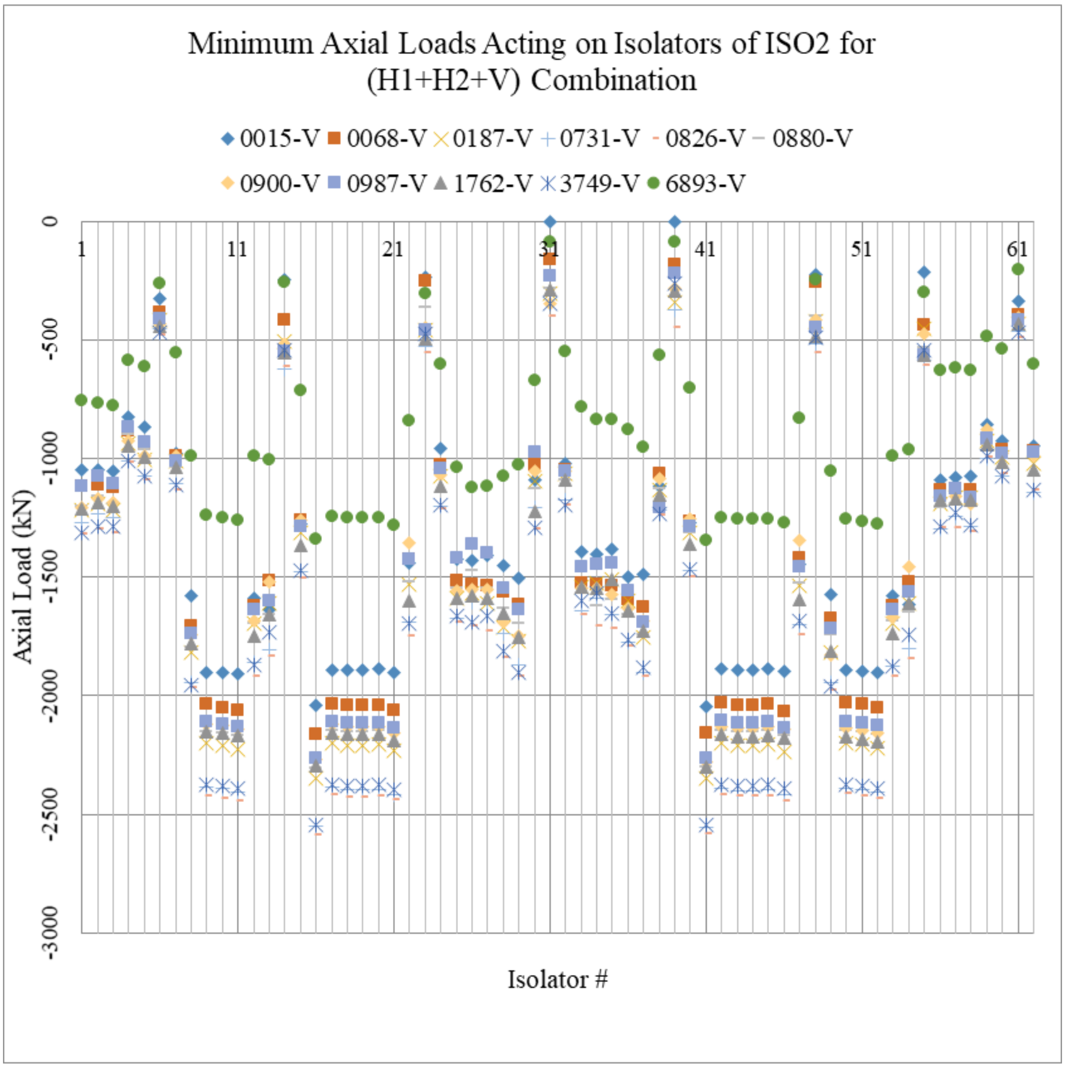

Figure 3.20. Minimum Axial Loads Acting on Each Isolator ISO2 from 11GMs with Vertical Components

While vertical components of ground motions increase the maximum axial loads on isolators, decrease the minimum axial loads. Such that tensile loads are generated from GM0015 on isolators 31 and 39.

Consequently, including the vertical component makes the axial load on columns more sensitive to earthquake records.

3.1.2. Analysis and Results of ISO4

In this part, evaluations made for ISO2 in previous part are repeated for ISO4 in order to make comparison between buildings having different number of floors.

3.1.2.1. Base Shear Results of ISO4

Maximum SRSS base shear values are presented in Figure 3.21.

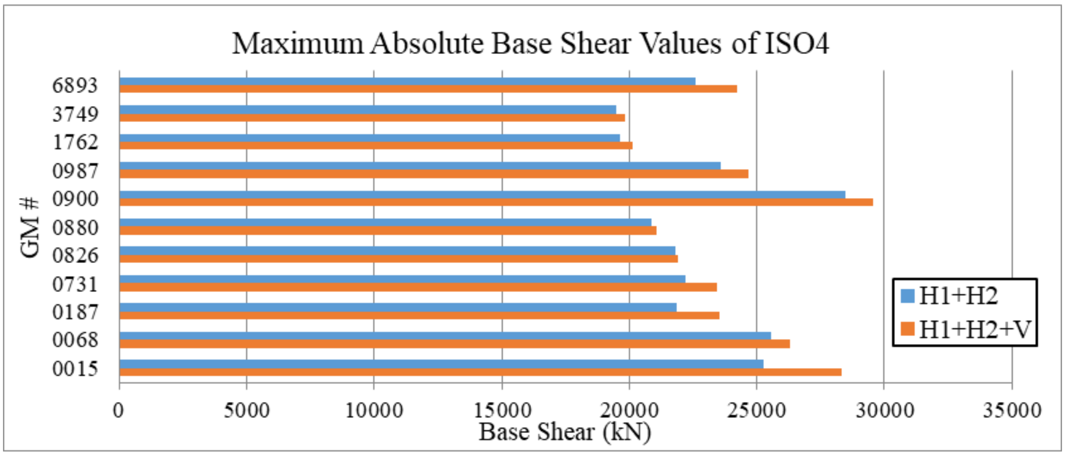

Figure 3.21. Maximum SRSS Base Shear Values of ISO4 from 11 GMs

Base reactions are higher as in ISO2 system when vertical component is included in analysis for selected 11 GMs.

Base reactions of ISO4 system obtained from NTHA for 11 GMs with and without vertical component are listed in Table 3.20. Mean base reactions of different 3 GM sets are presented in Table 3.21.

Table 3.19. Base Shear Coefficients of ISO4 Obtained from NTHA for 11 GMs

GM #	Base Shear Coefficients	
	H1+H1	H1+H2+V
0015	11.47%	12.86%
0068	11.60%	11.93%
0187	9.93%	10.67%
0731	10.08%	10.63%
0826	9.90%	9.94%
0880	9.48%	9.57%
0900	12.93%	13.41%
0987	10.71%	11.21%
1762	8.92%	9.13%
3749	8.84%	9.01%
6893	10.26%	10.99%

Table 3.20. Base Shear Values of ISO4 Obtained from NTHA for 11 GMs

GM #	Vb(kN)		
	H1+H1	H1+H2+V	Difference (%)
0015	25268.87	28338.42	12.15%
0068	25559.05	26291.63	2.87%
0187	21868.80	23519.84	7.55%
0731	22198.02	23414.18	5.48%
0826	21802.79	21903.99	0.46%
0880	20891.97	21075.88	0.88%
0900	28492.78	29552.70	3.72%
0987	23604.83	24695.34	4.62%
1762	19647.23	20120.03	2.41%
3749	19475.67	19859.19	1.97%
6893	22609.70	24204.69	7.05%

Table 3.21. Mean Base Shear Values of each GM Set Obtained from NTHA for ISO4

GM Sets	Vb (kN)
7 GMs Horizontal Components	23393.59
11 GMs Horizontal Components	22856.34
11 GMs Horizontal+ Vertical Components	23906.90

According to the presented results, similar with ISO2 system, considering vertical components of motions in analysis increases the base shear values significantly. Selecting eleven GMs rather than 7 GMs does not cause an identifiable change in base shear values. As it can be seen from figures, base shear values are higher in between 1-13 % when vertical component is included in analysis for selected 11 GMs. The change in base shear coefficients is approximately 1%, similar with ISO2, for selected ground motion records.

3.1.2.2. PFA Results for ISO4

SRSS peak floor accelerations for ISO4 system are demonstrated in Figure 3.22 for selected 11 GMs without vertical component.

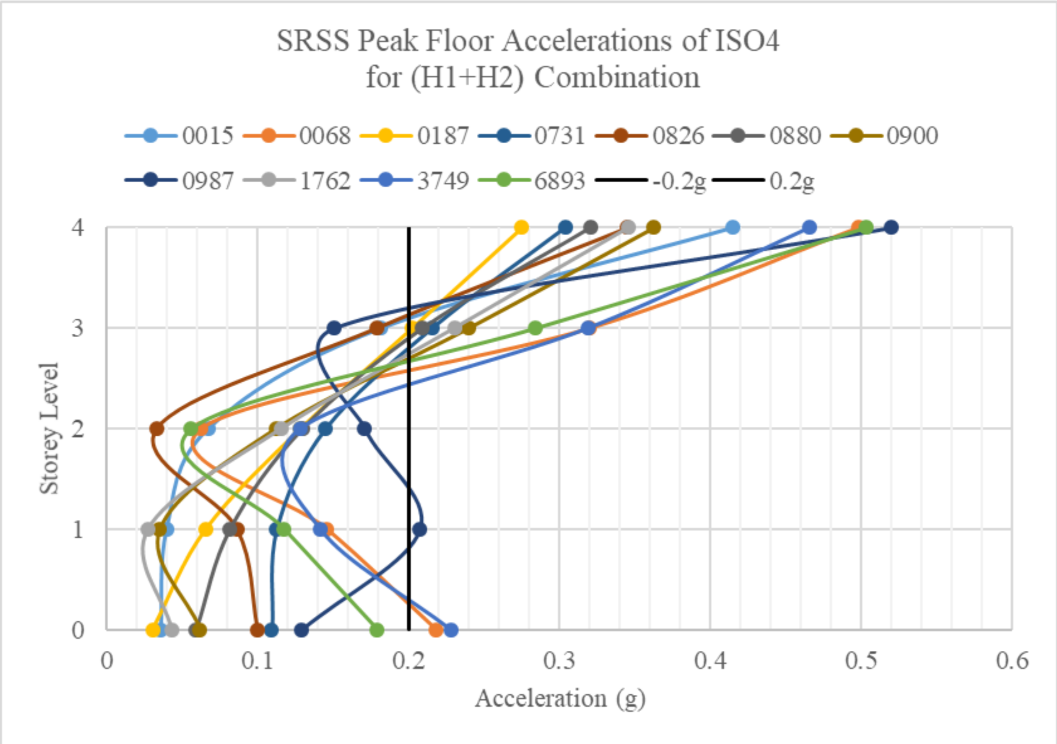

Figure 3.22. SRSS PFA of ISO4 from 11 GMs without Vertical Components

Peak floor accelerations for ISO4 system are presented in Figure 3.23 for selected 11 GMs with vertical component.

PFA results observed at the top floor of ISO4 system obtained from NTHA for 11 GMs with and without vertical component are listed in Table 3.22. Mean PFA values obtained from different 3 GM sets are presented in Table 3.23.

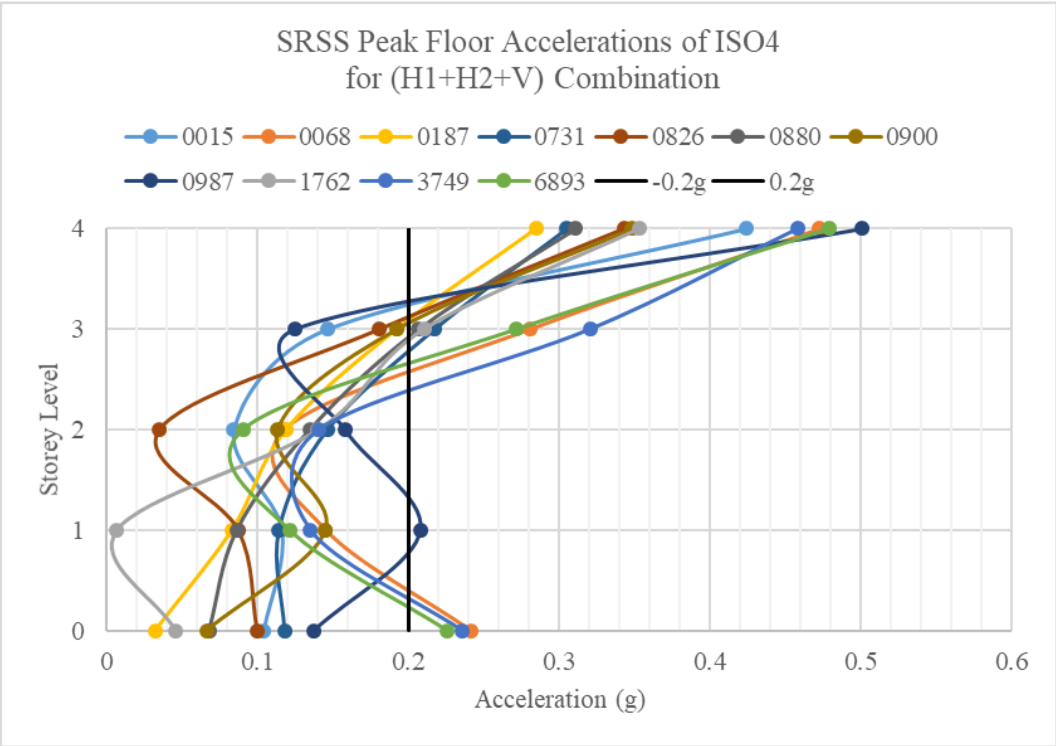

Figure 3.23. SRSS PFA of ISO4 from 11 GMs with Vertical Components

Table 3.22 PFA (g) of ISO4 Obtained from NTHA for 11 GM Records

GM #	SRSS PFA (g)		
	H1+H1	H1+H2+V	Difference (%)
0015	0.4145	0.4241	2.33%
0068	0.4978	0.4726	-5.06%
0187	0.2749	0.2845	3.50%
0731	0.3037	0.3047	0.33%
0826	0.3451	0.3430	-0.60%
0880	0.3202	0.3106	-3.00%
0900	0.3623	0.3484	-3.83%
0987	0.5197	0.5006	-3.67%
1762	0.3454	0.3527	2.12%
3749	0.4653	0.4579	-1.59%
6893	0.5034	0.4788	-4.88%

Table 3.23. Mean PFA (g) of each GM Set Obtained from NTHA for ISO4

GM Sets	SRSS PFA (g)
7 GMs Horizontal Components	0.3770
11 GMs Horizontal Components	0.3957
11 GMs Horizontal+ Vertical Components	0.3889

According to the results, it is clearly seen that selecting four more ground motions or using vertical components of GMs do not have any considerable effect on PFA values of ISO4 system like ISO2 system too.

3.1.2.3. IDR (%) Results for ISO4

Inter-storey drift ratios (%) distributed through the floors in x and y directions for ISO4 system are presented in Figures 3.24 and 3.25 for selected 11 GMs without vertical components.

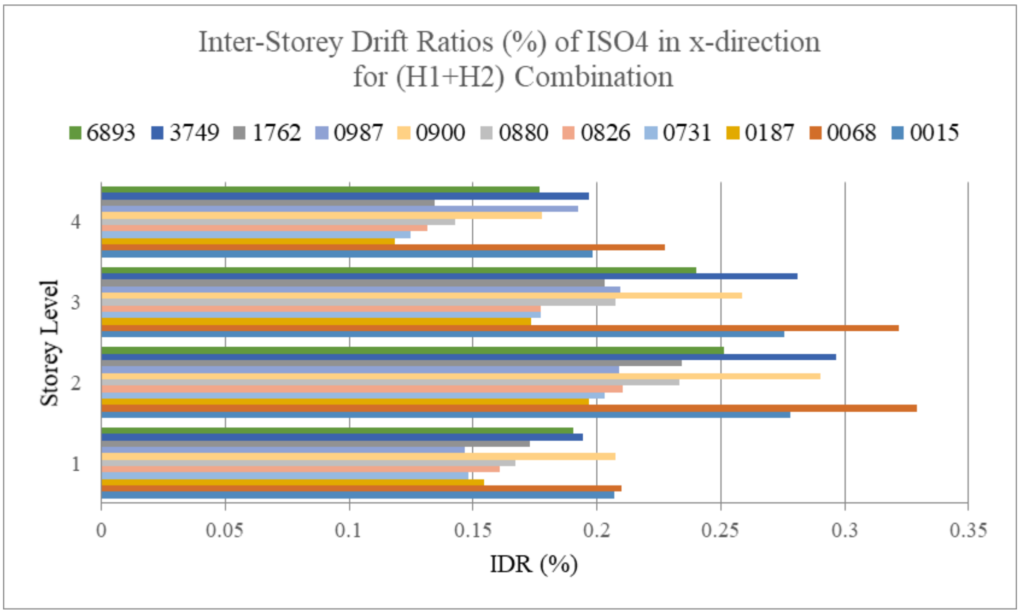

Figure 3.24. IDR (%) through Floors of ISO4 (in x-direction) from 11 GMs without Vertical Components

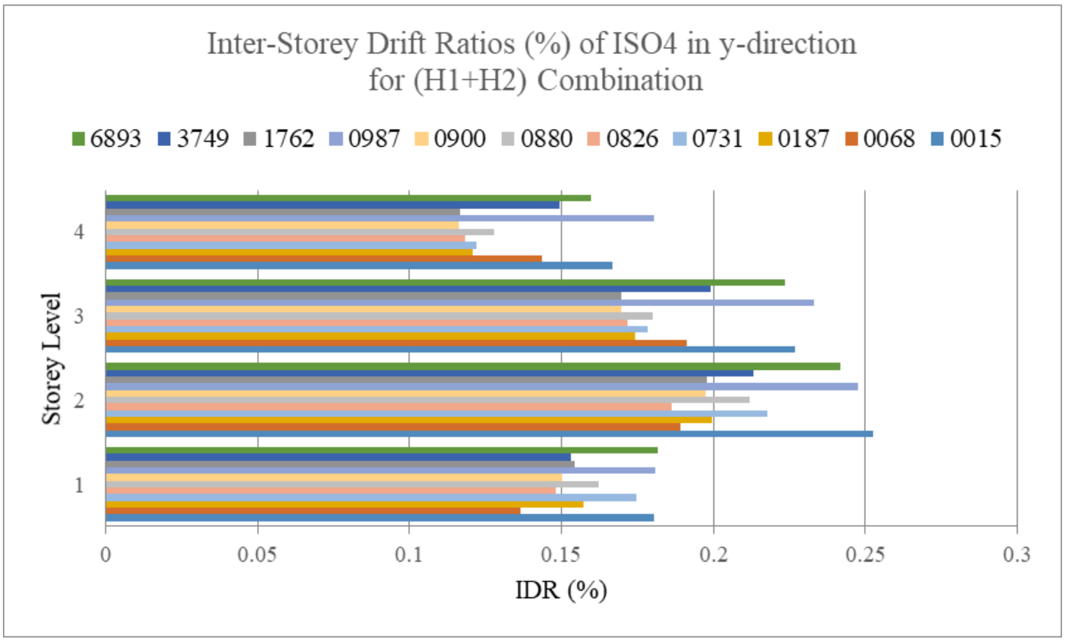

Figure 3.25. IDR (%) through Floors of ISO4 (in y-direction) from 11 GMs without Vertical Components

Inter-storey drift ratios (%) distributed through the floors in x and y directions for ISO4 system are demonstrated in Figures 3.26 and 3.27 for selected 11 GMs with vertical components.

Maximum IDR (%) results of ISO4 system obtained from NTHA for 11 GMs with and without vertical components are listed in Table 3.24. Mean IDR (%) obtained from different 3 GM sets are presented in Table 3.25.

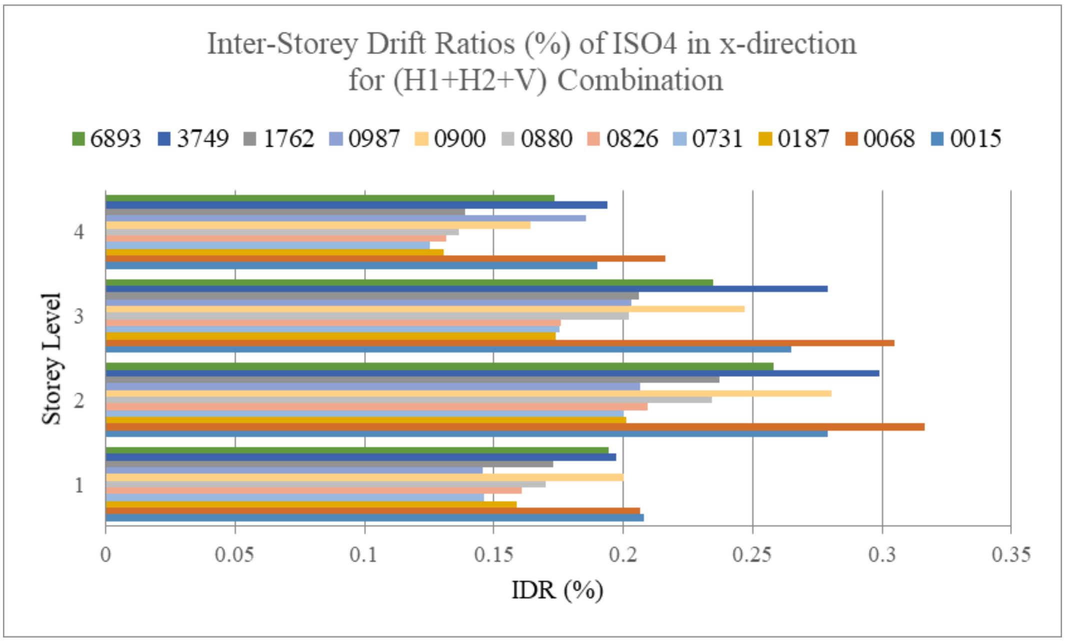

Figure 3.26. IDR (%) through Floors of ISO4 (in x-direction) from 11 GMs with Vertical Components

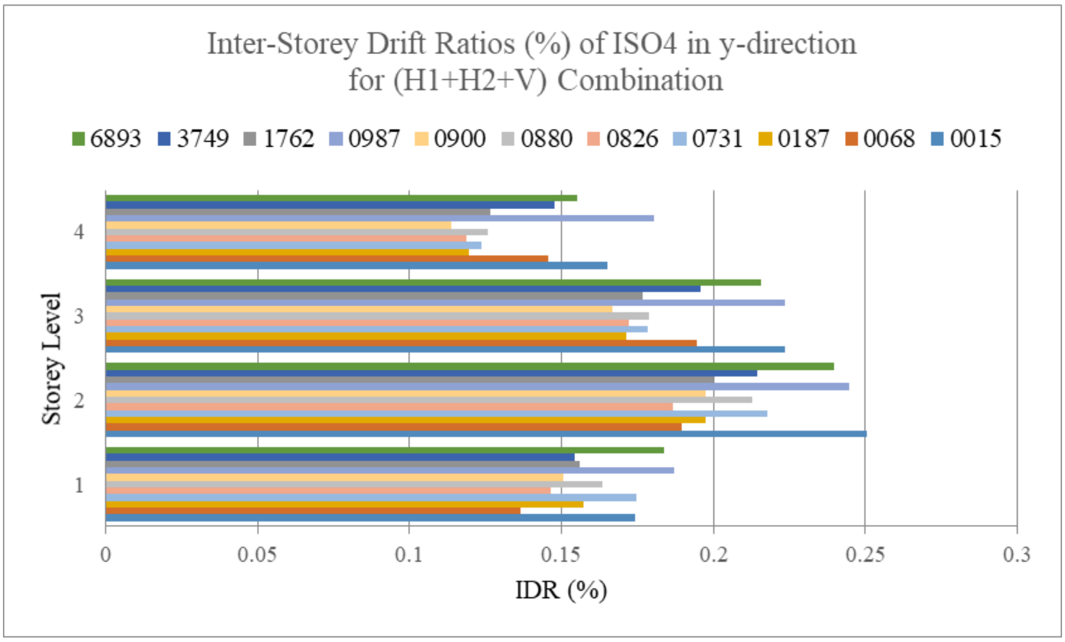

Figure 3.27. IDR (%) through Floors of ISO4 (in y-direction) from 11 GMs with Vertical Components

Table 3.24. Maximum IDR (%) Results of ISO4 Obtained from NTHA for 11 GMs

GM #	Max. IDR in x-direction (%)			Max. IDR in y-direction (%)		
	H1+H1	H1+H2+V	Difference (%)	H1+H1	H1+H2+V	Difference (%)
0015	0.2780	0.2791	0.39%	0.2525	0.2502	-0.89%
0068	0.3290	0.3162	-3.90%	0.1912	0.1946	1.80%
0187	0.1968	0.2010	2.12%	0.1996	0.1973	-1.11%
0731	0.2030	0.2004	-1.28%	0.2177	0.2178	0.05%
0826	0.2106	0.2095	-0.50%	0.1864	0.1867	0.14%
0880	0.2332	0.2341	0.38%	0.2121	0.2127	0.28%
0900	0.2903	0.2805	-3.37%	0.1972	0.1973	0.07%
0987	0.2096	0.2065	-1.47%	0.2476	0.2447	-1.17%
1762	0.2343	0.2373	1.27%	0.1979	0.1997	0.91%
3749	0.2967	0.2988	0.73%	0.2132	0.2144	0.56%
6893	0.2513	0.2581	2.71%	0.2416	0.2397	-0.81%

Table 3.25. Mean IDR (%) of each GM Set Obtained from NTHA for ISO4

GM Sets	Max. IDR in x-direction (%)	Max. IDR in y-direction (%)
7 GMs Horizontal Components	0.2610	0.2119
11 GMs Horizontal Components	0.2484	0.2143
11 GMs Horizontal+ Vertical Components	0.2474	0.2141

Any of the GMs does not exceed the maximum limits defined in specifications, which are explained in the beginning of this chapter.

According to presented results, using vertical component of GMs has not a considerable effect on IDR (%) parameters for ISO4 system too.

3.1.2.4. ISD Results for ISO4

The importance of isolation system displacement (ISD) parameter for isolation system design is discussed in previous part. It is also mentioned that system displacement is obtained from the SRSS (Square Root of the Sum of the Squares) of the displacements in x and y directions for each time instants of the ground motions. Obtained ISD in meters for 11 GMs with and without vertical components are presented in Figures 3.28 and 3.29 respectively.

Maximum SRSS ISD values of ISO2 system for 11 GMs are presented in Table 3.26. Mean ISD obtained from different 3 GM sets are presented in Table 3.27.

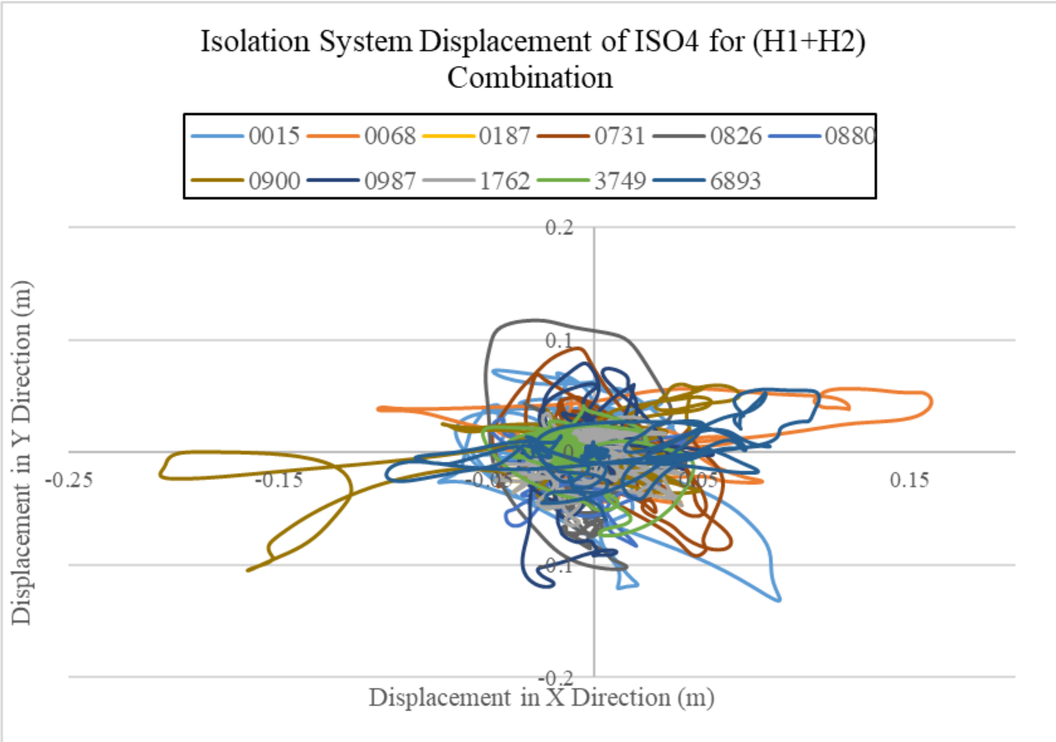

Figure 3.28. ISD of ISO4 from 11 GMs without Vertical Components

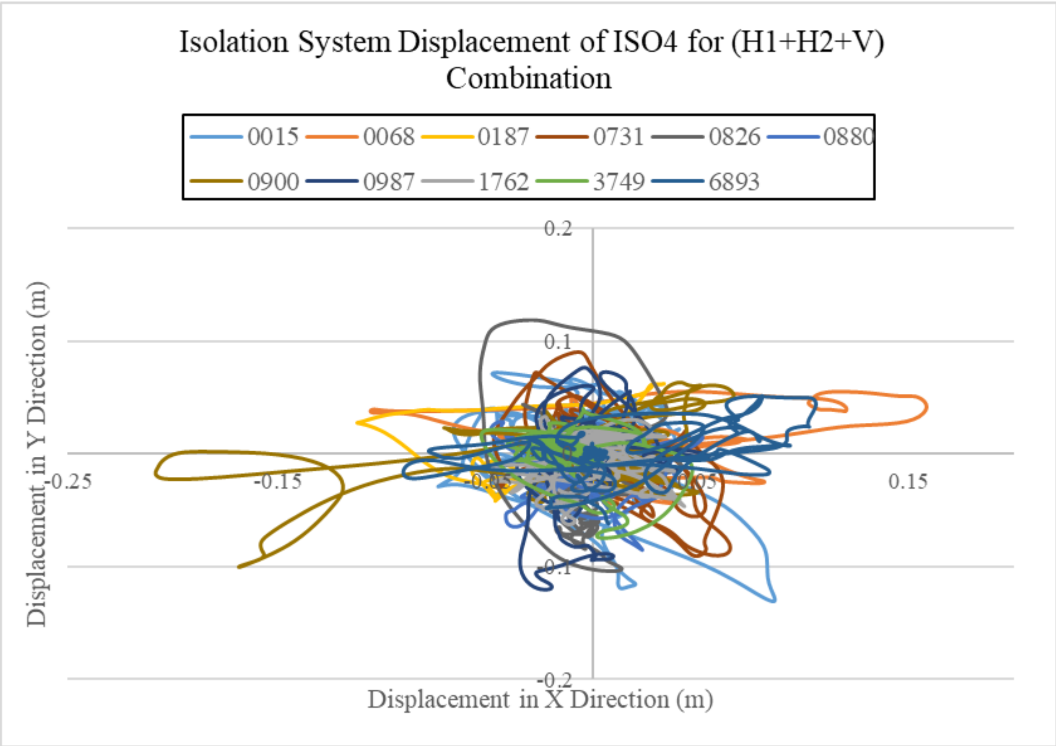

Figure 3.29. ISD of ISO4 from 11 GMs with Vertical Components

Table 3.26. Maximum SRSS ISD of ISO4 Obtained from NTHA for 11 GMs

GM #	Isolator Displacement (cm)		
	H1+H1	H1+H2+V	Difference (%)
0015	15.8282	15.6344	-1.22%
0068	16.6939	16.4370	-1.54%
0187	10.8491	11.5655	6.60%
0731	10.5637	10.8878	3.07%
0826	12.1827	12.3638	1.49%
0880	8.5343	8.8252	3.41%
0900	20.7380	20.8910	0.74%
0987	12.1610	12.2550	0.77%
1762	6.5626	6.3660	-3.00%
3749	7.4188	7.4756	0.77%
6893	11.8421	11.5557	-2.42%

Table 3.27 Mean SRSS ISD of each GM Set Obtained from NTHA for ISO4

GM Sets	Isolator Displacement (cm)
7 GMs Horizontal Components	12.9466
11 GMs Horizontal Components	12.1249
11 GMs Horizontal+ Vertical Components	12.2052

According to the results, selecting 11 ground motions rather than 7 ground motions decreases the obtained mean ISD like ISO2. When the vertical components of GMs are considered, even if the system displacement slightly increases, this rise is too small to consider.

3.1.2.5. Bending Moment of Columns and Shear Walls

The same column and shear wall selected for ISO2 are evaluated for ISO4. Maximum bending moment values of the selected column in x and y directions are demonstrated in Figure 3.30 and 3.31.

Maximum bending moment values of selected column for ISO4 system for 11 GMs are represented in Table 3.28 and mean bending moment values obtained from different 3 GM sets are presented in Table 3.29.

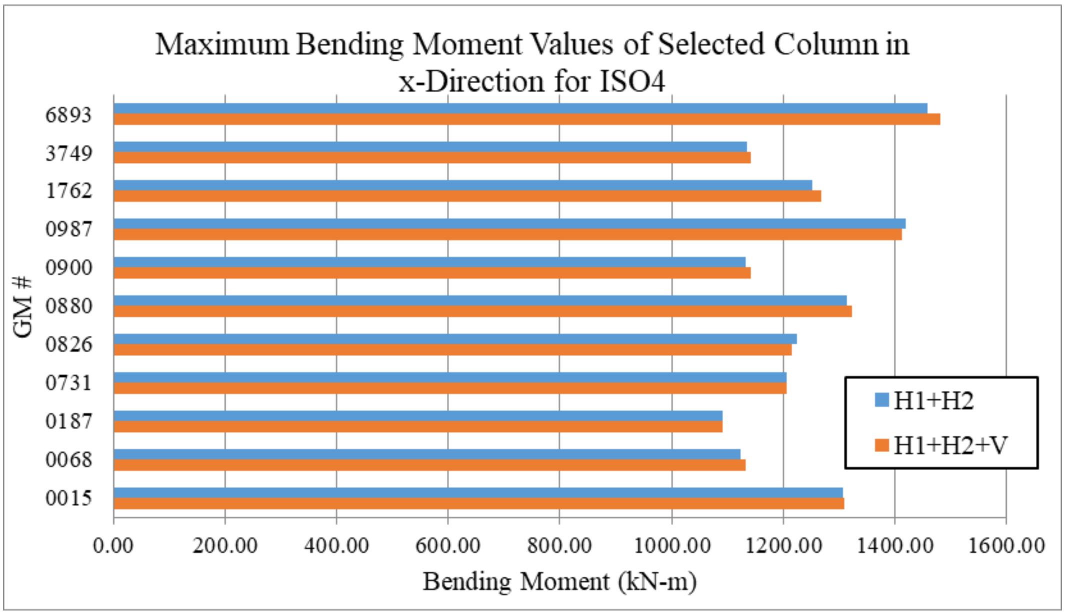

Figure 3.30. Maximum Bending Moment Values of Selected Column (in x-direction) for ISO4 from 11 GMs

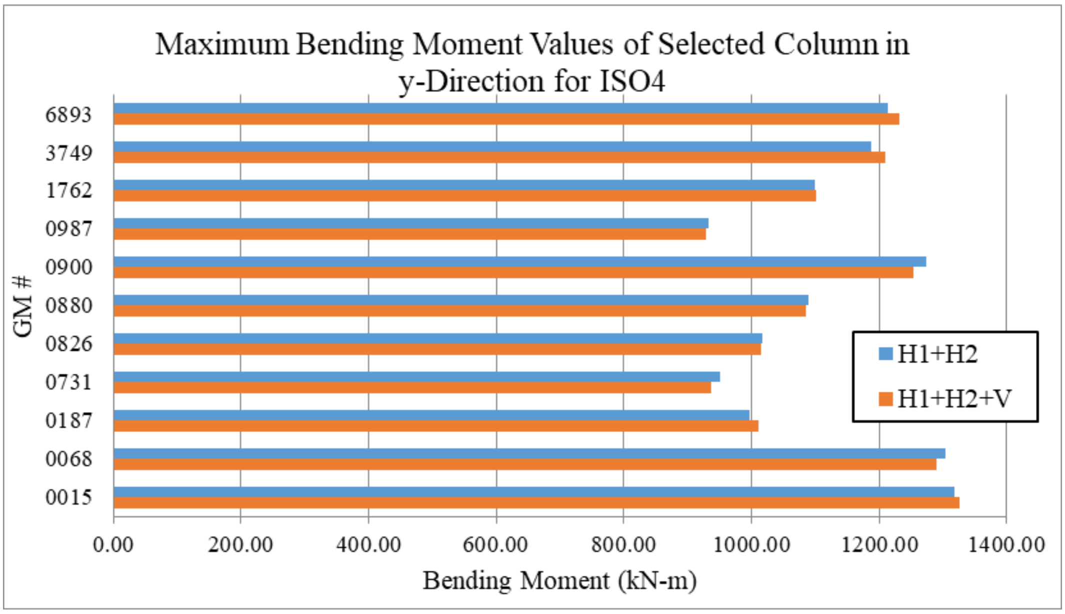

Figure 3.31. Maximum Bending Moment Values of Selected Column (in y-direction) for ISO4 from 11 GMs

Table 3.28. Values of Bending Moment of Selected Column of ISO4 Obtained from NTHA for 11GMs

GM #	Mx(kNm)			My(kNm)		
	H1+H1	H1+H2+V	Difference(%)	H1+H1	H1+H2+V	Difference(%)
0015	1306.76	1308.29	0.12%	1317.16	1325.71	0.65%
0068	1123.24	1131.59	0.74%	1304.96	1289.23	-1.21%
0187	1090.77	1091.49	0.07%	997.79	1010.92	1.32%
0731	1205.59	1204.99	-0.05%	950.65	937.46	-1.39%
0826	1224.63	1214.36	-0.84%	1016.61	1016.09	-0.05%
0880	1313.64	1322.56	0.68%	1088.83	1085.22	-0.33%
0900	1132.88	1142.29	0.83%	1273.94	1253.54	-1.60%
0987	1419.70	1412.02	-0.54%	932.79	928.13	-0.50%
1762	1252.45	1268.60	1.29%	1099.59	1100.63	0.09%
3749	1134.02	1141.30	0.64%	1188.58	1210.53	1.85%
6893	1457.47	1481.42	1.64%	1214.33	1232.76	1.52%

Table 3.29. Mean Values of Bending Moment of Selected Column of each GM Set Obtained from NTHA for ISO4

GM Sets	Mx (kNm)	My(kNm)
7 GMs Horizontal Components	1186.70	1160.27
11 GMs Horizontal Components	1241.92	1125.93
11 GMs Horizontal+ Vertical Components	1247.17	1126.38

According to obtained results, while selecting 4 more records increase the bending moment value in x-direction, it decreases the bending moment in y-direction. Additionally, the effect of vertical component on bending moment values of selected column is too small to consider.

Maximum bending moment values of the selected shear wall in x and y directions are demonstrated in Figures 3.32 and 3.33.

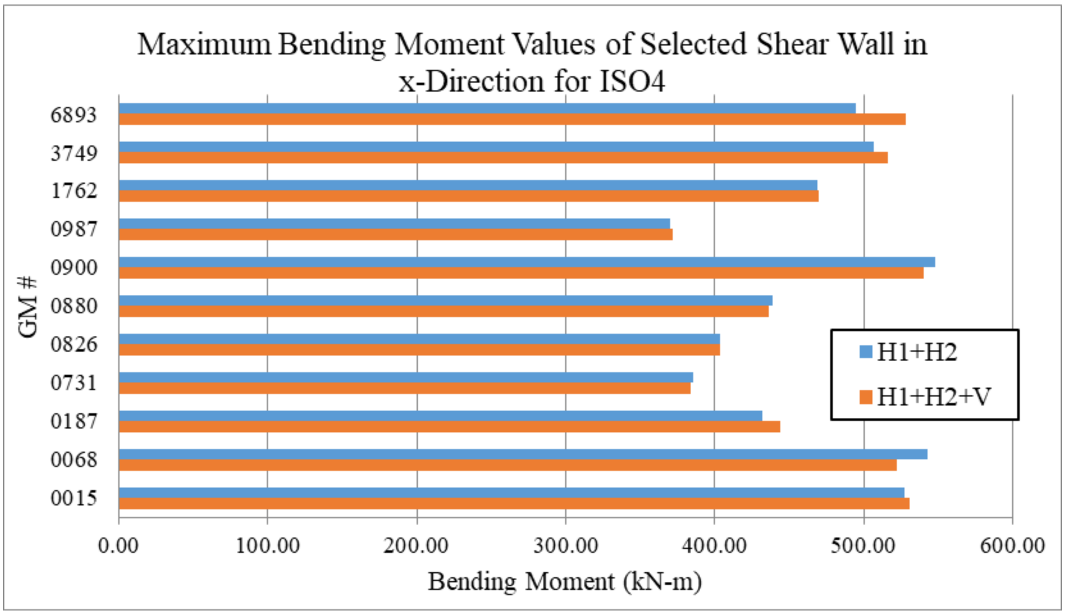

Figure 3.32. Maximum Bending Moment Values of Selected Shear Wall (in x-direction) for ISO4 from 11 GMs

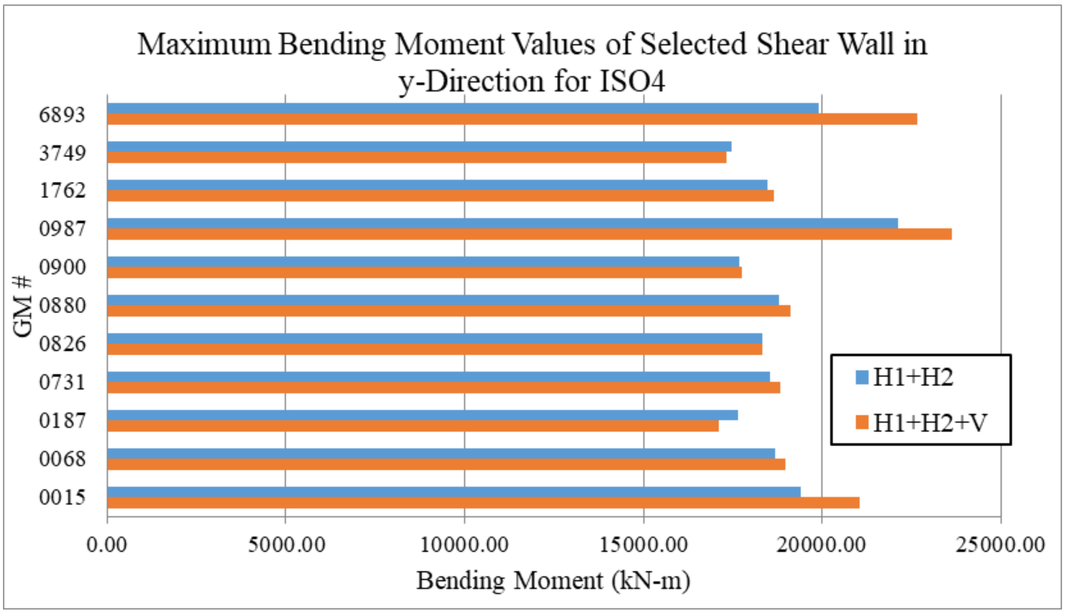

Figure 3.33 Maximum Bending Moment Values of Selected Shear Wall (in y-direction) for ISO4 from 11 GMs

Maximum bending moment values of selected shear wall for ISO4 system for 11 GMs are represented in Table 3.30 and mean bending moment values obtained from different 3 GM sets are presented in Table 3.31.

Table 3.30. Values of Bending Moment of Selected Shear Wall of ISO4 Obtained from NTHA for 11GMs

GM #	Mx(kNm)			My(kNm)		
	H1+H1	H1+H2+V	Difference(%)	H1+H1	H1+H2+V	Difference(%)
0015	527.89	530.87	0.56%	19415.61	21039.60	8.36%
0068	543.28	522.48	-3.83%	18695.22	18963.57	1.44%
0187	432.17	444.26	2.80%	17660.80	17104.20	-3.15%
0731	385.19	384.08	-0.29%	18559.10	18828.20	1.45%
0826	403.50	403.22	-0.07%	18317.83	18314.68	-0.02%
0880	438.61	436.09	-0.57%	18785.60	19119.45	1.78%
0900	547.85	539.98	-1.44%	17689.34	17745.61	0.32%
0987	370.02	372.15	0.58%	22146.79	23624.71	6.67%
1762	469.15	469.88	0.15%	18458.75	18642.21	0.99%
3749	507.23	516.48	1.82%	17479.98	17340.58	-0.80%
6893	494.76	528.12	6.74%	19915.79	22677.02	13.86%

Table 3.31. Mean Values of Bending Moment of Selected Shear Wall of each GM Set Obtained from NTHA for ISO4

GM Sets	Mx (kNm)	My(kNm)
7 GMs Horizontal Components	483.17	18326.52
11 GMs Horizontal Components	465.42	18829.53
11 GMs Horizontal+ Vertical Components	467.96	19399.99

Similar with the results of ISO2 system, selecting 4 more motions decrease the bending moment value in x-direction, and increase the value in y-direction for shear wall. While the effect of vertical ground motion is too small in weak axis of shear wall, the effect is more significant in strong axis. Even so, the effects are not so significant.

3.1.2.6. Axial Loads Acting on Isolators for ISO4

In order to examine the changes in axial loads acting on isolators, maximum and minimum axial loads carried by each isolator are evaluated for 11 different ground motions for ISO4 system. While negative values represent the compression on isolators, because friction pendulum isolators do not carry any tensile load, zero values expose that the related isolators are under the influence of tension.

Maximum and minimum loads acting on each isolator for 11 GMs without vertical components in ISO4 system are demonstrated in Figures 3.34 and 3.35.

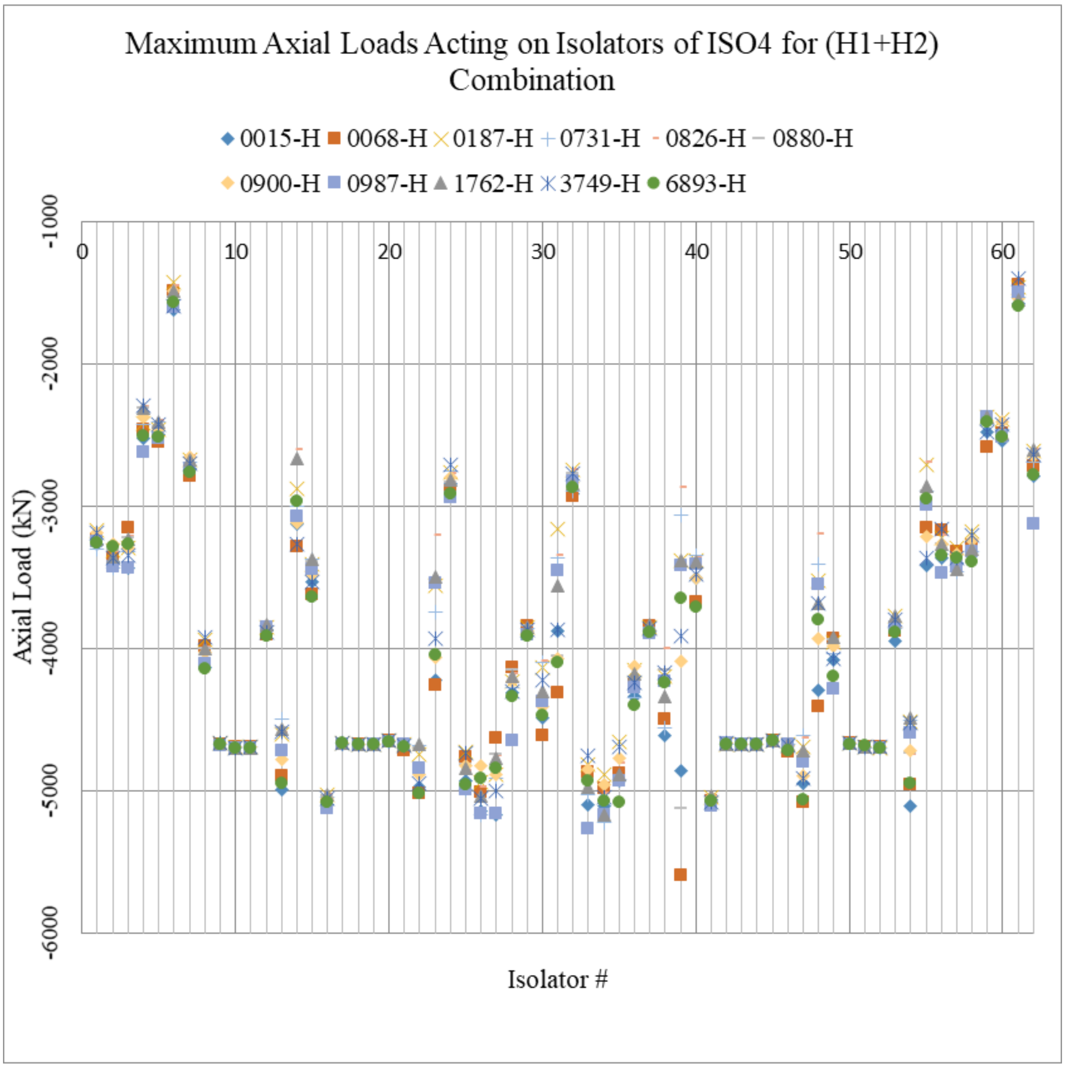

Figure 3.34. Maximum Axial Loads Acting on Each Isolator of ISO2 from 11 GMs without Vertical Components

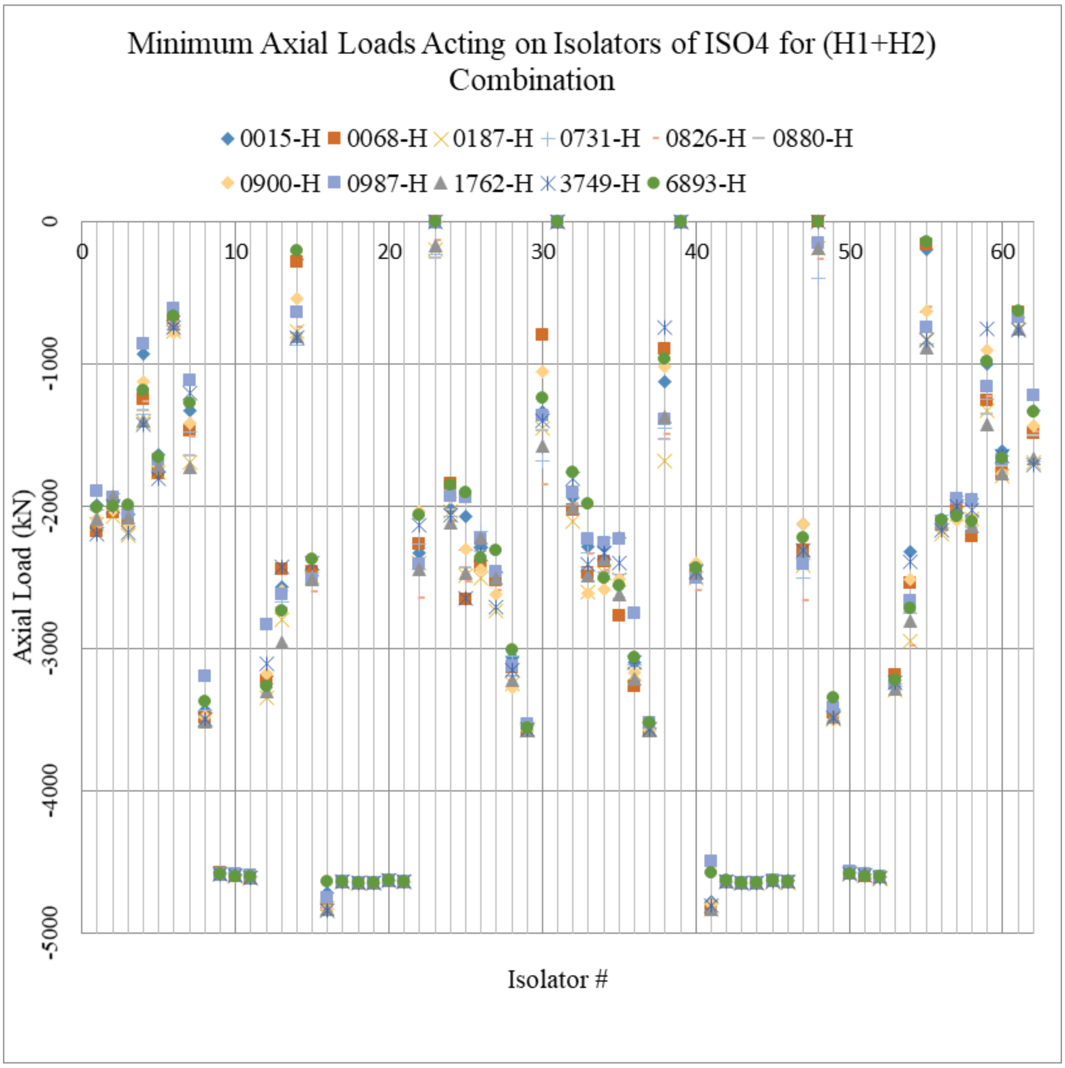

Figure 3.35. Minimum Axial Loads Acting on Each Isolator of ISO2 from 11 GMs without Vertical Components

While maximum axial loads are varying between 1000kN and 6000 kN (compression), minimum loads scatter between 0 and 5000 kN (compression). Tensile loads are generated by some GMs without vertical components on isolators 25, 34, 43 and 58.

For 11 GMs with vertical components, maximum and minimum axial loads are presented in Figures 3.36 and 3.37.

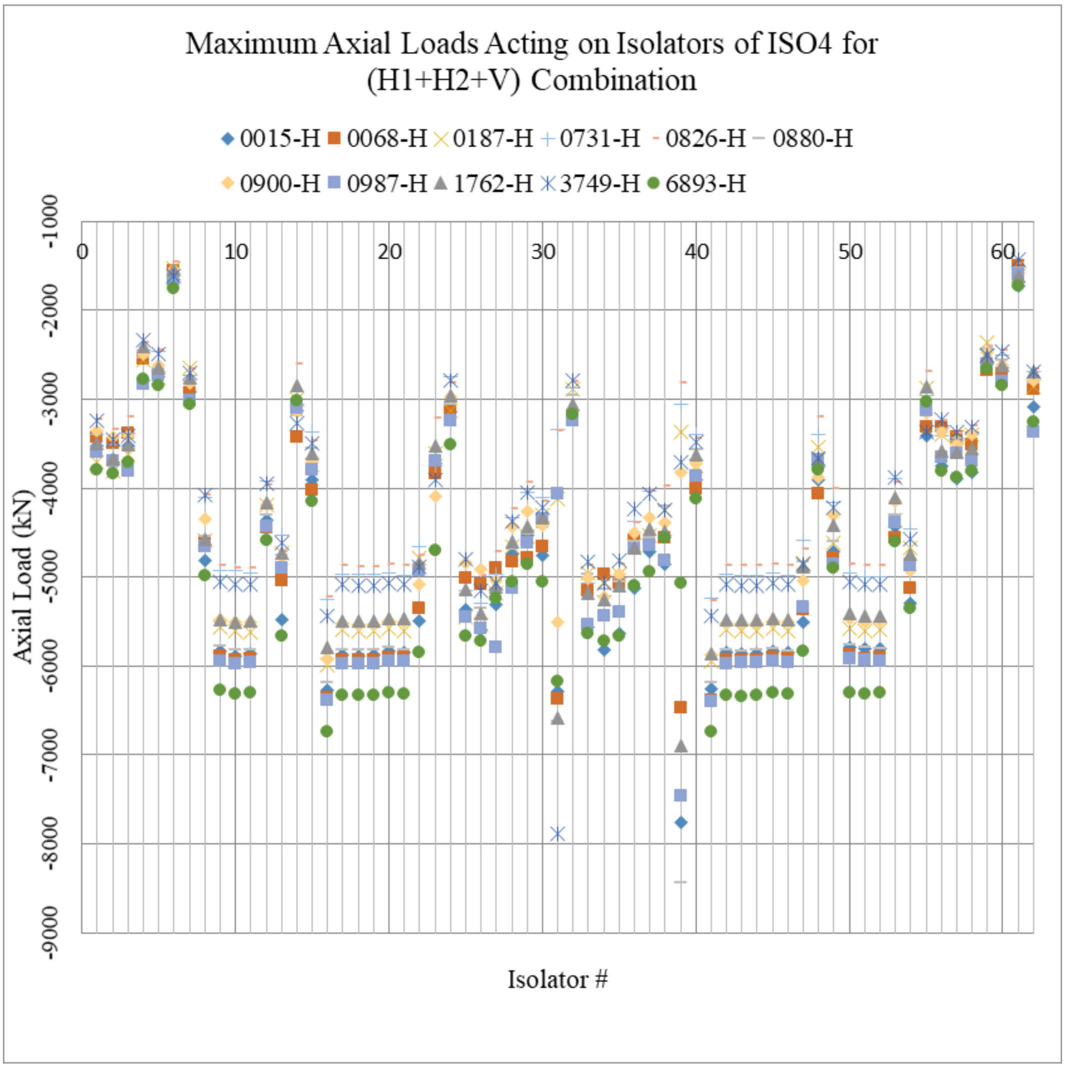

Figure 3.36. Maximum Axial Loads Acting on Each Isolator of ISO2 from 11 GMs with Vertical Components

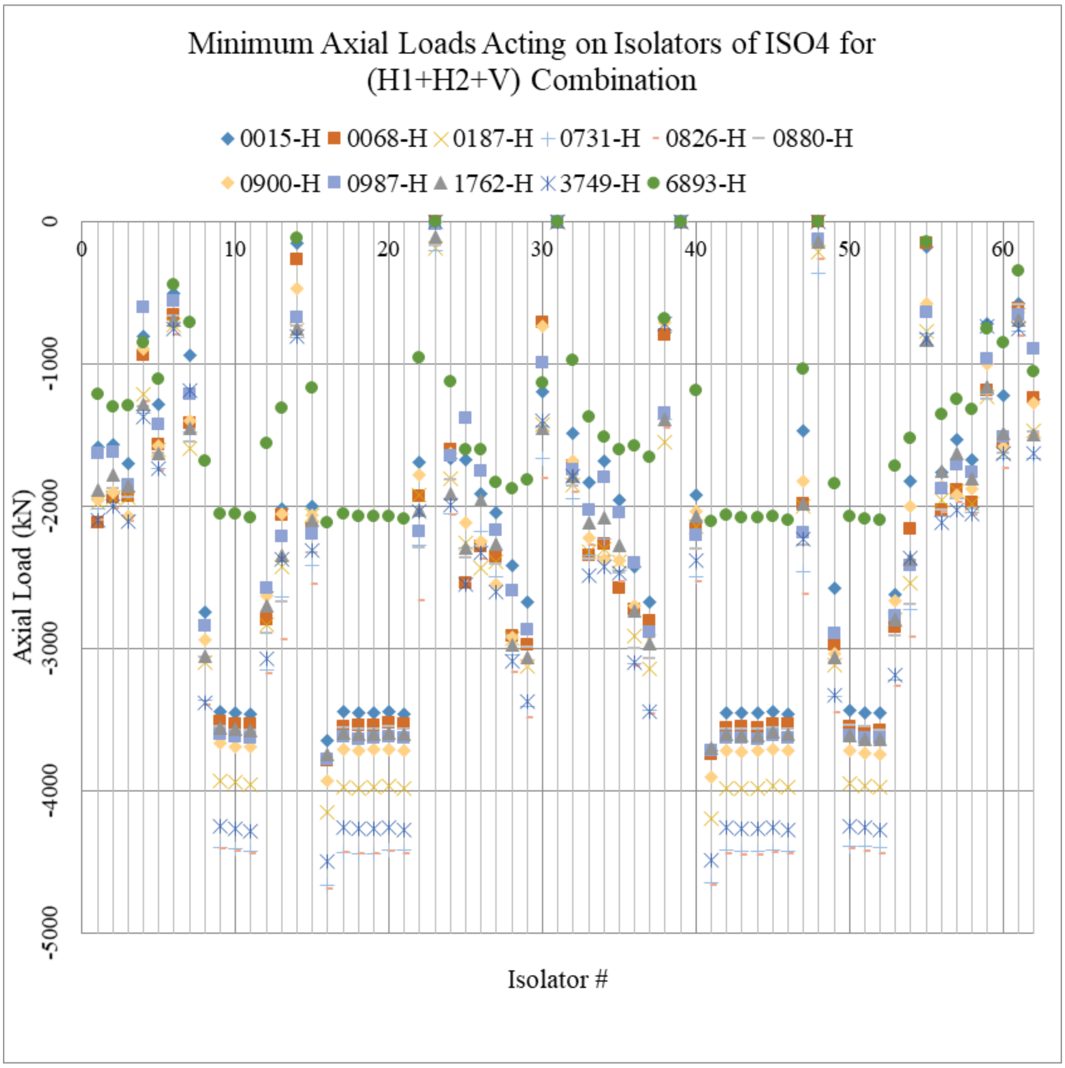

Figure 3.37. Minimum Axial Loads Acting on Each Isolator of ISO2 from 11 GMs with Vertical Components

While vertical components of ground motions increase the maximum axial loads on isolators, decrease the minimum axial loads. When compared with ISO2 system, the changes are more dramatic. It means that, vertical component makes columns of 4-storey buildings more sensitive than 2-storey buildings.

3.1.3. Analysis and Results of ISO7

In this part, evaluations made for ISO2 and ISO4 are repeated for ISO7 in order to make comparison between buildings having different number of floors.

3.1.3.1. Base Shear Results of ISO7

Maximum SRSS base shear values are presented in Figure 3.38.

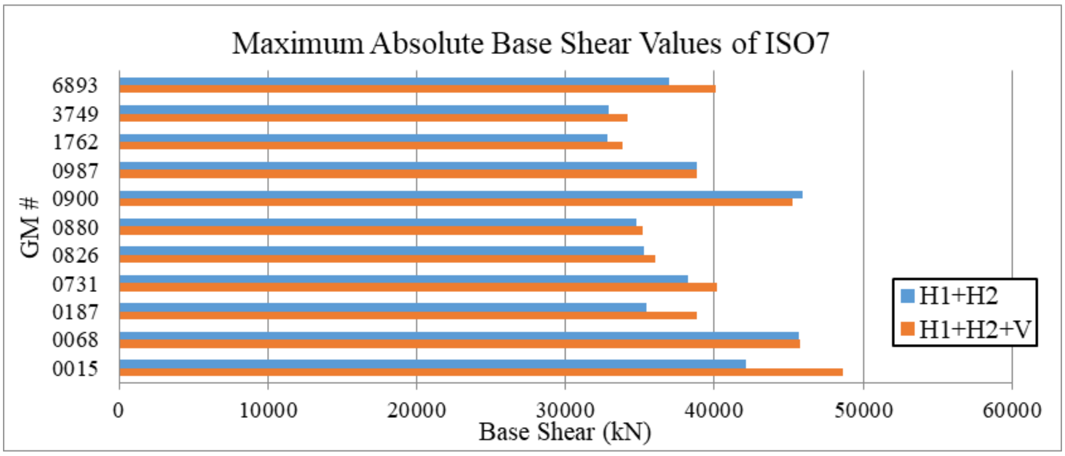

Figure 3.38. Maximum SRSS Base Shear Values of ISO7 from 11 GMs

Similar with ISO2 and ISO4 systems, base shear values are higher when vertical component is included in analysis for selected 11 GMs.

Base shear values of ISO7 system obtained from NTHA for 11 GMs with and without vertical component are listed in Table 3.33. Mean IDR (%) parameters of different 3 GM sets are presented in Table 3.34.

Table 3.32. Base Shear Coefficients of ISO7 Obtained from NTHA for 11 GMs

GM #	Base Shear Coefficients	
	H1+H1	H1+H2+V
0015	11.48%	13.24%
0068	12.44%	12.48%
0187	9.66%	10.56%
0731	10.41%	10.94%
0826	9.62%	9.80%
0880	9.48%	9.59%
0900	12.52%	12.32%
0987	10.57%	10.57%
1762	8.95%	9.22%
3749	8.97%	9.31%
6893	10.06%	10.93%

According to the presented results, similar with the other two systems, considering vertical components of motions in analysis increases the base shear values significantly for ISO7 system. Selecting eleven GMs rather than 7 GMs does not cause an identifiable change in base shear values.

As it can be seen from figures, base shear values are higher in between 0-16 % when vertical component is included in analysis for selected 11 GMs. The change in base shear coefficients are 1% and smaller, similar with ISO2 and ISO4, for selected ground motion records.

Table 3.33 Base Shear Values of ISO7 Obtained from NTHA for 11 GMs

GM #	Vb(kN)		
	H1+H1	H1+H2+V	Difference (%)
0015	42144.10	48630.70	15.39%
0068	45666.84	45804.38	0.30%
0187	35459.93	38790.71	9.39%
0731	38213.89	40175.01	5.13%
0826	35311.59	35996.08	1.94%
0880	34806.02	35211.32	1.16%
0900	45966.68	45239.17	-1.58%
0987	38800.97	38805.36	0.01%
1762	32843.29	33837.35	3.03%
3749	32920.48	34198.83	3.88%
6893	36940.24	40124.65	8.62%

Table 3.34. Mean Base Shear Values of each GM Set Obtained from NTHA for ISO7

GM Sets	Vb (kN)
7 GMs Horizontal Components	39311.13
11 GMs Horizontal Components	38097.64
11 GMs Horizontal+ Vertical Components	39710.32

3.1.3.2. PFA Results of ISO7

SRSS Peak floor accelerations for ISO7 system are demonstrated in Figure 3.39 for selected 11 GMs without vertical component.

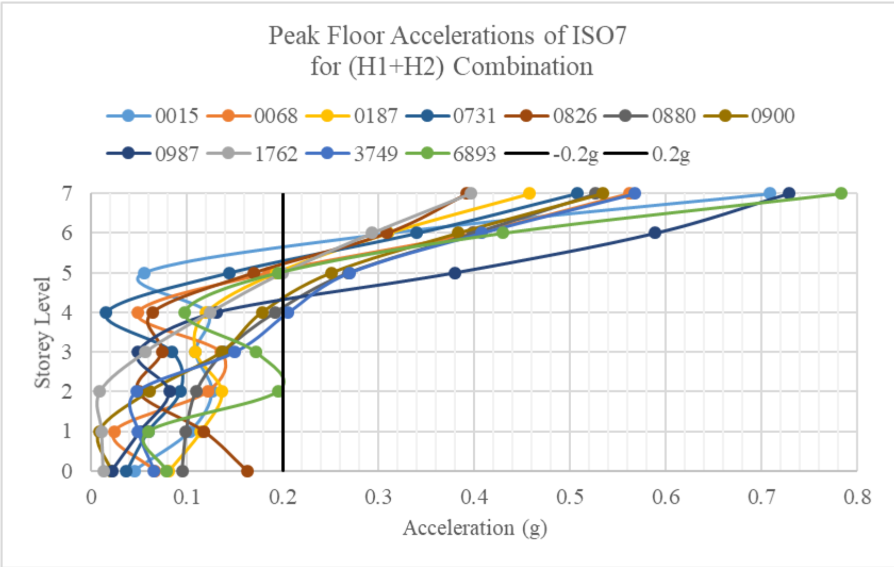

Figure 3.39. SRSS PFA of ISO7 from 11 GMs without Vertical Components

SRSS peak floor accelerations for ISO7 system are presented in Figure 3.40 for selected 11 GMs with vertical component.

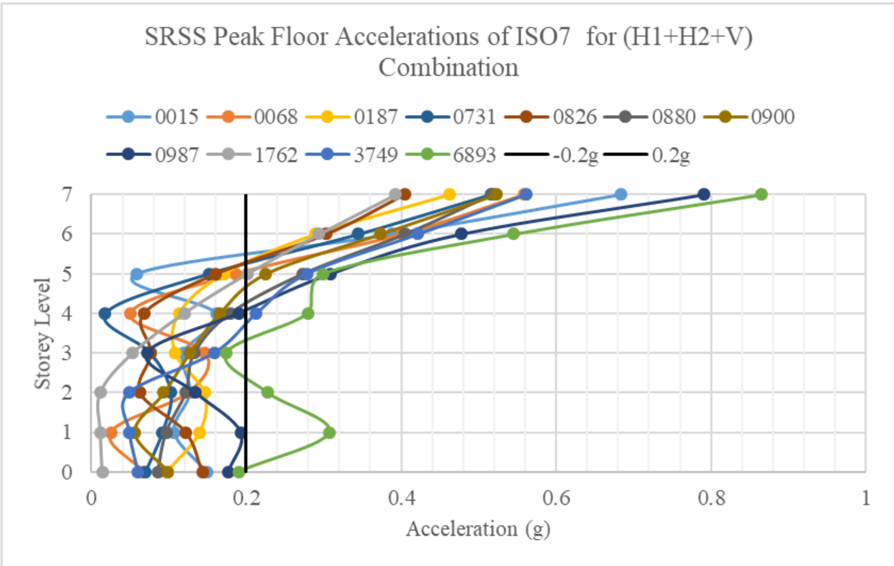

Figure 3.40. SRSS PFA of ISO7 from 11 GMs with Vertical Components

PFA results observed at the top floor of ISO7 system obtained from NTHA for 11 GMs with and without vertical component are listed in Table 3.35. Mean PFA values obtained from different 3 GM sets are presented in Table 3.36.

Table 3.35. PFA (g) of ISO7 Obtained from NTHA from 11 GM Records

GM #	SRSS PFA (g)		
	H1+H1	H1+H2+V	Difference (%)
0015	0.7088	0.6832	-3.62%
0068	0.5616	0.5584	-0.58%
0187	0.4577	0.4624	1.03%
0731	0.5070	0.5154	1.66%
0826	0.3922	0.4045	3.16%
0880	0.5266	0.5171	-1.80%
0900	0.5339	0.5234	-1.97%
0987	0.7283	0.7913	8.65%
1762	0.3958	0.3927	-0.78%
3749	0.5679	0.5609	-1.23%
6893	0.7829	0.8654	10.55%

Table 3.36. Mean PGA (g) of each GM Set Obtained from NTHA for ISO7

GM Sets	SRSS PFA (g)
7 GMs Horizontal Components	0.5519
11 GMs Horizontal Components	0.5602
11 GMs Horizontal+ Vertical Components	0.5704

According to the results, it is clearly seen that selecting four more ground motions or using vertical components of GMs do not have any considerable effect on PFA values of ISO7 system as similar as the other two systems too.

3.1.3.3. IDR (%) Results for ISO7

Inter-storey drift ratios (%) distributed through the floors in x and y directions for ISO7 system are presented in Figures 3.41 and 3.42 for selected 11 GMs without vertical components.

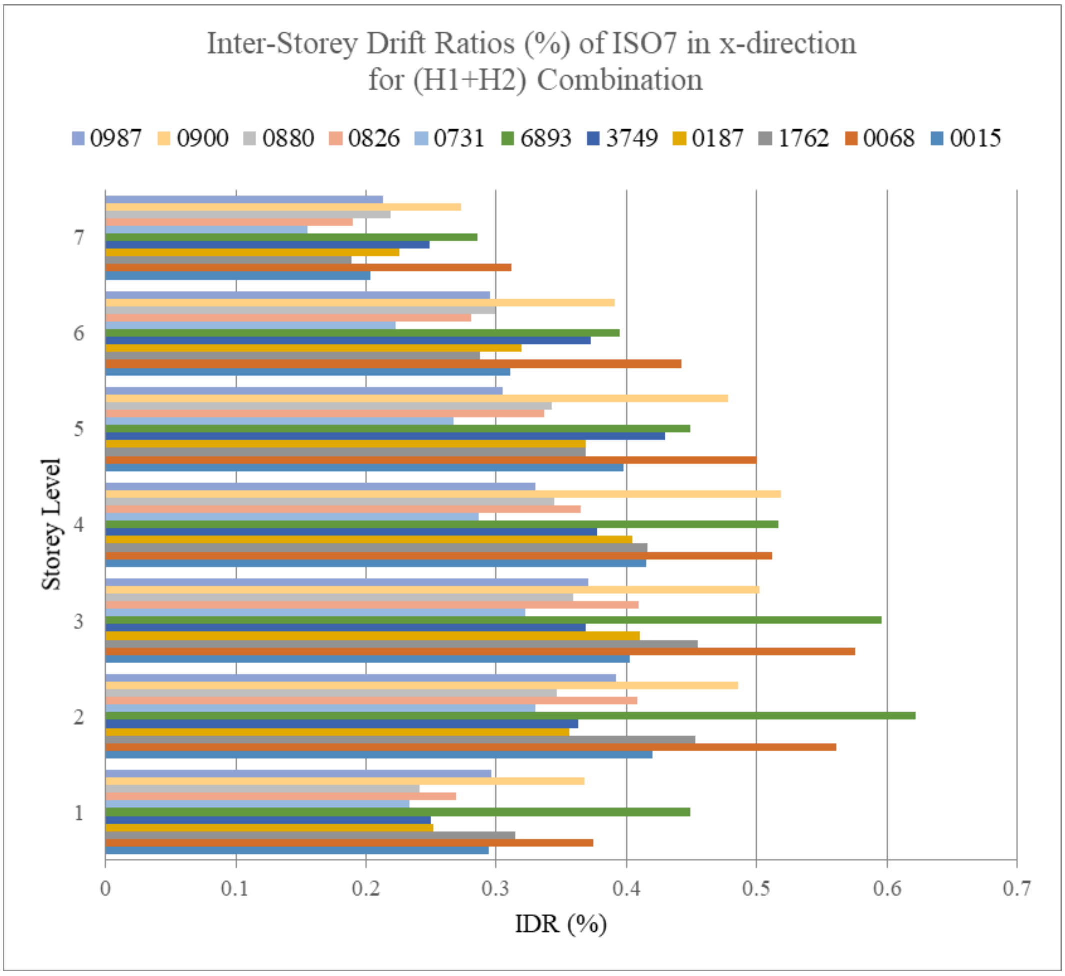

Figure 3.41. IDR (%)) through Floors of ISO7 (in x-direction from 11 GM Records without Vertical Component)

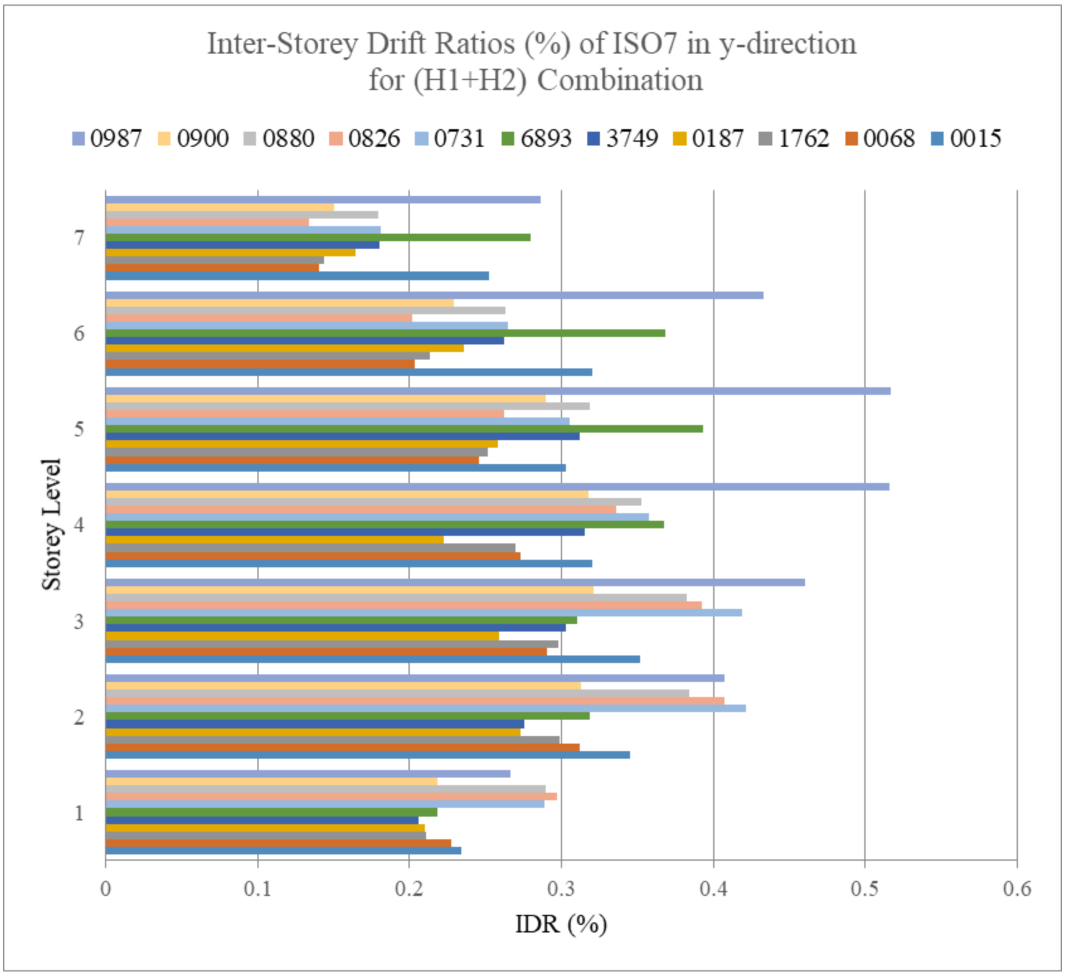

Figure 3.42. IDR (%) through Floors of ISO7 (in y-direction) from 11 GM Records without Vertical Component

Inter-storey drift ratios (%) distributed through the floors in x and y directions for ISO7 system are demonstrated in Figures 3.43 and 3.44 for selected 11 GMs with vertical components.

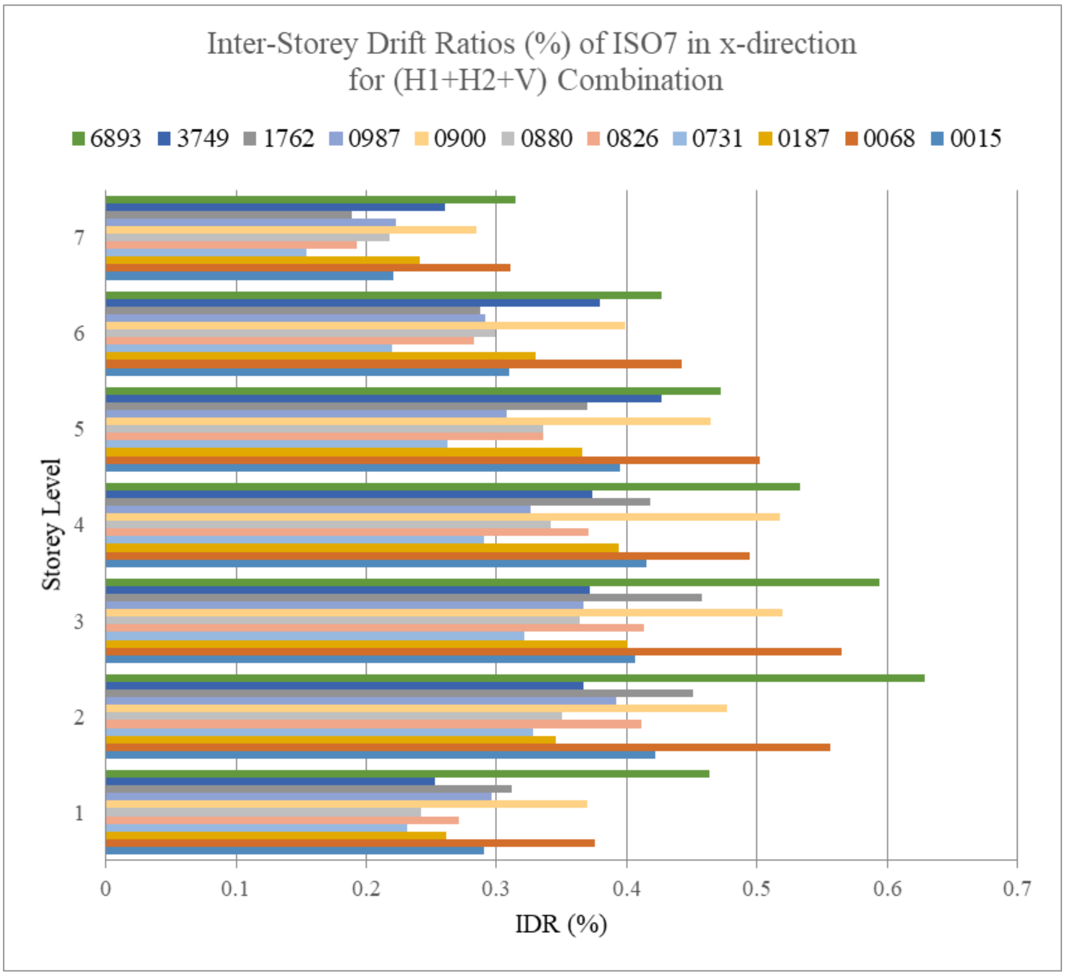

Figure 3.43. IDR (%) through Floors of ISO7 (in x-direction) from 11 GM Records with Vertical Component

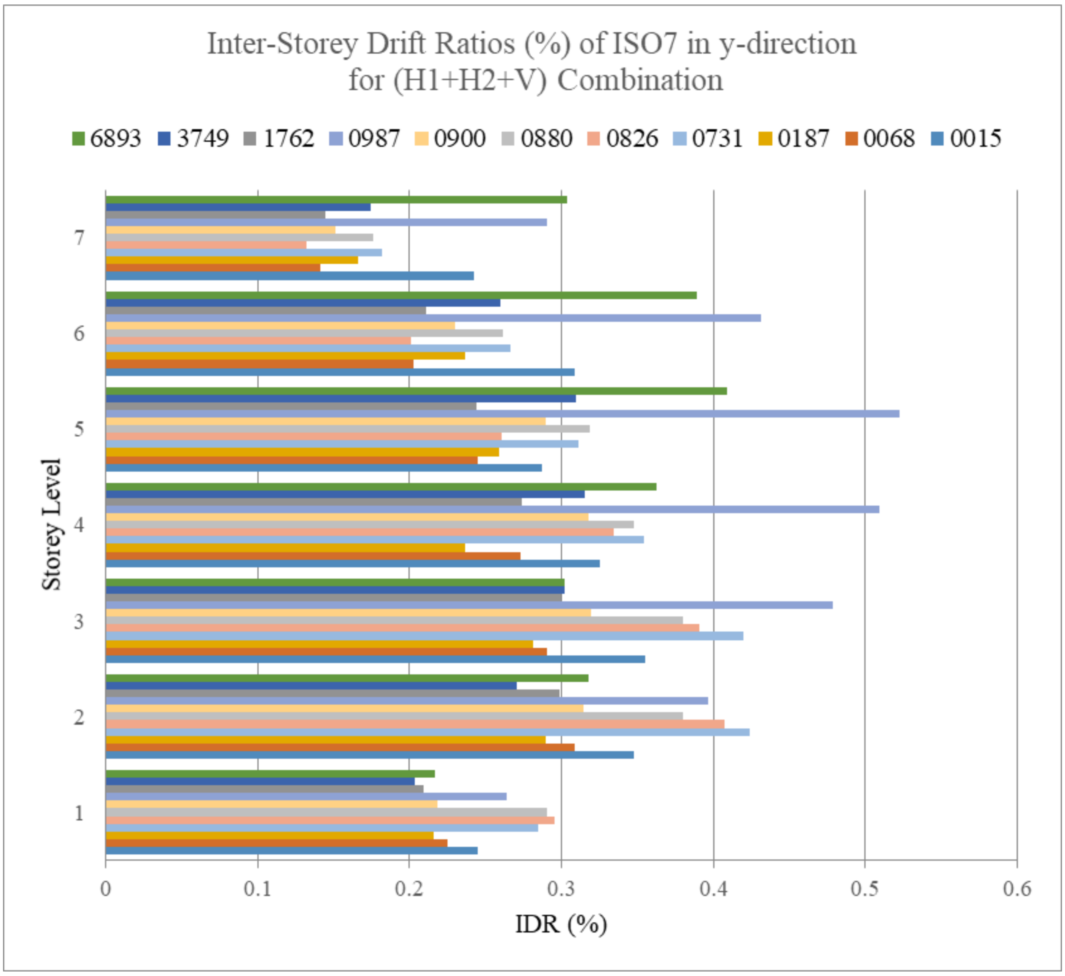

Figure 3.44. IDR (%) through Floors of ISO7 (in y-direction) from 11 GM Records with Vertical Component

Maximum IDR (%) results of ISO7 system obtained from NTHA for 11 GMs with and without vertical components are listed in Table 3.37. Mean IDR (%) obtained from different 3 GM sets are presented in Table 3.38.

Table 3.37. Maximum IDR (%) Results of ISO4 Obtained from NTHA for 11 GMs

GM #	Max. IDR in x-direction (%)			Max. IDR in y-direction (%)		
	H1+H1	H1+H2+V	Difference (%)	H1+H1	H1+H2+V	Difference (%)
0015	0.4201	0.4217	0.38%	0.3519	0.3552	0.95%
0068	0.5752	0.5651	-1.76%	0.3116	0.3087	-0.92%
1762	0.4551	0.4575	0.53%	0.2984	0.2994	0.34%
0187	0.4105	0.4005	-2.45%	0.2727	0.2899	6.30%
3749	0.4293	0.4269	-0.55%	0.3152	0.3150	-0.05%
6893	0.6223	0.6292	1.11%	0.3929	0.4087	4.02%
0731	0.3300	0.3277	-0.69%	0.4210	0.4235	0.59%
0826	0.4095	0.4129	0.82%	0.4075	0.4068	-0.17%
0880	0.3592	0.3635	1.21%	0.3842	0.3801	-1.05%
0900	0.5184	0.5197	0.26%	0.3211	0.3198	-0.42%
0987	0.3916	0.3917	0.05%	0.5170	0.5220	0.98%

Table 3.38. Mean IDR (%) of each GM Set Obtained from NTHA for ISO2

GM Sets	Max. IDR in x-direction (%)	Max. IDR in y-direction (%)
Set 1	0.4347	0.3397
Set2	0.4474	0.3630
Set 3	0.4469	0.3663

Any of the GMs does not exceed the maximum limits defined in specifications, which are explained in the beginning of this chapter.

According to presented results, using vertical component of GMs has not a considerable effect on IDR (%) parameters for ISO7 system too.

3.1.3.4. ISD Results for ISO7

The system displacement is obtained from the SRSS (Square Root of the Sum of the Squares) of the displacements in x and y directions for each time instants of the ground motions. Obtained ISD in meters for 11 GMs with and without vertical components are presented in Figures 3.45 and 3.46 respectively.

Maximum SRSS ISD values of ISO7 system for 11 GMs are presented in Table 3.39. Mean ISD obtained from different 3 GM sets are presented in Table 3.40.

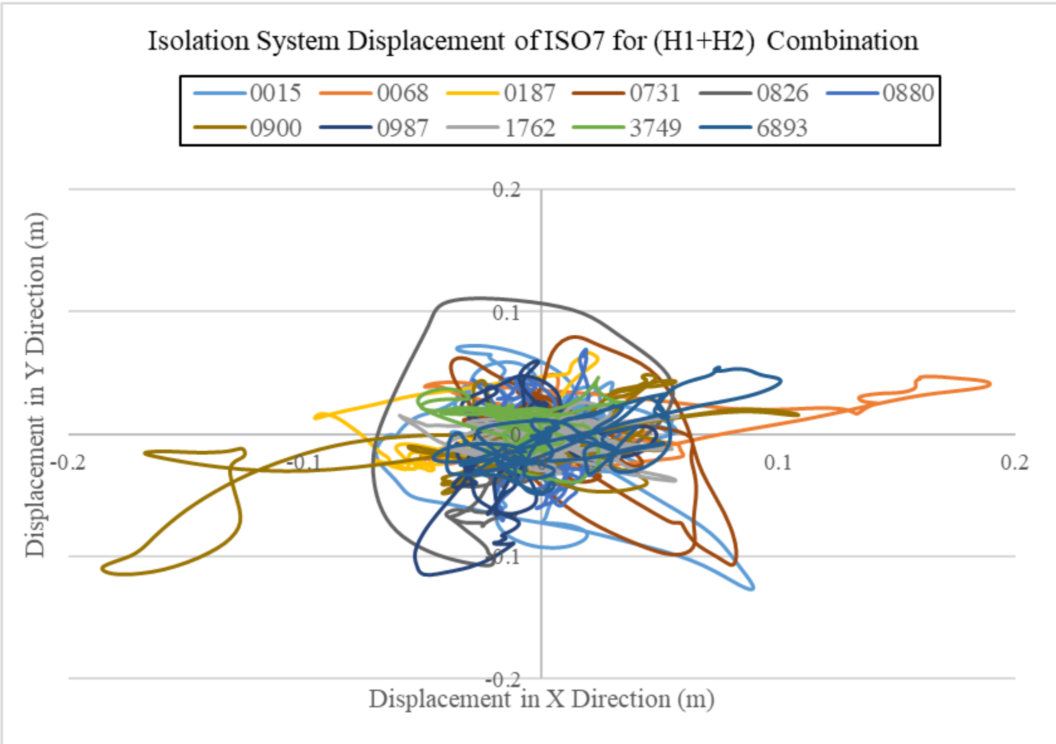

Figure 3.45. ISD of ISO7 from GM Records without Vertical Components

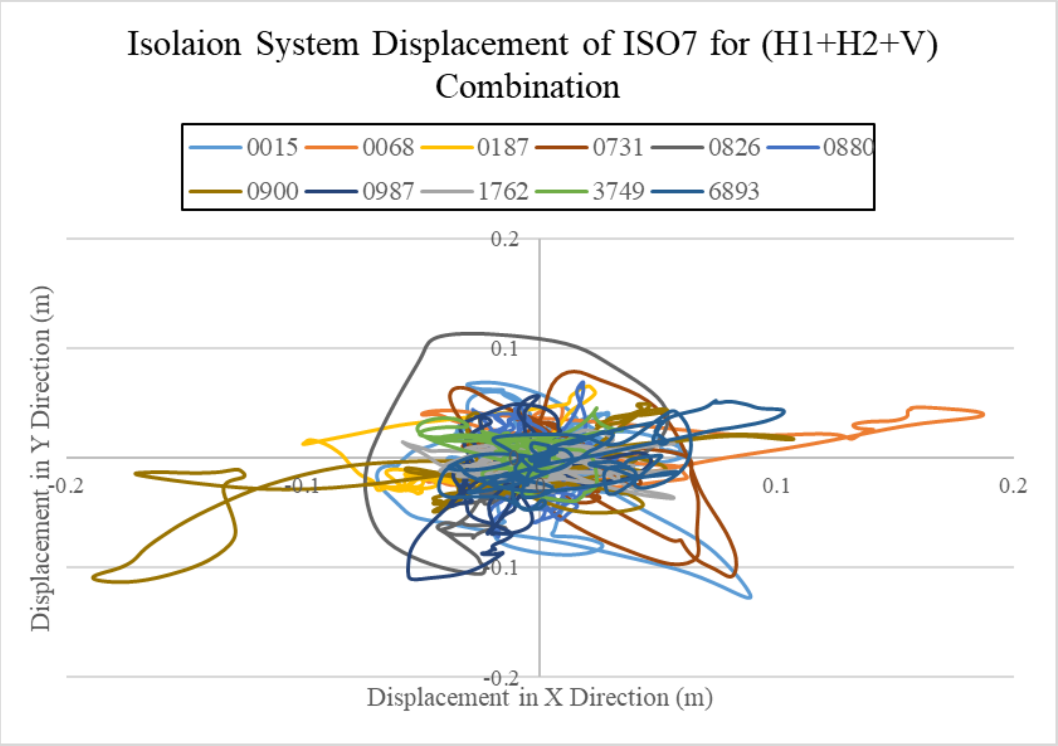

Figure 3.46. ISD of ISO7 from GM Records with Vertical Components

Table 3.39. Maximum SRSS ISD of ISO7 Obtained from NTHA for 11 GM Records

GM #	Isolator Displacement (cm)		
	H1+H1	H1+H2+V	Difference (%)
0015	15.47	15.51	0.23%
0068	19.38	19.15	-1.23%
0187	9.69	10.10	4.24%
0731	13.36	13.47	0.86%
0826	11.56	11.87	2.74%
0880	7.25	7.41	2.24%
0900	21.62	21.83	0.99%
0987	12.49	12.29	-1.58%
1762	6.79	6.71	-1.26%
3749	6.00	5.94	-0.97%
6893	11.00	11.16	1.44%

Table 3.40. Mean SRSS ISD of each GM Set Obtained from NTHA for ISO7

GM Sets	Isolator Displacement (cm)
7 GMs Horizontal Components	13.2528
11 GMs Horizontal Components	12.2370
11 GMs Horizontal+ Vertical Components	12.3128

As seen from the results, selecting 11 ground motions rather than 7 ground motions decreases the obtained mean ISD like ISO2 and ISO4. The change in displacement when vertical components of GMs are considered is too small to consider.

3.1.3.5. Bending Moment of Columns and Shear Walls

The same column and shear wall selected for ISO2 and ISO4 are evaluated for ISO7. Maximum bending moment values of the selected column in x and y directions are demonstrated in Figures 3.47 and 3.48.

Maximum bending moment values of selected column for ISO4 system for 11 GMs are represented in Table 3.41 and mean bending moment values obtained from different 3 GM sets are presented in Table 3.42.

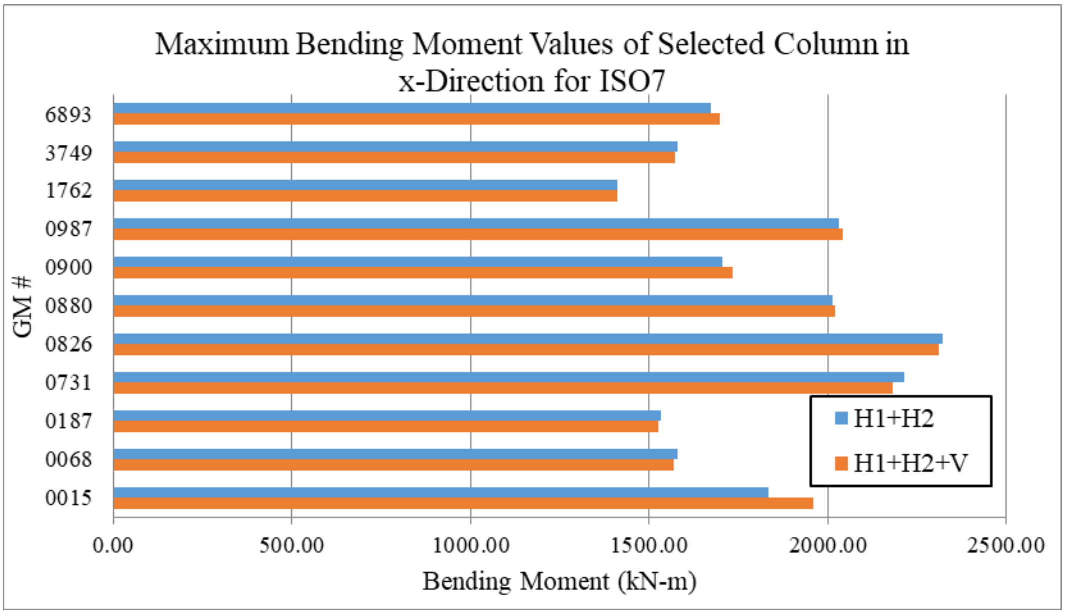

Figure 3.47. Maximum Bending Moment Values of Selected Column (in x-direction) for ISO7 from 11 GMs

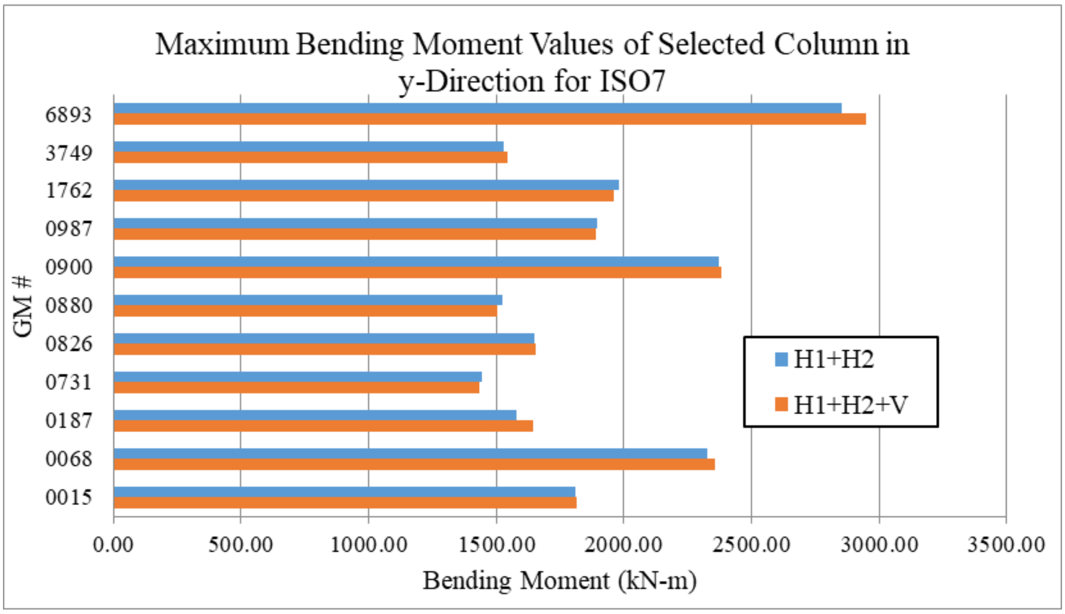

Figure 3.48. Maximum Bending Moment Values of Selected Column (in y-direction) for ISO7 from 11 GMs

Table 3.41. Values of Bending Moment of Selected Column of ISO7 Obtained from NTHA for 11GMs

GM #	Mx(kNm)			My(kNm)		
	H1+H1	H1+H2+V	Difference(%)	H1+H1	H1+H2+V	Difference(%)
0015	1833.20	1958.45	6.83%	1812.64	1817.55	0.27%
0068	1578.91	1570.55	-0.53%	2324.92	2358.32	1.44%
0187	1532.36	1524.45	-0.52%	1581.52	1646.89	4.13%
0731	2214.98	2180.66	-1.55%	1446.24	1436.26	-0.69%
0826	2319.88	2309.43	-0.45%	1648.43	1654.20	0.35%
0880	2013.46	2021.48	0.40%	1522.71	1502.33	-1.34%
0900	1704.15	1733.13	1.70%	2373.97	2382.78	0.37%
0987	2029.69	2043.02	0.66%	1897.34	1890.55	-0.36%
1762	1413.14	1409.65	-0.25%	1978.73	1961.42	-0.87%
3749	1581.22	1572.16	-0.57%	1531.43	1546.90	1.01%
6893	1674.48	1697.72	1.39%	2854.77	2951.51	3.39%

Table 3.42. Mean Values of Bending Moment of Selected Column of each GM Set Obtained from NTHA for ISO7

GM Sets	Mx (kNm)	My(kNm)
7 GMs Horizontal Components	1779.75	1799.06
11 GMs Horizontal Components	1808.68	1906.61
11 GMs Horizontal+ Vertical Components	1820.06	1922.61

According to obtained results, selecting 4 more records increase the bending moment value in both two directions. Additionally, the effect of vertical component on bending moment values of selected column is too small to consider.

Maximum bending moment values of the selected shear wall in x and y directions are demonstrated in Figures 3.49 and 3.50.

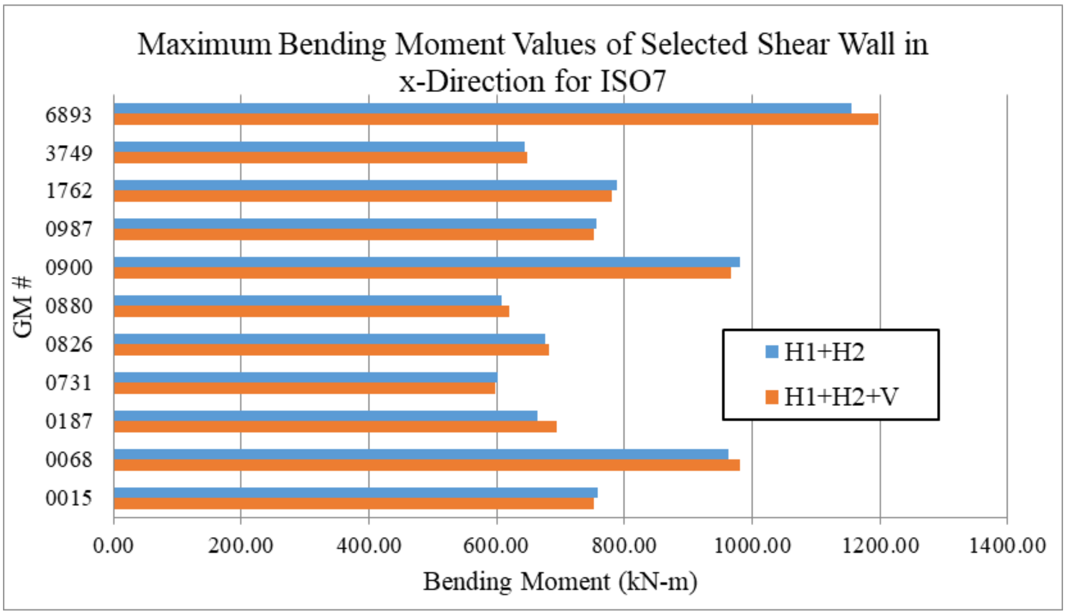

Figure 3.49. Maximum Bending Moment Values of Selected Shear Wall (in x-direction) for ISO7 from 11 GMs

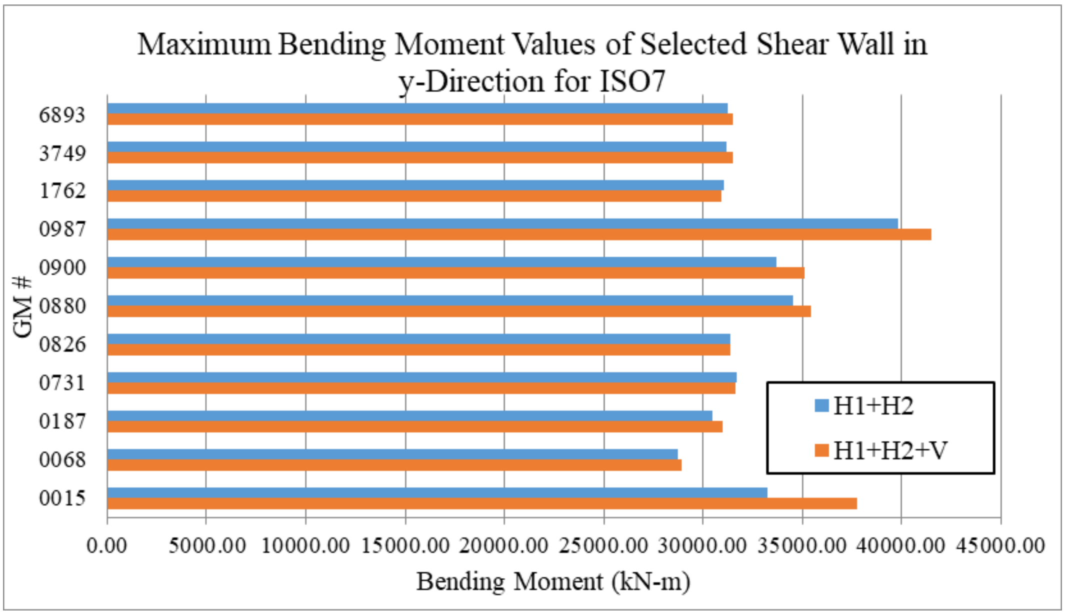

Figure 3.50. Maximum Bending Moment Values of Selected Shear Wall (in y-direction) for ISO7 from 11 GMs

Maximum bending moment values of selected shear wall for ISO4 system for 11 GMs are represented in Table 3.30 and mean bending moment values obtained from different 3 GM sets are presented in Table 3.31.

Table 3.43. Values of Bending Moment of Selected Shear Wall of ISO7 Obtained from NTHA for 11GMs

GM #	Mx(kNm)			My(kNm)		
	H1+H1	H1+H2+V	Difference(%)	H1+H1	H1+H2+V	Difference(%)
0015	758.31	751.76	-0.86%	33273.97	37788.42	13.57%
0068	963.94	980.57	1.73%	28755.77	28908.33	0.53%
0187	663.84	693.44	4.46%	30510.70	31019.59	1.67%
0731	600.92	597.11	-0.64%	31700.42	31666.54	-0.11%
0826	676.73	681.89	0.76%	31371.12	31385.14	0.04%
0880	608.55	620.02	1.89%	34556.85	35477.54	2.66%
0900	981.99	966.49	-1.58%	33682.10	35153.44	4.37%
0987	755.53	751.29	-0.56%	39826.56	41539.58	4.30%
1762	788.35	779.88	-1.07%	31090.58	30903.35	-0.60%
3749	643.52	647.01	0.54%	31197.31	31537.35	1.09%
6893	1156.30	1197.25	3.54%	31283.14	31528.43	0.78%

Table 3.44. Mean Values of Bending Moment of Selected Shear Wall of each GM Set Obtained from NTHA for ISO7

GM Sets	Mx (kNm)	My(kNm)
7 GMs Horizontal Components	745.87	31953.87
11 GMs Horizontal Components	781.63	32477.14
11 GMs Horizontal+ Vertical Components	787.88	33355.25

Different from the results of ISO2 and ISO4 system, selecting 4 more motions increase the bending moment value in both directions for shear wall. While the effect of vertical ground motion is too small in weak axis of shear wall, the effect is more significant in strong axis. Even so, the effects are not so significant.

3.1.3.6. Axial Loads Acting on Isolators

In order to examine the changes in axial loads acting on isolators, maximum and minimum axial loads carried by each isolator are evaluated for 11 different ground motions for ISO7 system. While negative values represent the compression on isolators, because friction pendulum isolators do not carry any tensile load, zero values expose that the related isolators are under the influence of tension.

Maximum and minimum loads acting on each isolator for 11 GMs without vertical components in ISO7 system are demonstrated in Figures 3.51 and 3.52.

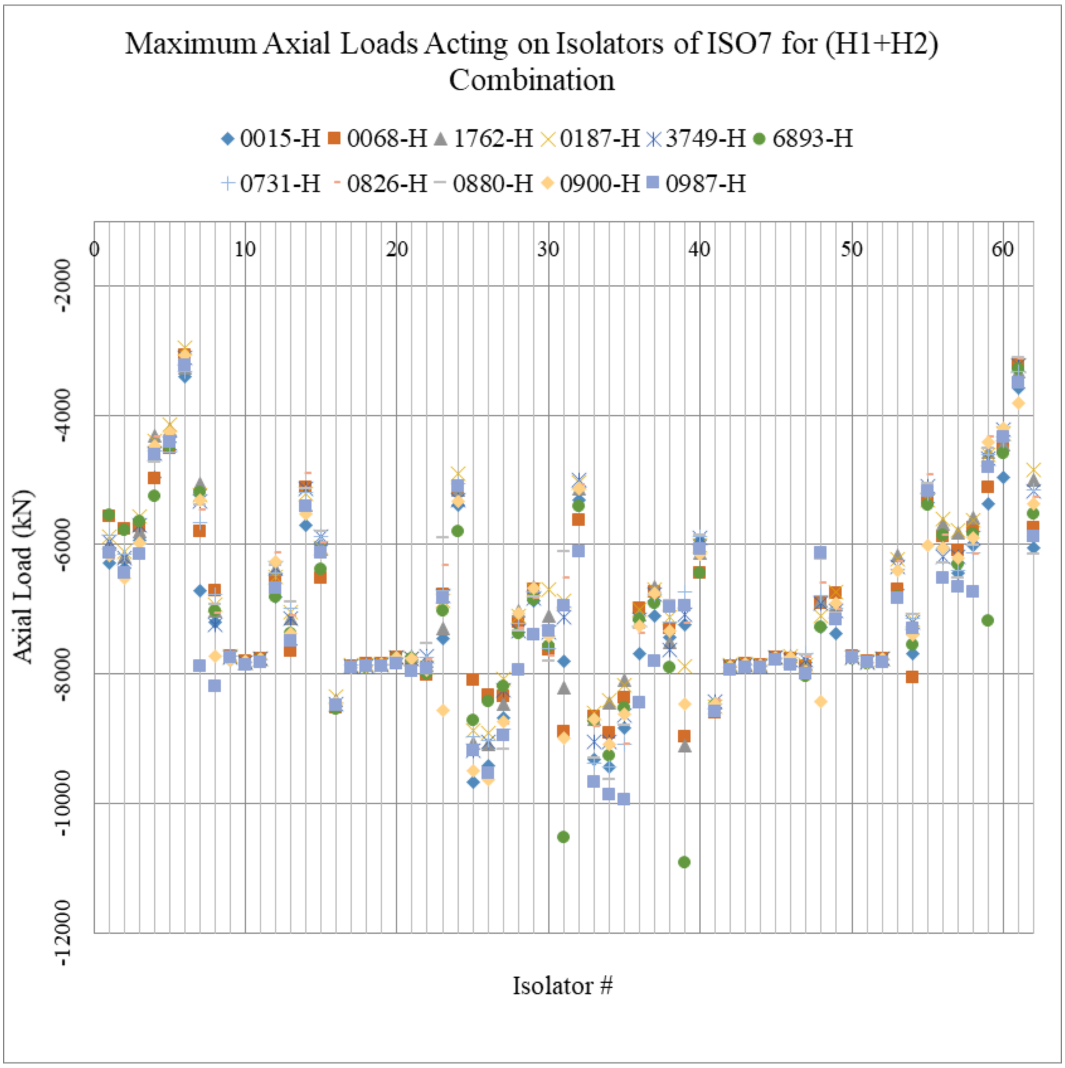

Figure 3.51. Maximum Axial Loads Acting on Each Isolator of ISO7from 11 GM Records without Vertical Component

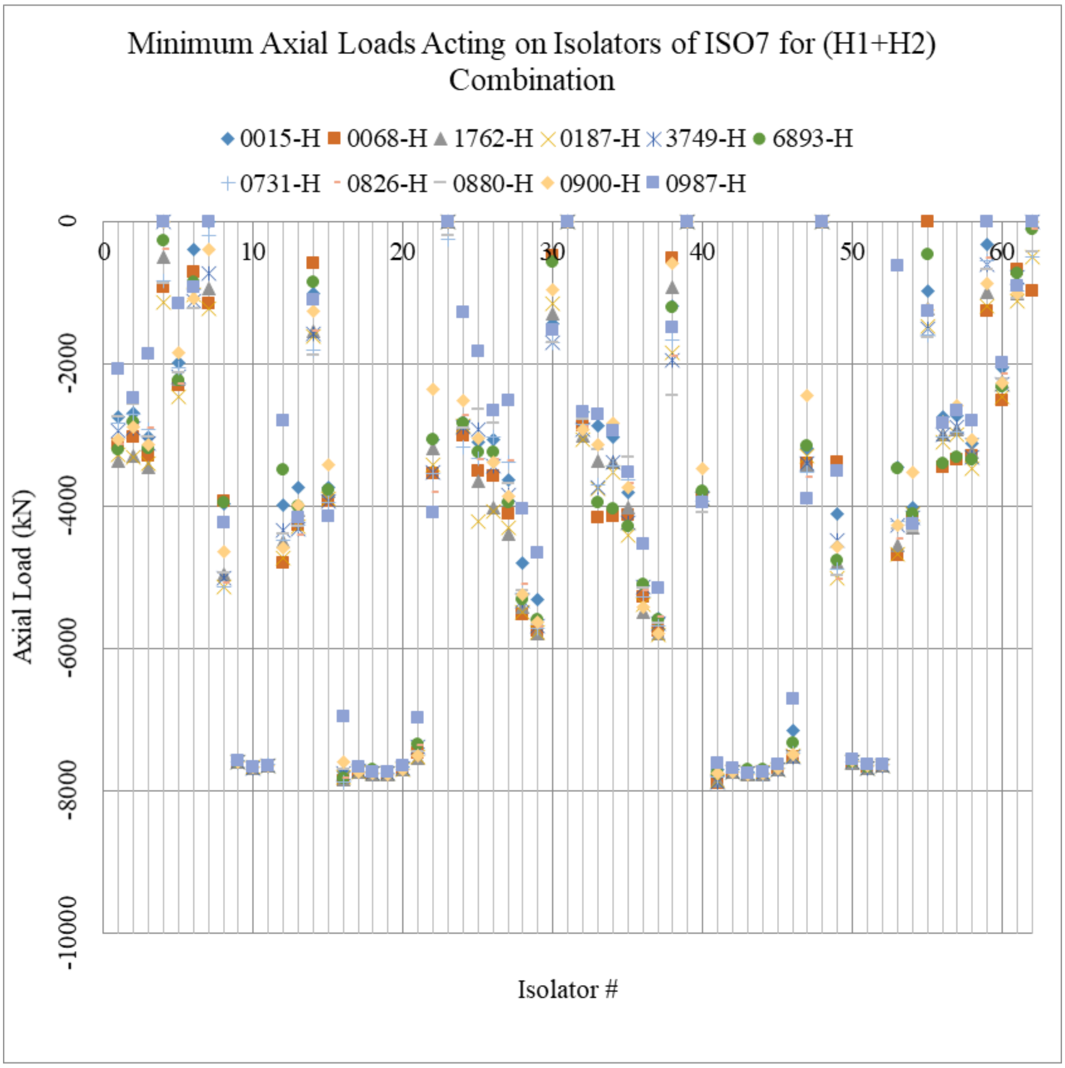

Figure 3.52. Minimum Axial Loads Acting on Each Isolator of ISO7from 11 GM Records without Vertical Component

While maximum axial loads are varying between 3000kN and 11000 kN (compression), minimum loads scatter between 0 and 8000 kN (compression). Tensile loads are generated by some GMs without vertical components on isolators 4, 7, 23, 31, 39, 48, 55, 59 and 62.

For 11 GMs with vertical components, maximum and minimum axial loads are presented in Figures 3.53 and 3.54.

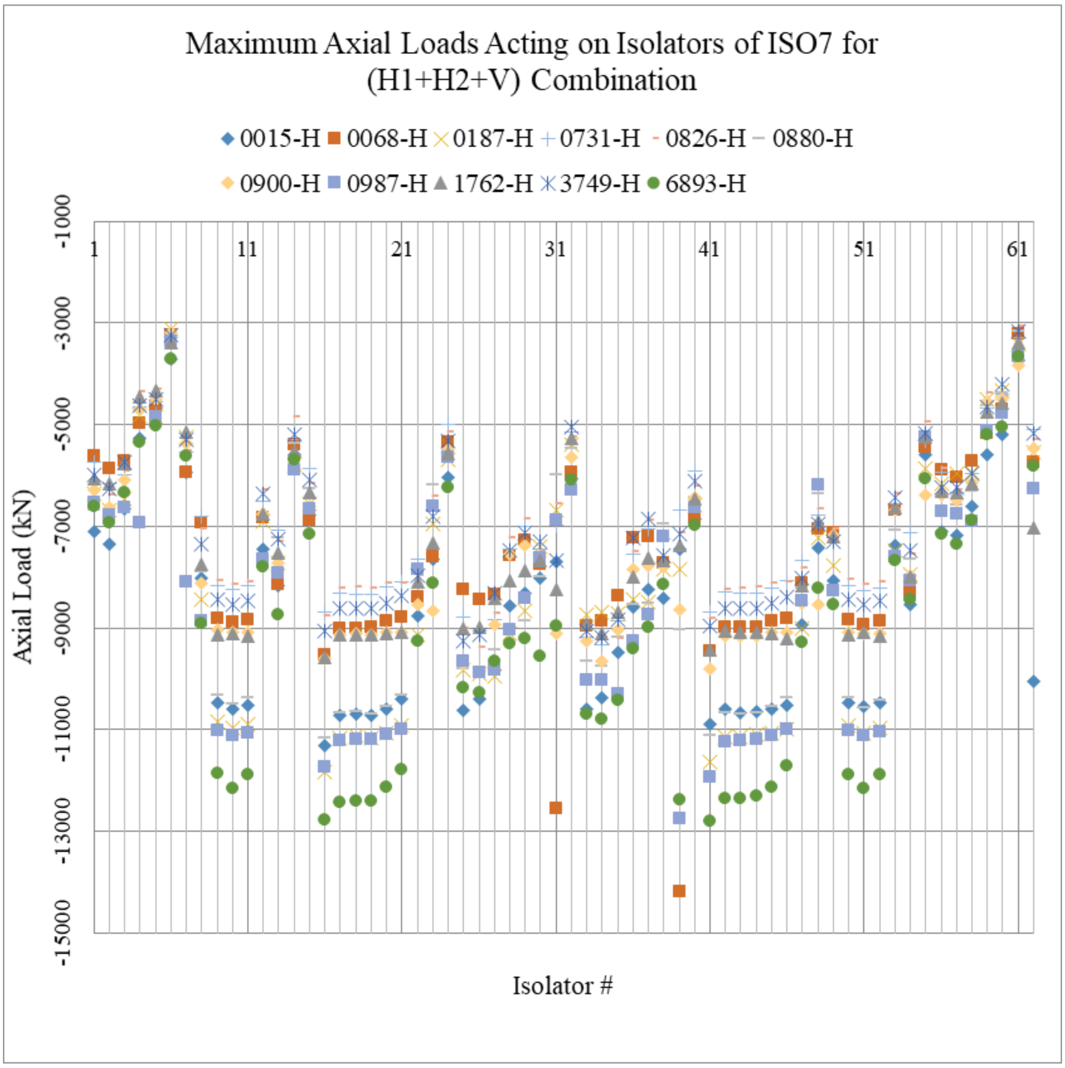

Figure 3.53. Maximum Axial Loads Acting on Each Isolator of ISO7from 11 GM Records with Vertical Component

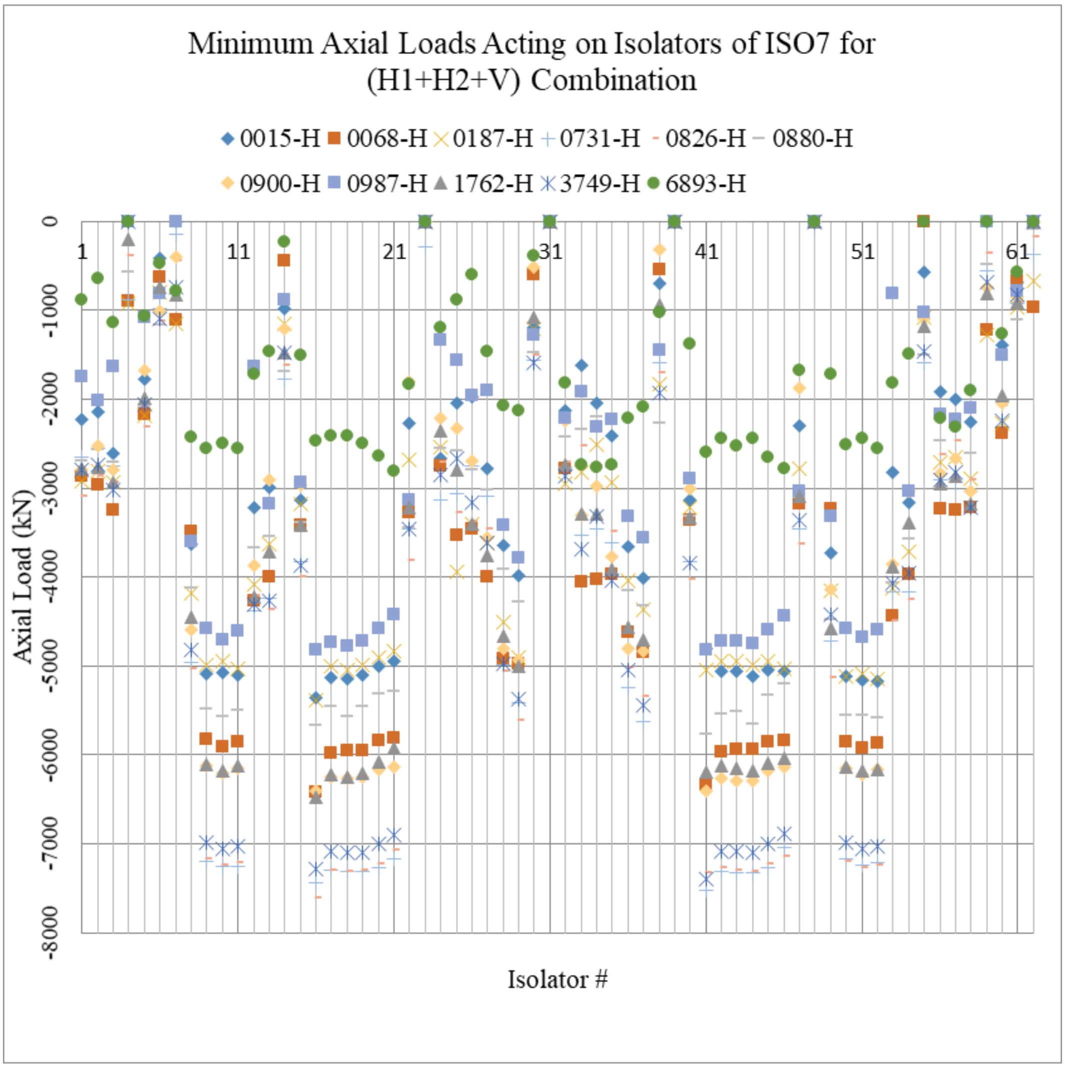

Figure 3.54. Minimum Axial Loads Acting on Each Isolator of ISO7from 11 GM Records with Vertical Component

While vertical components of ground motions increase the maximum axial loads on isolators, decrease the minimum axial loads approximately 100 kN. When compared with the other two systems, the changes are more dramatic. In other words, as the number of floors increases, the sensitivity of the axial loading columns to the vertical ground motions increase.

CHAPTER 4

DISCUSSION OF RESULTS

From non-linear time history analysis, obtained base shear values of the corresponding structural systems are demonstrated in Figure 4.1.

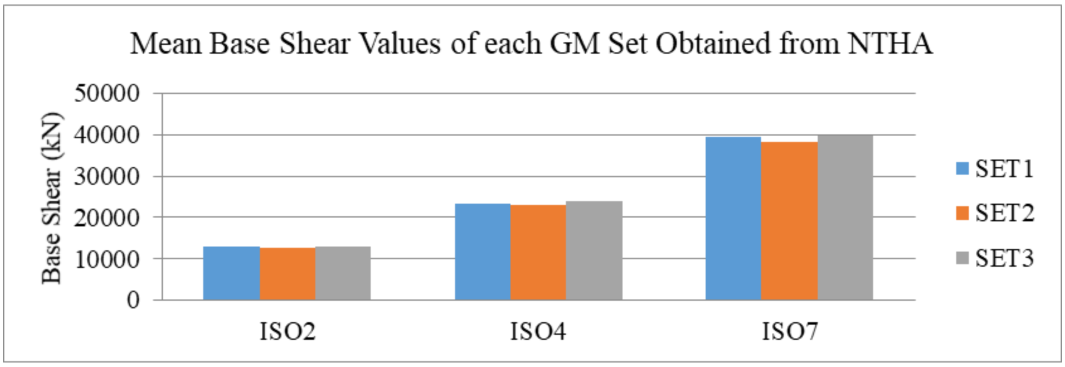

Figure 4.1. Mean Base Shear Values of Each GM Set Obtained from NTHA

Changes in base shear values of each base isolated 2, 4 and 7 storey structural systems from NTHA are provided in Table 4.1.

When four more GMs are selected, reduction ratios of base shear values are %2.85, %2.30, and % 3.09 for ISO2, ISO4 and ISO7, respectively. It is obvious that selecting 11 GMs rather than 7 GMs causes a decrease in base shear values for all systems but the reductions are not dependent with the numbers of the storeys that the structures have.

Taking vertical components of GMs into account and selecting 11 GMs rat is clearly

Table 4.1. Change in Base Shear Values

Structural Systems	GM Set Relations	Change in Vb (kN)
ISO2	11H/7H	-2.85%
	11H+V/11H	3.81%
	11H+V/7H	0.86%
ISO4	11H/7H	-2.30%
	11H+V/11H	4.60%
	11H+V/7H	2.19%
ISO7	11H/7H	-3.09%
	11H+V/11H	4.23%
	11H+V/7H	1.02%

increases the base reaction values. The increment ratios of base shear values are 3.81%, 4.60% and 4.23% for ISO2, ISO4 and ISO7, respectively. However, any effect of having different numbers of storeys on base reactions for base isolated systems could not be proven.

PFA (g) results are determined in the same way with the base reaction results. Obtained SRSS PFA values of the corresponding structural systems are provided in Figure 4.2. Change ratios of each base isolated structural system from NTHA are provided in Table 4.2.

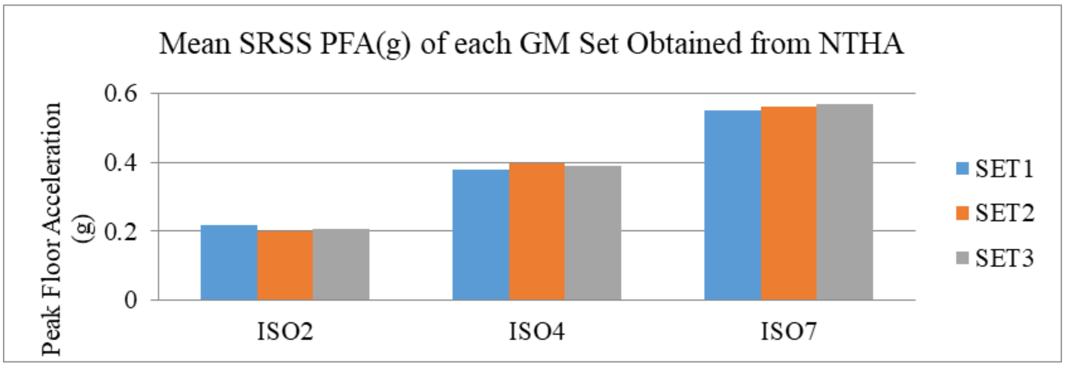

Figure 4.2. Mean SRSS PFA (g) of each GM Set Obtained from NTHA

According to the presented results, it is obvious that selecting four more ground motions or using vertical components of GMs do not have any noticeable effect on PFA values of base isolated systems.

Maximum inter-storey drift ratios are evaluated by numbers of storeys and different sets of GMs too. Obtained IDR (%) values of the corresponding structural systems are provided in Figures 4.3 and 4.4. Changes in maximum IDR of each base isolated 2, 4 and 7 storey structural systems from NTHA are provided in Table 4.3.

Table 4.2. Change in PFA (g)

Structural Systems	GM Set Relations	Change in SRSS PFA
ISO2	11H/7H	-2.12%
	11H+V/11H	0.14%
	11H+V/7H	-1.98%
ISO4	11H/7H	4.96%
	11H+V/11H	-1.72%
	11H+V/7H	3.16%
ISO7	11H/7H	1.50%
	11H+V/11H	1.82%
	11H+V/7H	3.35%

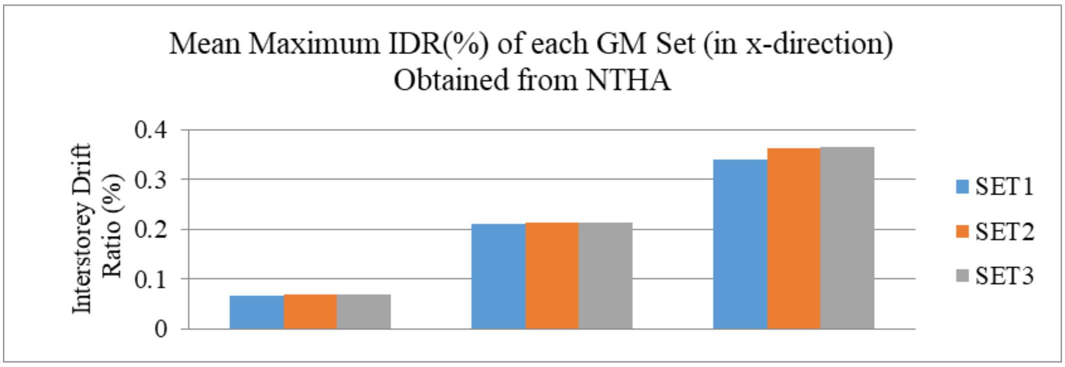

Figure 4.3. Mean Maximum IDR (%) of each GM Set (in x-direction) Obtained from NTHA

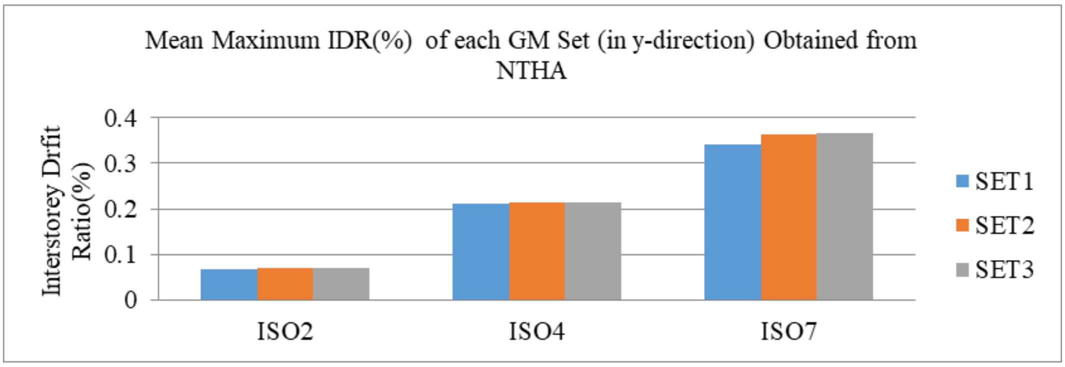

Figure 4.4. Mean Maximum IDR (%) of each GM Set (in y-direction) Obtained from NTHA

Table 4.3. Change in Maximum IDR

Structural Systems	GM Set Relations	Change in IDR in x-direction	Change in IDR in y-direction
ISO2	11H/7H	-4.58%	2.95%
	11H+V/11H	0.38%	1.29%
	11H+V/7H	-4.22%	4.28%
ISO4	11H/7H	-4.83%	1.13%
	11H+V/11H	-0.40%	-0.09%
	11H+V/7H	-5.21%	1.04%
ISO7	11H/7H	2.92%	6.86%
	11H+V/11H	-0.11%	0.91%
	11H+V/7H	2.81%	7.83%

Based on the presented results, selecting four more ground motions or using vertical components of GMs do not have any considerable effect on PFA values of base isolated systems independent from storey numbers.

One of the most important factors, isolation system displacement, is evaluated in the scope of this work. Obtained SRSS ISD values of the corresponding structural systems are provided in Figure 4.5. Changes in ISD of each base isolated 2, 4 and 7 storey structural systems from NTHA are provided in Table 4.4.

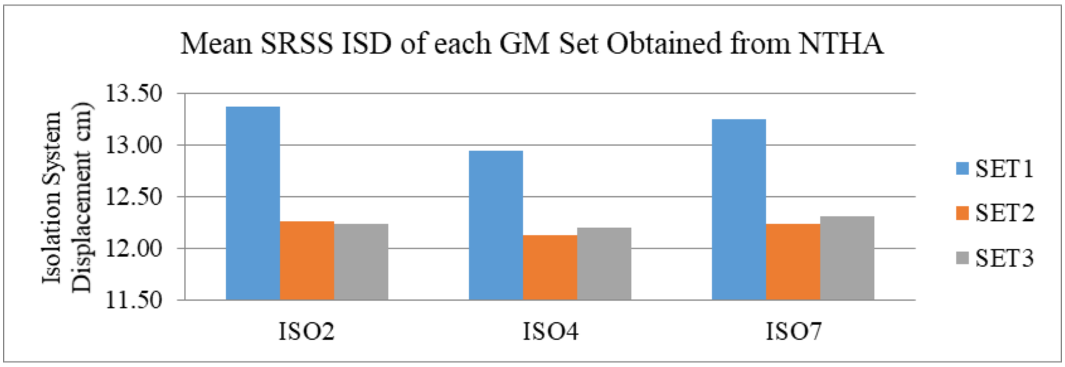

Figure 4.5. Mean SRSS ISD of each GM Set Obtained from NTHA

It is clearly seen that selecting four more GMs dramatically decreases the ISD value. For ISO2, ISO4 and ISO7 systems, SRSS ISD values decrease %8.24, %6.35 and %7.66 respectively. This means that the reduction ratio decreases as the number of storey increases. However, based on the results, taking into account the vertical components of ground motions has no identifiable effect on SRSS ISD.

Table 4.4. Change in SRSS ISD

Structural Systems	GM Set Relations	Change in ISD
ISO2	11H/7H	-8.24%
	11H+V/11H	-0.21%
	11H+V/7H	-8.43%
ISO4	11H/7H	-6.35%
	11H+V/11H	0.66%
	11H+V/7H	-5.73%
ISO7	11H/7H	-7.66%
	11H+V/11H	0.62%
	11H+V/7H	-7.09%

Bending moments of a selected column and a selected shear wall for each structural system have been evaluated in this study. Obtained bending moment vales of corresponding column in x and y directions for three structural systems are provided in Figure 4.6 and Figure 4.7, respectively. Changes in moment values of each base isolated 2, 4 and 7 storey structural systems from NTHA are provided in Table 4.5.

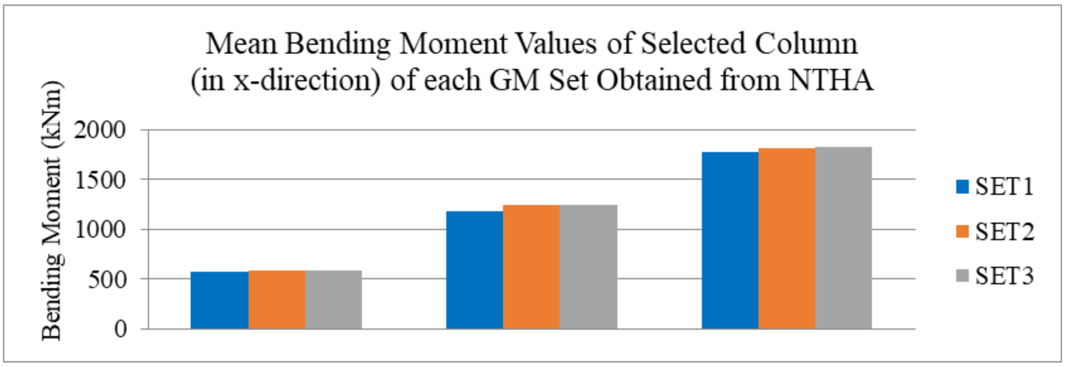

Figure 4.6. Mean Bending Moment Values of Selected Column (in x-direction) of each GM Set Obtained from NTHA

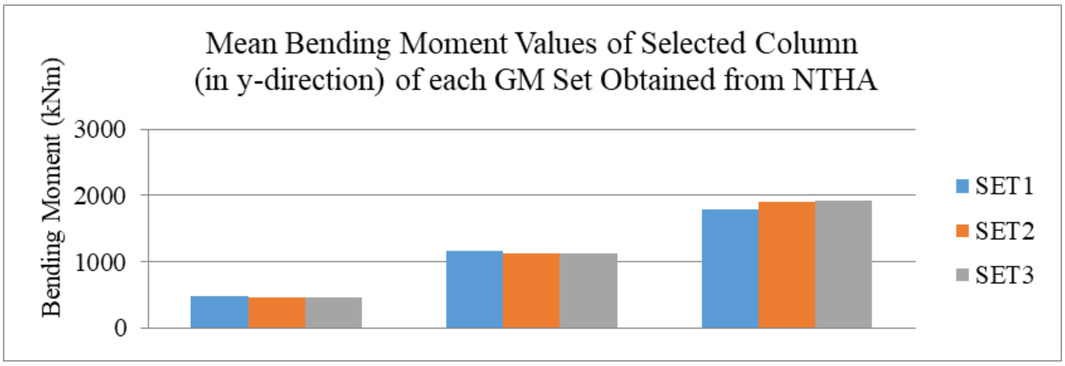

Figure 4.7. Mean Bending Moment Values of Selected Column (in y-direction) of each GM Set Obtained from NTHA

Table 4.5. Changes in Moment Values of Selected Column

Structural Systems	GM Set Relations	Change in Bending Moment in x-direction	Change in Bending Moment in y-direction
ISO2	11H/7H	1.87%	-4.53%
	11H+V/11H	0.80%	0.95%
	11H+V/7H	2.68%	-3.63%
ISO4	11H/7H	4.65%	-2.96%
	11H+V/11H	0.42%	0.04%
	11H+V/7H	5.10%	-2.92%
ISO7	11H/7H	1.63%	5.98%
	11H+V/11H	0.63%	0.84%
	11H+V/7H	2.26%	6.87%

According to the results, selecting more ground motion records increase the bending moment of column in x-direction. However, in y-direction, while the moment values decrease for ISO2 and ISO4 systems, more records increase the moment values for ISO7 system. Moreover, the effect of including vertical components of records on bending moment of column under 1%.

Obtained bending moment vales of corresponding shear wall in x and y directions for three structural systems are provided in Figure 4.8 and Figure 4.9, respectively. Changes in moment values of each base isolated 2, 4 and 7 storey structural systems from NTHA are provided in Table 4.6.

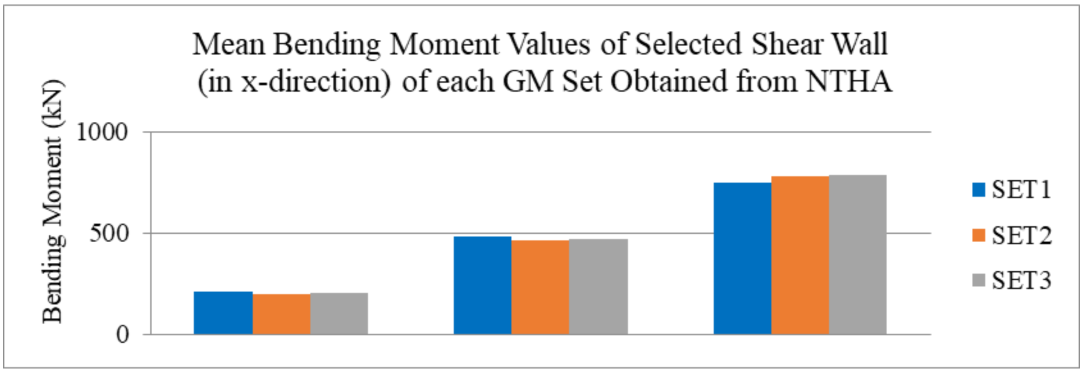

Figure 4.8. Mean Bending Moment Values of Selected Shear Wall (in x-direction) of each GM Set Obtained from NTHA

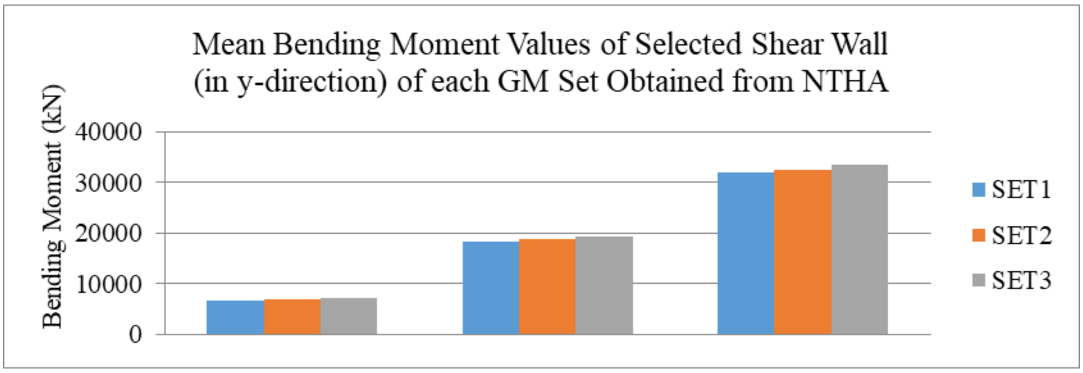

Figure 4.9. Mean Bending Moment Values of Selected Shear Wall (in x-direction) of each GM Set Obtained from NTHA

Selecting more ground motion records and including their vertical components increase the bending moment values in strong axis of shear wall. However, the results of weak axis are not identifiable.

Consequently, the effects of selecting 4 more motions or including vertical components on bending moments of columns and shear walls ae not in a general trend.

The last parameter evaluated in this study is the axial load on the isolators located in the systems. Obtained average maximum axial loads of the isolators located in

Table 4.6. Changes in moment values of Selected Shear Wall

Structural Systems	GM Set Relations	Change in Bending Moment in x-direction	Change in Bending Moment in y-direction
ISO2	11H/7H	-4.24%	3.05%
	11H+V/11H	1.19%	2.12%
	11H+V/7H	-3.11%	5.23%
ISO4	11H/7H	-3.67%	2.74%
	11H+V/11H	0.55%	3.03%
	11H+V/7H	-3.15%	5.86%
ISO7	11H/7H	4.80%	1.64%
	11H+V/11H	0.80%	2.70%
	11H+V/7H	5.63%	4.39%

corresponding structural systems are provided in Figure 4.10 and changes in average maximum axial loads are provided in Table 4.7.

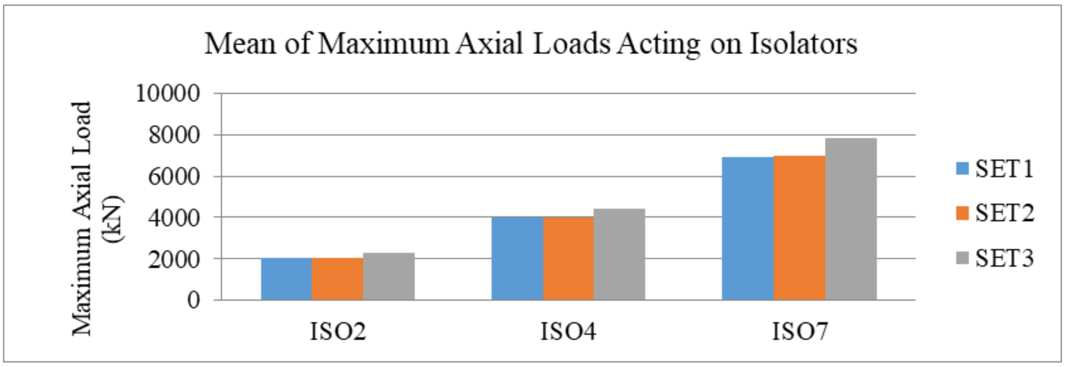

Figure 4.10. Mean Average Maximum Axial Loads Acting on Isolators of each GM Set Obtained from NTHA

Based on the provided results, change ratios are -% 0.07, -% 0.23 and % 0.36 for ISO2, ISO4 and ISO7 systems respectively. This means that selecting 11 GMs rather than 7 GMs has not an identifiable effect in maximum axial loads acting on isolators.

Table 4.7. Change in Average Maximum Axial Loads on Isolators

Structural Systems	GM Set Relations	Change in Max. Average Axial Loads on Isolators
ISO2	11H/7H	-0.07%
	11H+V/11H	11.08%
	11H+V/7H	11.00%
ISO4	11H/7H	-0.23%
	11H+V/11H	11.69%
	11H+V/7H	11.44%
ISO7	11H/7H	0.36%
	11H+V/11H	12.46%
	11H+V/7H	12.86%

Considering vertical components of GMs has a significant effect on maximum axial loads on isolators. While, the average maximum load increases with a ratio of %11.08 for ISO2 systems, the increment ratios are %11.69 and %12.46 for ISO4 and ISO7 systems respectively. It indicates that in higher-rise buildings, the vertical components of GMs affect the axial loads acting on isolators much more.

Obtained average minimum axial loads of the isolators located in corresponding structural systems are provided in Figure 4.11 and changes in average maximum axial loads are provided in Table 4.8.

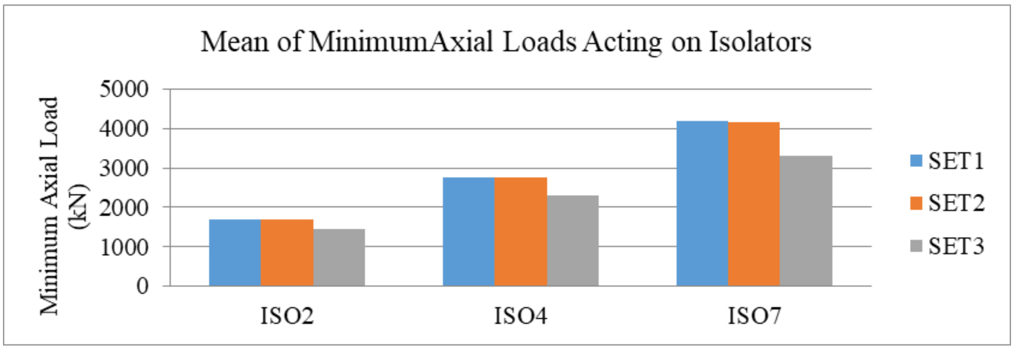

Figure 4.11. Mean Average Minimum Axial Loads Acting on Isolators of each GM Set Obtained from NTHA

Table 4.8. Change in Average Minimum Axial Loads Acting on Isolators

Structural Systems	GM Set Relations	Change in Min. Average Axial Loads on Isolators
ISO2	11H/7H	0.06%
	11H+V/11H	-14.19%
	11H+V/7H	-14.15%
ISO4	11H/7H	-0.10%
	11H+V/11H	-15.89%
	11H+V/7H	-15.98%
ISO7	11H/7H	-0.88%
	11H+V/11H	-20.66%
	11H+V/7H	-21.36%

Selecting four more GMs has not a significant effect on minimum axial loads acting on isolators as well as the maximum axial loads. Considering the vertical components of GMs has a significant effect on minimum axial loads carried by isolators, around %15~20. While the reduction ratios are %14.19 and %15.89 for ISO2 and ISO4 system, for ISO7 system, the ratio increases up to %20.66. Moreover, as stated in Chapter 3, vertical earthquake can create a tensile load on some isolators. According to the provided results, vertical components of GMs decrease the minimum axial loads acting on isolators as well as increase the maximum loads as the number of floors increases. Furthermore, according to the scatter diagrams provided in Chapter 3, the variation of the axial loads on isolators in FPS systems increase with the vertical component of ground motions and this variability becomes greater as the number of floors increases.

NTHA is an analysis procedure that takes very long time and the number of selected GMs affect the elapsed time during the analysis. Analysis duration is a very important parameter for structural designers because of the limited project durations and budgets. Elapsed times of three sets for ISO2, ISO4 and ISO7 systems are demonstrated in Figure 4.12.

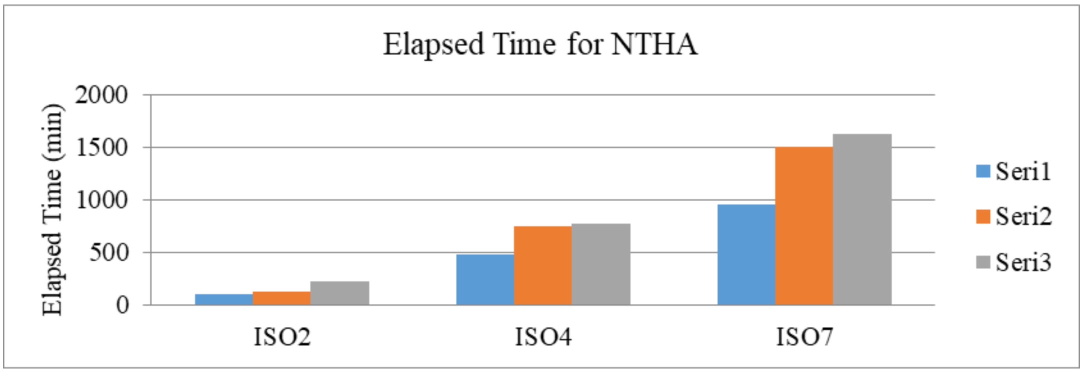

Figure 4.12. Elapsed Time for Each GM Set

As a result of all evaluations in this chapter, the most affected parameters from the earthquake regulation revision in Tukey are base reactions of structures and axial loads carried by isolators for base isolated systems. Moreover, isolation system displacements decrease when 11 GMs selected rather than 7 GMs. Additionally, time spent on analysis increases by approximately 1.5 times because of the code revision. It is not determined that the revision of earthquake regulation caused a significant change on the other evaluated parameters.

CHAPTER 5

SUMMARY AND CONCLUSIONS

5.1. Summary

In this study, the effects of selecting and scaling 11 GMs instead of 7 GMs including vertical components, which is a revision made in Turkish seismic code, on seismic response of base-isolated structures are investigated. Different sets of GMs are created and compared with each other in the cases of structures having three different numbers of floors as 2, 4 and 7. Seismic analysis is executed for Isparta, which is the first-degree seismic zone in Turkey. Non-linear time history analysis methods of base-isolated systems regulated in TEC2007 and TBEC2019 are compared in terms of seismic design parameters and elapsed time for FPS.

5.2. Conclusions

- The values of base increase significantly when the vertical component of GM is included in analysis. Selecting four more GM for time history analysis influences the base reactions however, the effect is not significant.
- Inter-storey drift ratios and peak floor accelerations changes with vertical components of GMs in NTHA without a general trend.
- The vertical component of ground motion has no influence on the value of maximum displacement of FPS. However, the maximum displacement value calculated by taking the mean of 11 GMs is approximately %8 low compared with the mean of 7 GMs. It is an expected result according to the average SRSS horizontal spectra of selected records. Even if the procedure of selection of ground motion records is described in detail, it is a subjective procedure. The result may change by selecting different ground motion records. Therefore, it is not a correct inference to say the regulation in the seismic code causes a decrease in the maximum displacement of friction pendulum bearings.

- The results of bending moment values vary according to the axes of columns and shear walls. Both selecting more records and considering vertical motion affects bending moments but these changes are not in a general trend.
- The axial loads carried by friction pendulum bearings are not influenced by the number of selected ground motions. However, the inclusion of the vertical component of the earthquake in the analysis increases the variation about the axial forces on friction pendulum bearings. While the maximum loads increase, the minimum loads decrease. Additionally, as the number of floors increases, the increases and decreases in axial loads on the bearings increase incrementally, even tensile loads occur on some bearings. Even if the response of the isolation system is affected by the tensile loads occurred on bearings, from the designer's perspective, the tension in the isolation system should be avoided. As a result, the revision in the Turkish seismic code has significantly affected the axial loads acting on friction pendulum bearings in the design of base-isolated buildings.
- The regulation in seismic code increases the analysis duration of base-isolated buildings because new code requires to select more ground motion records and to include the vertical components of these records. As the number of floors increases, analysis can take more than a daylong. This is a big challenge for a designer because of the limited project durations and budgets.

5.3. Recommended Future Studies

According to the analysis results, the number of ground motion records used in NTHA for base isolated structures does not have much effect on FPS response. The main differences are created by the vertical components of earthquakes. The influence of vertical component of an earthquake on FPS could be extended by considering more irregular or fully symmetrical structures and taller buildings. Moreover, ground motions could be selected from a more restricted set, for example, near-fault records. Additionally, all the parameters discussed in this study could be investigated for other types of base isolation systems like LRB, HDRB etc. for future studies.

REFERENCES

[1] "PEER Ground Motion Database." [Online]. Available: https://ngawest2.berkeley.edu/site.

[2] T. M. Al-Hussaini, V. A. Zayas, and M. C. Constantinou, "Seismic Isolation of Multi-Story Frame Structures Using Spherical Sliding Isolation Systems," 1994.

[3] F. Amaral and Luis Guerreiro, "Effect of Vertical Component of Earthquake on the Response of Pure-Friction Base-Isolated Structures," Adv. Mater. Res., vol. 743, pp. 105–109, 2013.

[4] ASCE, ASCE/SEI 7-10 Minimum Design Loads for Buildings and Other Structures. 2010.

[5] B. Ö. Ay and S. Akkar, "A procedure on ground motion selection and scaling for nonlinear response of simple structural systems," Earthq. Eng. Struct. Dyn., 2012.

[6] J. J. Bommer and A. S. Elnashai, "Displacement spectra for seismic design," J. Earthq. Eng., 1999.

[7] B. Carpani, "Base Isolation From a Historical Perspective," in 16WCEE, 2017.

[8] P. Clemente and G. Buffarini, "Base isolation: design and optimization criteria," Seism. Isol. Prot. Syst., 2010.

[9] Computers and Structures, "SAP2000 Advanced Version 20.0.0." 2016.

[10] A. Islam, M. Jameel, and M. Uddin, "Simplified design guidelines for seismic base isolation in multi-storey buildings for Bangladesh National Building Code (BNBC)," Int. J. Phys. Sci., 2011.

[11] A. Kamrava, "Seismic Isolators and their Types," Curr. World Environ., 2015.

[12] T. E. Kelly, W. H. Robinson, and R. I. Skinner, Seismic Isolation for Designers and Structural Engineers. 2006.

[13] F. Mazza, “Effects of near-fault vertical earthquakes on the nonlinear incremental response of r.c. base-isolated structures exposed to fire,” Bull. Earthq. Eng., 2016.

[14] F. Naeim and J. M. Kelly, Design of Seismic Isolated structures: From Theory to Practice. 1999.

[15] G. Ozdemir and M. C. Constantinou, “Evaluation of equivalent lateral force procedure in estimating seismic isolator displacements,” Soil Dyn. Earthq. Eng., 2010.

[16] N. T. Özcan, “Site Specific Probabilistic Seismic Hazard Analysis for Isparta,” 2015.

[17] L. Petti, F. Polichetti, A. Lodato, and B. Palazzo, “Modelling and Analysis of Base Isolated Structures with Friction Pendulum System Considering near Fault Events,” Open J. Civ. Eng., 2013.

[18] Prota Software, “Prota Structure 2018.” 2018.

[19] M. Rabiei, “Effects Of Vertical Ground Motions On The Seismic Response Of Isolated Structures With XY-Friction Pendulum System,” 14th World Conference on Earthquake Engineering (14WCEE). 2008.

[20] M. Rabiei and F. Khoshnoudian, “Response of multistory friction pendulum base-isolated buildings including the vertical component of earthquakes,” Can. J. Civ. Eng., 2011.

[21] S. Shekhar, S. P. Shukla, and S. Zafar, “Seismic Isolation Devices,” no. October, 2018.

[22] M. of H. R. of Turkey, Deprem Yalıtımlı Olarak İnşa Edilecek Hastanelere Ait Proje ve Yapım İşlerinde Uyulması Gereken AsgariStandartlar. 2018.

[23] Turkish Standards Institute (TSE), Turkish Earhquake Code (TEC2007). 2007.

[24] Turkish Standards Institute (TSE), “Requirements for Design and Construction of Reinforced Concrete Structures (TS500),” 2000.

[25] Turkish Standards Institute (TSE), Turkish Building Earthquake Code (TBEC2019). 2019.

[26] Turkish Standards Institute (TSE), Design Loads for Buildings (TS498). 1997.

[27] G. P. Warn and A. S. Whittaker, “Vertical Earthquake Loads on Seismic Isolation Systems in Bridges,” J. Struct. Eng., 2008.

[28] E. L. Wilson, Three-Dimensional Static and Dynamic Analysis of Structures. 2002.

CURRICULUM VITAE

PERSONAL INFORMATION

Surname, Name	: Elcik Erol, Bengü
Nationality	: Turkish (TC)
Date and Place of Birth	: 19 October 1990, Burdur
E-mail	: e166958@metu.edu.tr

EDUCATION

Degree	**Institution**	**Year of Graduation**
BS	METU Civil Engineering	2014
High School	Anadolu Öğretmen High School, Burdur	2008

WORK EXPERIENCE

Year	**Place**	**Enrollment**
2013-Present	PROTA Mühendislik	Structural Design Engineer

FOREIGN LANGUAGES

Advanced English